UNITED NATIONS EDUCATIONAL, SCIENTIFIC AND CULTURAL ORGANIZATION
INTERNATIONAL ATOMIC ENERGY AGENCY
INTERNATIONAL CENTRE FOR THEORETICAL PHYSICS
I.C.T.P., P.O. BOX 586, 34100 TRIESTE, ITALY, CABLE: CENTRATOM TRIESTE

H4.SMR/1011 - 18

Fourth Workshop on Non-Linear Dynamics and Earthquake Prediction

6 - 24 October 1997

The Physics of Earthquakes

L. KNOPOFF

University of California at Los Angeles
Dept. of Physics and Astronomy
Institute of Geophysics and Planetary Physics
Los Angeles, California
U.S.A.

SCALE INVARIANCE OF SMALL EARTHQUAKES: THE MYTH AND THE REALITY

L. Knopoff

Department of Physics and Astronomy
and Institute of Geophysics and Planetary Physics
University of California, Los Angeles

1. EARTHQUAKE ENERGY DISTRIBUTIONS

Over the last decade the well-known power-law distribution of earthquake energies [1-3] has frequently been taken to be evidence of self-organization under scale-invariant conditions and hence to imply that the earthquake process is one of self-organized criticality [4-8]. In the earthquake case this argument is misleading; there are alternative explanations for understanding the power law.

To review, the power laws are derived from analysis of earthquake catalogs, which are usually a listing of five parameters, namely the hypocenters – which are the locations in three dimensions of the points of initiation of the earthquake fracture–, the times of initiation of the earthquake fracture, and the magnitudes. The magnitude M of an earthquake is proportional to the base ten logarithm of the energy radiated to distant sites. There are two hints that dynamical processes are important: 1) earthquakes are fractures – and fractures cannot develop instantly –, and 2) earthquakes radiate vibratory wave motions of stress and displacement to distant points. The phenomenon of radiation implies that dissipative processes are at work even during the brief seconds of

the earthquake fracture event. We cannot ignore radiation since it is the one method we have of knowing that most earthquakes have actually taken place.

On a standard picture, the nature of fracture requires that we start with an elastic medium that has been prestressed up to some critical fracture threshold, at which moment fracture initiates locally and the zone of fracture spreads over some surface. The detection of wave radiation by seismographs, as well as the human experience of large earthquakes, is testimony to the rapidity of the fracture process; the crack edge velocities are of the order of shear wave velocities and in crustal rocks, these are of the order of 3 km/sec. Maximum particle velocities during slip are estimated to be of the order of a few meters/sec. The rate of loading of prestress is slow, thereby accounting for the long interval between successive large earthquakes; typical loading slip rates are of the order of several cm/year. The energy radiated in an earthquake is undoubtedly a measure of the linear dimensions of the fracture: the larger the fracture, the larger the magnitude of the earthquake. As we shall see, the limits to the size of an earthquake fracture are strongly influenced by the geometrical fluctuations in the prestress and of the fracture strengths.

To establish an intuitive understanding of the magnitudes of earthquakes, each increase of one magnitude corresponds to a 30-fold increase in energy. A magnitude 8 earthquake is an enormous event, capable of causing great death and property damage in populated areas; a magnitude 8 earthquake is a rare event locally on the scale of human lifetimes, and occurs only once every 132 years or so on the average in Southern California[9]. A magnitude 3 earthquake is perceptible only very locally, and causes no damage and occurs about once every two days in Southern California on the average; the magnitude 3 earthquakes occur about 2×10^4 more frequently than magnitude 8 events, but are felt by few people because of their small size and localization. Magnitude 8 events are huge earthquakes and are felt over wide regions.

The cumulative energy distribution in small earthquakes is

$$N(E) \sim E^{-B}. \tag{1}$$

(Seismologists prefer to use the cumulative distribution rather than the pdf.) The power law is a universal, found in all regions of the earth where there are tectonic earthquakes; observationally the exponent is 2/3 everywhere in the world with only small fluctuations; there are also heuristic arguments that give the exponent precisely. The relation (1) is known to hold for small earthquakes, since these are the only ones observable in sufficient quantity that their statistics can be identified. We know very little about the energy distribution of large earthquakes since they are rare events, and since magnitudes have only been measured since definition in 1935. The catalog for Southern California earthquakes, which spans 60+ years, is the temporally longest local catalog in the world. In that interval the largest earthquake was a magnitude 7.5 event; the last earthquake in the magnitude 8 range took place in 1857. How can one do statistics of large earthquakes if only 16 independent events with $M \geq 6.4$

have occurred in 63 years, and the strongest earthquake known has not occurred at all in the interval? So our quantitative knowledge of the large-energy end of the spectrum is poor, as given by this relatively short, although longest of catalogs.

If the finite temporal sample of a 60-year long (or less) catalog is valid as a long-term average, the total energy radiated by earthquakes $\int EdN$ under the power law (1) diverges if the upper limit to earthquake energy size is infinite, since $B < 1$. Since the energy budget for generating earthquakes, derived from processes in the interior of the earth, is finite, it is clear that the power law cannot extend to the largest energies, and that there must be a rolloff or cutoff in the distribution. This argues for the presence of at least two branches to the distribution: a low energy branch for which the power law is observed and is due to some universal process, and a high energy branch which does not fit the power law for small earthquakes and for which we have very little data. The high energy branch may or may not have its own power law distribution, but we do not know anything about that. I shall argue that the low energy branch, which we know is valid for frequent small earthquakes, is indeed due to a universal process (no surprise here), although the nature of the process may turn out to be something of a surprise. I shall also argue that the high energy branch is a response to physical processes that are strongly influenced by the geometry of earthquake faults locally. Since the geometry of faults varies from region to region, i.e. fault maps in Peru are different from those in Japan, etc., it will follow that the high energy branch must have a local character rather than a universal one, unless the major faults on which large earthquakes occur have some universal character of their own; this seems unlikely. The power law branch of the distribution cannot imply self-organized criticality (SOC) since the development of SOC depends on the presence of a power law tail at the large energy end of the distribution. Our power law is at the wrong end of the distribution.

The larger the region of potential energy storage before the earthquake, the larger the earthquake. If there is a rolloff or cutoff in the energy distribution, then there must be a corresponding characteristic length scale in the geometry of earthquakes. In Southern California, all small earthquakes are located in the uppermost 15 km of the earth's crust, which is only about 1/400 of the earth's radius; larger earthquakes may have fractures that extend as deeply as 18 or 19 km. Let us take 15 km to define the characteristic length. A critical depth is an appropriate measure of the crossover in the distribution since small fractures would be likely to grow as circles or ellipses without intersecting either the lower or upper boundaries of the seismogenic slab, while larger earthquakes would be constrained to grow horizontally, with a roughly rectangular geometry. Thus the statistics of large earthquakes would not be expected to follow the same rules as the small ones, since the fluctuations that stop growth would be expected to have different distributions on the two scales. In many other parts of the world, earthquakes occur at much greater depths, so the rolloff magnitude corresponding to the characteristic length scale is not expected to

be a universal; instead it probably varies significantly from region to region.

The rupture dimensions of small earthquakes increase by about a half-order of magnitude for each increase in earthquake magnitude: a magnitude 3 earthquake corresponds to a fracture dimension of about 300 m, a magnitude 5 earthquake to a fracture of about 3 km, etc. An earthquake with linear dimensions of 15 km corresponds to a magnitude 6.4 earthquake approximately; I take this to be the rolloff magnitude. The magnitude distribution for Southern California shows no kink at magnitude 6.4 nor at any other magnitude up to the largest (M=7.5) that has taken place in the last 60+ years. Further, the net slip in all earthquakes of the last 60 years is less than that of the slow slip in the plates that drive the earthquakes; this has been interpreted as implying that we are currently in an episode of deficiency of strong earthquakes in the magnitude 7 range and above[10]; on this interpretation, the pdf should have a peak at its large energy end, which is not observed at present; there should, of course, be a falloff at even larger energies. I will argue that at the largest energies, the geometry of faulting will require that there be a cutoff in the distribution at energies beyond the M=6.4 rolloff.

2. STRESS REDISTRIBUTION

What are the physical processes that determine the distributions of the two branches? The mechanism is centered on the physics of fracture. Because the earthquake catalogs do not indicate the relationship between the geometry of the fracture and the hypocenter, most authors have treated the catalogs as describing a point process. This interpretation is misleading. The geometry of fracture plays a vital role in the self-organization of seismicity; in detail, the precise points of origin of fractures may be rather minimally important.

The average slip $\langle u \rangle$ in a fracture is related to the average drop in stress $\langle \sigma \rangle$ from that in the prestressed state to that in the final state. From simple dimensional arguments based on Hookean elasticity, the scaling is

$$\langle u \rangle \sim \frac{\langle \sigma \rangle}{\mu} L \tag{2}$$

where μ is the elastic modulus of the material astride the crack and L is some critical length, presumably related to the geometry of the crack. Consider the application of (2) to the great ($M \approx 8$) San Francisco earthquake of 1906. The mean slip was about 4.5 m. The fracture length was about 450 km, which implies that there was a huge momentum exchange over the short time of the earthquake. (The energy released was of the order of 10^{24} erg, which is an enormous amount, and is of the order of the energy that would be released in a hypothetical 100 megaton explosion.) If we use typical values of stress drop of 100 bars (= 10MPa = 10^8dy/cm^2) and of shear modulus of 3×10^4 MPa (= 3×10^{11} dy/cm^2), one gets a scale size L for this earthquake of about 15 km, give or take a factor of π or less. The coincidence with the thickness of

the seismogenic zone may or may not be real; I believe there are arguments favoring the association. The enormous discrepancy between the scale size and the fracture length implies that slip ceases when the fracture length is of the order of 15 km. Thus the fracture in this great earthquake must be described as a moving patch of rupture of size 15 km; at the time the extremities of the fracture began to slip, the parts close to the point of initiation had healed a minute or two earlier; only $\sim$ 15km of the fracture slips at any instant. Thus healing may play as important a part in the self-organization as the condition for initiation of fracture; we will have to understand the dynamics, not only of initiation of slip, but also of cessation of slip. If the value of 15 km for the healing scale size is valid, then perhaps the process of healing has a different influence on the fracture of large earthquakes than it has on small ones.

In general, the drop in stress on a fracture is accompanied by a redistribution of stress in the neighborhood. Immediately to the side of the fracture, the stress is also lowered because of the continuity conditions on stress. Beyond the end of the fracture the stress after fracture is increased. The stresses in 1-D and 2-D scalar static cracks satisfy Laplace's equation; one can apply Gauss' theorem and show that the net change in stress on any closed curve is zero. As a consequence, there is no way to relieve the inexorable buildup of stress from tectonic sources in this model, and ultimately this model must explode in a "non-earthquake". This is not the case for dynamic cracks which are dissipative, having a dynamics controlled by the wave equation. It is the increase in stress outside the crack and in its plane that provides for the self-organizing principle in usual use. The stresses are decreased on the fractured segment and increased outside it. The range of the stresses L outside the cracks is scaled by 15 km for the larger fractures or by the size of the fracture for the smaller fractures, $L = \min[15\text{km}, \ell]$, where ℓ is the length of the crack. The change in scale size is usually ignored in simple models of seismicity that take finite fracture sizes into account. In even simpler sandpile models, the scale size for the redistribution is uniformly nearest-neighbor, i.e. it is the lattice spacing. However this is clearly a model of a dislocation rather than a fracture; it is assumed in dislocation models that healing, or restoration of strength, takes place before the neighboring lattice site can break, whereas on crack models, healing does not take place until after the crack has reached the length L. Evidently the dislocation model is undesirable: the model cannot develop the slip observed in large earthquakes; according to (2), the slip is vastly underestimated when compared with observation since the scale size L is so small.

The basis for the self-organization is thus that the stress drops on the fractured segment and increases in its plane outside it. The tectonic stress in the plane elevates the stress level slowly over the entire region, causing a new segment to rupture, which in turn causes further stress redistribution. Thus the succession of fractures and the reloading by plate tectonics generates a system of stresses that fluctuate in time and space. Fractures are initiated when the prestress is brought to the level of the fracture strength. Fractures stop growing

when they encounter a fluctuation in the difference between the local fracture strength and the prestress that is too great for the stress at the edge of the crack to deliver; the fluctuation is set up by the past history of fractures. From the Green's function for cracks with smooth edges, under either dynamic or static conditions of fracture, the stress enhancement at the edge of a crack is

$$\sigma_{edge} \sim \langle\sigma\rangle(L/d)^{1/2} \tag{3}$$

up to some numerical factors that take complex geometry into account, where σ and L are as before, where the average of the stress drop $\langle\sigma\rangle$ is taken over the active region of slip as measured by L, and where d is a distance of tapering at the edge of the crack that is introduced to avoid singularities; d is scaled by L but is less than it. Thus the larger cracks among the low-energy part of distribution have a greater likelihood that they will increase in size than smaller cracks; this statement does not hold for large L, that is for the largest cracks. The distance d is not a mere mathematical convenience: it can be shown that the edge of a crack must have a transition zone of dimension d, that lies between the regions of complete slip on the inside and the region of locking on the outside of the crack[11]; in this zone the material deforms nonelastically such as by inducing plastic deformation, slip-plane gliding, microfracturing, granulation, etc. In the case of earthquake faults, this requires that a zone of weaker material be developed around the fault laterally before or during the earthquake and whose strength rises again some time after the earthquake; thus the strength of this zone itself fluctuates over time. Such weak zones have been identified as wave guides from observations of aftershocks of the very strong Landers earthquake (M=7.3, 1992) in Southern California[12].

3. MODELS OF LARGE EARTHQUAKES

Earthquake systems are clearly self-organizing. I have indicated that these systems are not SOC for geophysical reasons; I show that they are not SOC for physical reasons as well. We study models of large earthquakes to see what the qualitative properties of the self-organization are. A number of models of self-organization in earthquake systems have been constructed in which it is assumed that the power law is the only branch to the distribution. Since power laws imply self-similarity, it has been assumed that the earthquake histories are developed on the simplest of landscapes of the spatial distribution of fracture strengths, namely constant distributions. However, for spatially homogeneous threshold models of fracture, the power laws that are developed must have infinitely long tails. Thus for these models, there is a finite probability that a fracture will develop that extends across the entire model; at this point a fracture develops that stops for reasons other than the internal fluctuations of difference between fracture strength and prestress; these cracks are of infinite length for periodic boundary conditions, or they encounter unbreakable barriers at ends (which are extraordinary inhomogeneities of strength), etc. We

call these events runaways; they are lattice-size effects. In other words, the runaway events interact with the computational boundaries and develop fractures that are not stopped for the same reasons as the smaller events; they are not members of the same universality class; the largest earthquakes in nature are true earthquakes. After a runaway the subsequent evolutionary history is overwhelmed by and is a consequence of the reset of the stress conditions by the interaction with the boundaries, and no longer reflects a process that is characteristic of an infinite region; to restate in simple terms, after a fracture encounters the boundaries, we begin to be concerned with surface rather than volume effects. The situation does not improve if one introduces dynamics and radiation damping into a finite lattice system. It has been shown that evolutionary seismicity on a finite homogeneous lattice with dynamics and radiation and with rapid healing, develops a very long transient episode of activity that has the power law property, but even here the system ultimately organizes itself into a lattice-wide event[13] which, as remarked, is physically unacceptable. Indeed the power law in the transient phase does not describe an ensemble of random events. Instead, the events before the runaway are highly correlated: since the stress after any fracture is roughly uniform, all parts of it are likely to reach the threshold stress at about the same time, after a suitable elapsed time for reloading. Thus the next event on this segment has a very high probability of being about the same length as its predecessor. Thus the power law in these models reflects the numbers of clusters and the number of fractures in each cluster.

Numerical simulations focus on the high energy branch of the distribution rather than the low energy branch. If computational lattice sizes correspond to a size that is larger than the largest fractures observed, then the simulations of stress redistribution are dominated by the large and largest earthquakes. It follows that the primary goal of these simulations cannot be one of using the power law distribution known for small earthquakes as a target. We restrict attention in the models to the organization of the large earthquakes, for which we have no statistical guidelines.

Can inhomogeneous distributions of fracture strength stabilize the process and restrict the occurrence of runaways? Recent work[14] has shown that there is a strong relationship between fracture strength and geometry of faulting, and that an irregular geometry implies an irregular fracture strength. To elaborate this notion, we must first define an earthquake fault. The mapped faults are sites where large earthquake ruptures of the past have intersected the surface of the earth; they are manifestations of the damage to the crust performed by large events. Because of their size, small fractures are unlikely to intersect the surface, but large fractures will, especially if $M \geq 6.4$. Thus fault maps give the surface expression of the geometry of large fractures. The dating of ancient fractures on faults at the surface is a campaign that is only just beginning[9,15]. The fact that major faults have extensive offsets that are very much larger than the slips in individual great earthquakes, tells us that large earthquakes recur on the same fault structures. Although they are themselves

strong, so that they do not slip in earthquakes very often, these faults are zones of local weakness since the largest earthquakes do not take place in the fresh rock adjoining the old faults; most often, new earthquakes take place on old structures. Faults however grow very slowly by extension of existing structures and new ones are probably initiated, but most contemporary earthquakes take place on pre-existing fault structures. At some time after a fracture on a fault has taken place, the walls of the fault must be sutured or locked in order that deformational stress be accumulated over the long time interval before the next large earthquake occurs on it. We have proposed above that the process of healing in the large events is relatively rapid and and a large part of the strength is restored during the rupture itself.

No fault is perfectly planar or perfectly smooth, because nothing in the real, macroscopic world is smooth. Without geometrical roughness of fault surfaces, there would be no ability to store deformational prestress, since faults would always slip. But roughness is found on a variety of scales. On large scales, the macroscopic geometry of faults includes offsets, bifurcations, echeloning, etc.; at sites of nonplanar geometry, bifurcations into secondary branches can take place. Thus faults form networks; in the case of Southern California faulting, the San Andreas Fault (SAF), which is the boundary between the Pacific and North American plates, dominates the activity on the network. In the past 60+ years, there has been virtually no activity down to the very smallest of magnitudes on the SAF; all of the very strong earthquakes of this interval have occurred on secondary faults of the network. Thus any model of the seismicity of large earthquakes should be done on a network of intersecting fault, rather than on the single faults of popular models up to this time.

Despite these remarks, let us see how far we can get by studying single faults. In the case of in-plane deformations which are appropriate for earthquakes, segments of faults that are not parallel to the regional shear stress will continue to accumulate normal stress; the normal stresses are not relieved by shear (earthquake) fractures. Thus the normal stress on these "bends" should be expected to build up monotonically under the inexorable increase of regional deformation by the loading due to plate tectonics. Under a Coulomb fracture criterion (or something similar), which states that the material will fracture when the shear stress exceeds a certain fraction of the normal stress, in 2-D the threshold stress for fracture of this bend segment should increase more and more, i.e. it becomes stronger and stronger. Thus the succession of earthquakes on this segment should increase monotonically in magnitude and with monotonically increasing time intervals. Once the fault becomes too strong, the fault should lock and plate tectonics be switched off. Since this does not happen in nature, there must be some form of relaxation of the normal stress with a time constant that is long compared to the recurrence time of large earthquakes. The relaxation must take place through seismic processes such as mountain building and non-seismic processes, such as erosion, folding, and most likely the fracture and growth of secondary faults. We can overestimate the relaxation time from the ratio of the heights of local mountains— and their roots— to the tectonic

rates of deformation, and reach a figure of about 10^5 years, give or take a large factor. The relaxation time must be longer than the interval times between large earthquakes; the interval between the two most recent large earthquakes on the Landers fault system was between 6000 and 9000 years[15], which places a lower bound on the relaxation time. Thus the normal stress accumulated in the last 10^4 to 10^5 years is stored in bends on the faults (and we suppose in other geometrical irregularities of fault structures), and hence these irregularities are of great local strength in comparison with the portions of the fault that are parallel to the regional stress. Thus fault structures that are not parallel to the regional stress are sites of great shear strength, and we must expect that large fluctuations in fracture strength would develop at these sites. Such geometrically induced fluctuations in threshold stress imprint a second extrinsic scale size (or many scale sizes) on the problem. Simulations under the geometrical constraints of very large fluctuations in fracture strength with long-time constant relaxation of stress, never display runaways or lattice-wide events; but then one can always argue that the computations have not been run for long enough times, so the case is not proved.

The geometry suggests that the long reaches of the SAF that are more or less parallel to the regional shear stress have relatively low shear strength[16], and are punctuated by occasional localized sites of great strength. In other words, the two plates would be likely to slip in a mode of almost continuous sliding were it not for a few sites at which they are prevented from doing so; at these sites the plates are "nailed" together. Thus these "asperities" are sites at which the potential energy of deformation is accumulated prior to great earthquakes; when these asperities break, they do so in very large events, and generate slip in very large earthquake fractures that extend to the next asperities or beyond. These are the characteristic earthquakes that have been reported for large earthquakes that seem to recur on the same sites[17]. They represent the largest earthquakes that are possible on the system and their magnitudes are limited by the spacing and strengths of the asperities.

Simulations on a 1-D straight fault with a spiky distribution of breaking strengths shows a large number of weak slip events in the valleys between the peaks of strength. Occasionally, strong earthquakes develop at the asperities that tear up to and stop at neighboring asperities as we expect. However there are enormous instabilities in these patterns in the form of abrupt changes in rates and sizes of events[18,19]; these instabilities are associated with abrupt stress transfer from one part of the fault to another through broken asperities that act as gates. Further, these patterns have extraordinarily different from those that are found to develop on models with large but smoothed fluctuations of breaking strengths. These instabilities of pattern from structure to structure, and instabilities of pattern evolution for a given structure, imply that the quality of the large-energy branch of the distribution is strongly dependent on local fault geometry and therefore cannot be expected to be a universal property.

As a first effort to simulate earthquake pattern development and evolution on

a network of faults, we have considered a simple case of stress interactions between two nearby, parallel faults with inhomogeneous distributions of fracture strengths[19]. We find a new type of instability of pattern in these simulations: extended lacunae in the seismic activity are developed on individual faults, wherein activity on extended portions of one fault ceases and activity is concentrated on the other fault. This form of activity-flipping is associated with the constraint that all points on at least one fault must ultimately break through, no matter how strong, or else plate tectonic motions cease. As a consequence, activity must develop at strong sites on one fault even though complementary faults may be locally weaker and would have been expected to be more likely to fracture had the fault been isolated. These instabilities are further testimony to the dependence of the large-energy branch on the local geometry of faulting on a two-dimensional network of faults capable of tearing in large earthquakes. The fact that these systems appear to be unstable due to a number of geometrical agents means that there is little likelihood at the present time of predicting interval times between events on the large earthquake branch of the distribution. But since this time scale is long compared to the human time scale, these issues are, for the moment, of academic interest, if it is our purpose to generate some insights into the possibilities of earthquake prediction.

4. AFTERSHOCKS

I return to the issue of the universality of the low-energy branch of the distribution. Because of the scaling of stress redistribution, large earthquakes must change the stress field significantly on the sites of occurrence of small earthquakes in the neighborhood, but the reverse is much less likely. This is another reason why SOC is unlikely to develop on the small-energy branch of the distribution; any self-organization on the small energy branch is likely to be heavily punctuated by activity on the large-energy branch. It would seem to be paradoxical to suggest that the universality of the small events is somehow connected with the non-universality of the larger ones. I argue that this is indeed the case.

A map of all earthquake epicenters in Southern California with a lower magnitude threshold on the low-energy branch of the distribution, is of course dominated by small earthquakes which are displayed in overwhelming numbers (Fig. 1). The map shows rather remarkably that many of the mapped faults on which large earthquakes are expected to occur, do not have any small earthquakes; but since there were no large earthquakes on these faults in the 60+ year interval of the catalog, these faults show no seismicity whatsoever in this interval. Most of these faults are expected to have strong earthquakes at some time in the future; the SAF has this property. This result is completely contrary to expectations based on sandpile or dislocation models of self-organizing systems, which assert that any given section of fault should experience the full

Fig. 1. — Epicenters of Southern California earthquakes with magnitudes greater than 3.5, 1935-1994. Most of the clusters of epicenters are due to aftershocks of large earthquakes.

spectrum of sizes of events, with small events occurring more frequently than large ones.

Some faults have many small shocks on or near on them. The densest clusters of these earthquakes can be identified as being the numerous small aftershocks of a few large earthquakes. These small earthquakes are the consequence of predecessor large ones, and these small earthquakes cannot organize themselves into a succession of events leading to future large earthquakes; these small events are the fallout of the large ones. Typically, large events occur without much preparation or build-up. However hopes for earthquake prediction must rest on observations of fluctuations in what seismicity there is before a large earthquake. Some of the small earthquakes on the map are not aftershocks of known identifiable large earthquakes in the 60+ year interval. Below, I suggest that aftershock series may last for much longer than 60 years, and hence these latter earthquakes may be aftershocks as well, but of large earthquakes that occurred before the start of the catalog.

Aftershocks are of course earthquakes that are highly localized around fracture zones of large earthquakes and are delayed by often many years after their parent event. Aftershocks themselves have been much studied, and are known to have at least two universal properties. The rate of occurrence of aftershocks is a universal and is given by Omori's law[20]

$$\dot{n} \sim 1/t \tag{4}$$

Observationally, the exponent on t may differ from 1 slightly, and adjustments in the specific form of the time dependence have been suggested, but we use this formula as a good starting point for discussion. Formula (4) is accurate at all magnitudes of the low-energy branch of the distribution; there are few aftershocks with magnitudes on the high-energy branch. A second universal is the observation that the magnitudes of earthquakes in an individual aftershock series fit the Gutenberg-Richter power law for small magnitude earthquakes remarkable well with the expected exponent B [21,22]; since the aftershock magnitudes are less than those of the parents, their magnitude distribution has a cutoff. The durations of the sequences (4) are extraordinarily long. In the best-documented aftershock series, which is that following the M=7.5 Kern County earthquake of 1952 in Southern California, aftershocks in the immediate neighborhood have a remarkably excellent fit to the Omori law, even after 43.5 years, a time that is a substantial fraction of the length of the complete catalog; for these earthquakes the fit to the power-law energy distribution is excellent: $1.5B = 1.03 \pm 0.04$. It is plausible to suppose that the law (4) holds for times longer than 60+ years.

If we strip off the known aftershocks from the map of Southern California epicenters, we are left with a much reduced set of small events. If we make the conjecture that the tail of the Omori distribution is very much longer than the 60+ year span of the Southern California catalog, we reach the conclusion that the majority of the residual events are also aftershocks of large events that occurred before the start of the catalog, and perhaps long before the start of the catalog. The catalog of small earthquake that remains, after all identifiable and presumed aftershocks are removed, is very small, accounting for perhaps 10% of the original total; these may also be aftershocks of early strong earthquakes, but we are not sure. Let us make the assumption that the earthquakes on the small-energy branch fit the Gutenberg-Richter law because they are aftershocks that fit the Gutenberg-Richter power law. This assumption is consistent with our conclusion from the analysis of the energy distribution that the numerous small events are the consequence of the few large ones, rather than being part of a self-organizing process leading to the large ones. Under this assumption, the self-organization of the small earthquakes is not punctuated by the stresses redistributed from the large earthquakes, but rather they are the punctuations themselves. This assumption regarding the length of the tail in the Omori law, means that earlier efforts to try to remove aftershocks by filters that made use of windows of finite width[23] were incorrect; this form of data analysis led to the observation that the residual events were independent. Under this assumption, the residual events are no longer independent. We must now shift our effort to try to understand the cause of the universality of the small energy branch of the distribution to a new and different problem, which is to try to understand the universality of the Omori/Utsu law of aftershocks.

The spatial distribution of aftershocks provides a clue to the problem. The distribution of aftershocks after the Landers earthquake was especially well documented[24], and the fact that the main rupture was on a system of vertical

faults removes many difficulties associated with the geometry of projection of hypocenters on the horizontal/map plane. The locations of the aftershocks form a cloud of dots that are up to several km from the rupture trace and within the accuracy of location cannot be assigned to the rupture trace itself; more of the aftershocks are near the rupture trace than far from it. Most of the aftershocks lie within 4 or 5 km of the rupture trace; Aki (personal communication) indicates that at least 80% of the aftershocks were more than 200 meters from the rupture trace.

There are two problems: Why are aftershocks located in the neighborhood of the fracture and not on the fault (as some authors would prefer), and what is the cause of the time delays? The solution to the problem of the time delays has been suggested by a number of authors to be due to relaxation of extraordinarily high stresses by non-elastic processes. I agree that relaxation is the answer to the time-delay problem, but this mode of solution runs into the first problem: where do the high stresses come from? Many authors suggest that irregularities of slip on the main fault might be the source of the high stresses. But the aftershocks are more or less uniformly distributed along the length of the main fracture and show no evidence of large irregularities on any scale. For the irregular-slip solution to hold, we would require that the irregularities of slip in the main fracture have very long wavelength fluctuations, since the shorter the distance scale of slip variations for a given amplitude of slip variations, the smaller the amplitude of the stress variations in the neighborhood. The amplitude of the slip variations in the main fault cannot be made too large, else the main fault would stop prematurely; the dynamics of large ruptures is a smoothing operator on slip, due to inertial effects, so it is difficult to generate rapid fluctuations in slip even for highly inhomogeneous faults. Further, it would be difficult to attribute a stochastically universal irregularity of slip that would contribute to the universality of the two observations of aftershock series.

An alternative to irregular slip is the following. We note first that the strength of the material a few km from the main fault is strong before the big earthquake since the sites of the aftershocks did not tear before the main shock. Second, from continuity conditions, the rupture on the main shock lowered the stress on the aftershock sites, and probably by a large amount. Thus, on a standard model, the aftershock sites would be even less likely to tear at any time after the main shock. Now we need a mechanical amplifier to increase the stress up to the fracture threshold at aftershock sites adjacent to the fault The solution to the dilemma is to propose that the main rupture also lowered the strength of the rock nearby the fault at the time of the main rupture, and to a level well below that of the residual stress, which is near the sliding friction or below it if there is dynamical overshoot. We suppose that the main shock shattered the rock nearby. The fragments are in contact at points of geometrical irregularity; these points are interconnected by a spiderweb of cracks, rather like the shattering of a windshield in an automobile collision— with different symmetry of course. Under a finite but small regional residual stress, weak cracks will have a large stress concentration at their edges, and these asperities

disappear in delayed time by stress corrosion at their edges. The process is much enhanced if the unbroken segments form asperities between two or more adjacent cracks which is the amplifier we seek. Stress corrosion is an active agent in promoting delayed collapse of a strong barrier region between two (or more) cracks[25]. The rates are much enhanced by the presence of water because of the enhanced solubility of silicates, and the possibility of developing granular rotations at high temperatures and confining pressures[26].

Thus aftershocks are a two-stage process. First, the large-slip event of the main shock triggers shattering of the near neighborhood over the time that it takes elastic waves to travel to the aftershock sites, which is of the order of a second or less. These fragments are prevented from further slipping by the geometrical irregularities of the shards. In the second stage the geometrical contacts between the shards disappears in accelerated creep by stress corrosion processes under the influence of the residual shear stress on the main fault. The magnitude distribution of the aftershocks is thus dependent on the amount of energy stored in the geometrical contacts of the shards, and the time delays are regulated by the stress corrosion process. If there is a low density of small cracks are produced by the shattering for example at some distance from the main fault, then the stresses are not amplified significantly and no aftershocks occur in this region. Simulations have reproduced part of this picture[25]. The model generates universality of the aftershocks by virtue of the universality of the shattering process. the model is not dependent on the specific properties of large-scale fault geometry or on the specifics of slip on individual faults. Seismological tests of this model are under way at this time.

In this development, we have introduced two new components of the physics of fracture, beyond those of simple elastic loading and brittle fracture presented in the earlier parts of this lecture. I suggest that 1) the walls of the small cracks that participate in the development of small earthquakes remain open for some time after formation, in order that 2) their edges can deteriorate in time under non-elastic decay processes. Thus we require that the healing rates for small cracks be long compared to the rupture times; these fractures must remain open for many decades. This is in contrast to the model of healing that we have developed for large earthquakes, in which healing is relatively rapid, and certainly shorter than the rupture time of the complete length of the fracture. How can this be? One possibility is to invoke the role of fluids in the fault zone and nearby. Fluids have been suggested as an active participant in the weakening process of faults, and that they might be agents in developing slip weakening prior to large-scale faulting. Further suppose that the immediate environment of the fault is strong because it is relatively dry. As large scale faulting develops, water may be squeezed out of the fault, into the fractures that it itself has formed in the neighborhood, thereby promoting short-term healing of the main fracture. The increased pressure of the fluids in the cracks nearby keeps the walls apart. Over long periods of time, this fluid can diffuse back into the fault zone and reheal the small cracks, thereby terminating the aftershock process, and preparing the region for the next great earthquake.

On this model, the presence of small earthquakes serves as a signature of low probability of occurrence of a strong shock. It does not however indicate when the strong shock will occur.

With regard to earthquake precursors, there are several indicators of the importance of fluids in fault zones and in fault networks to produce seismic precursors. Time limitations in this lecture, and space limitations on these printed pages, do not permit me to develop these ideas further. Some discussion along these lines have been identified in [27-29]].

Further research along these lines must take us in the direction of understanding better the physics of granular materials: how they are locked together, and how they unlock in the presence of fluids and under local shear stress.

5. DISCUSSION

I have proposed that a study of the universals of earthquake observations, namely the low-energy branch of the power-law distribution of earthquake energies and the properties of aftershocks, can lead to an understanding of the self-organization of earthquakes on several time scales. The consequences of these considerations have taken us away from the far too simple models of self-organization and the critical state that have appeared in the literature. In particular we have had to introduce a new component of the physics of fracture into the modeling over and above the usual considerations of elastic loading and brittle fracture; in particular we have been obliged to take into account the healing of cracks and the rates of healing; the physics of healing has bearing on the problems of plasticity, which I cannot discuss here. The future will see a much greater effort on understanding the interaction between geometry and fracture; we must expend a much greater effort at understanding the nature of deformation of granular materials since these materials are the real constituents of the fault zones and the nearby regions. In short, the application of simplistic physics is not enough to solve the problems of earthquakes. The problems are rich and well-deserving of serious attention, and there are many unsolved problems.

Acknowledgments

I thank M.S. Abinante, M.W. Lee and X.X. Ni for their kindness in acting as reflective and reflexive critics of some of these thoughts during the formative stages of this work.

References

[1] Gutenberg B., *Q. J. Geol. Soc. Lond.* **112** (1956) 1-14.
[2] Gutenberg B., Richter C.F., *Bull. Seismol. Soc. Amer.* **34** (1944) 185-188.
[3] Gutenberg B., Richter C.F., *Ann. di Geofisica* **9** (1956) 1-15.
[4] Bak P., Tang, C., *J. Geophys. Res.* **4** (1989) 15635-15637
[5] Sornette A., Sornette D., *Europhys. Lett.* **9** (1989) 197-202.
[6] Olami Z., Feder H.J.S., Christensen K., *Phys. Rev. Lett.* **68** (1992) 1244-1247.
[7] Olami Z., Christensen K., *Phys. Rev. A* **46** (1992) 1720-1723.
[8] Feder H.J.S., Feder J., *Phys. Rev. Lett.* **66** (1991) 2669-2672.
[9] Sieh K., Stuiver M., Brillinger D., *J. Geophys. Res.* **94** (1989) 603-623.
[10] Working Group on California Earthquake Probabilities, *Bull. Seismol. Soc. Amer.* **85** (1995) 379-439.
[11] Barenblatt G.I., *Adv. Appl. Mech.* **7** (1962) 55-129.
[12] Li Y.G., Vidale J.E., Aki K., and others, *Science* **265** (1994) 367-370.
[13] Xu H.J., Knopoff L., *Phys. Rev. E* **50** (1994) 3577-3581.
[14] Nielsen S., Knopoff L., in preparation.
[15] Sieh K., *Proc. Natl. Acad. Sci. USA* **93** (1996) 3764-3771.
[16] Zoback M.D., Zoback M.L., Mount V.S., and others, *Science* **238** (1987) 1105-1111.
[17] Schwartz D.P., Coppersmith K.J., *J. Geophys. Res.* **89** (1984) 5681-5698.
[18] Knopoff L., *Proc. Amer. Philosoph. Soc.* **137** (1993) 339-349.
[19] Knopoff L., *Proc. Natl. Acad. Sci. USA* **93** (1996) 3830-3837.
[20] Omori F., *J. Coll. of Science of Imper. Univ. of Japan* **7** (1894) 111-200.
[21] Utsu T., *Geophys. Mag.* **30** (1961) 521-605.
[22] Utsu T., *J. Faculty Science Hokkaido Univ. Ser. VII* **3** (1969) 129-195.
[23] Gardner J.K., Knopoff L., *Bull. Seismol. Soc. Amer.* **64** (1974) 1363-1367.
[24] Hauksson E., Jones L.M., Hutton K. and other, *J. Geophys. Res.* **98** (1993) 19835-19858.
[25] Yamashita T., Knopoff L., *Geophys. J. Roy. Astron. Soc.* **91** (1987) 13-26.
[26] Griggs D.T., Handin J., *Geol. Soc. Amer. Memoir* **79** (1960) 347-364.
[27] Knopoff L., Levshina T., Keilis-Borok V.I., Mattoni C., *J. Geophys. Res.* **101** (1996) 5779-5796.
[28] Yamashita T., Knopoff L., *Geophys. J. Roy. Astron. Soc.* **96** (1989) 389-399.
[29] Yamashita T., Knopoff L., *J. Geophys. Res.* **97** (1992) 19873-19879.

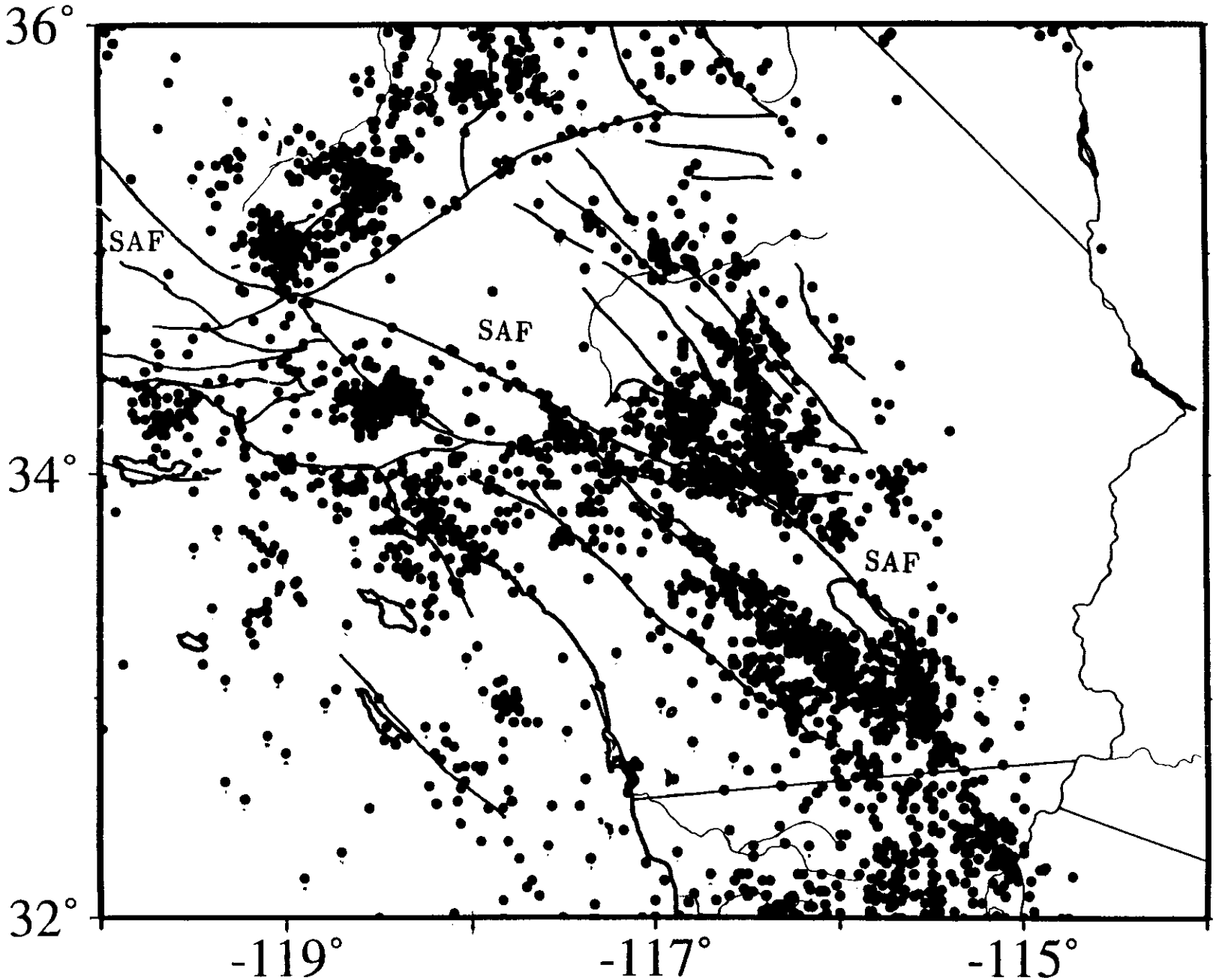
36°
34°
32°
-119°
-117°
-115°
SAF
SAF
SAF

Proc. Natl. Acad. Sci. USA
Vol. 93, pp. 3756–3763, April 1996
Colloquium Paper

This paper was presented at a colloquium entitled "Earthquake Prediction: The Scientific Challenge," organized by Leon Knopoff (Chair), Keiiti Aki, Clarence R. Allen, James R. Rice, and Lynn R. Sykes, held February 10 and 11, 1995, at the National Academy of Sciences in Irvine, CA.

A selective phenomenology of the seismicity of Southern California

L. KNOPOFF

Institute of Geophysics and Planetary Physics and Department of Physics, University of California, Los Angeles, CA 90024-1567

ABSTRACT **Predictions of earthquakes that are based on observations of precursory seismicity cannot depend on the average properties of the seismicity, such as the Gutenberg–Richter (G-R) distribution. Instead it must depend on the fluctuations in seismicity. We summarize the observational data of the fluctuations of seismicity in space, in time, and in a coupled space–time regime over the past 60 yr in Southern California, to provide a basis for determining whether these fluctuations are correlated with the times and locations of future strong earthquakes in an appropriate time- and space-scale. The simple extrapolation of the G-R distribution must lead to an overestimate of the risk due to large earthquakes. There may be two classes of earthquakes: the small earthquakes that satisfy the G-R law and the larger and large ones. Most observations of fluctuations of seismicity are of the rate of occurrence of smaller earthquakes. Large earthquakes are observed to be preceded by significant quiescence on the faults on which they occur and by an intensification of activity at distance. It is likely that the fluctuations are due to the nature of fractures on individual faults of the network of faults. There are significant inhomogeneities on these faults, which we assume will have an important influence on the nature of self-organization of seismicity. The principal source of the inhomogeneity on the large scale is the influence of geometry—i.e., of the nonplanarity of faults and the system of faults.**

The Magnitude-Frequency Law

Assume that our goal is the prediction of large earthquakes in a region as well studied as Southern California. Large earthquakes in Southern California occur so rarely that statistically based predictions of large earthquakes are not possible. We therefore try to limit the broad range of possible extrapolation scenarios that can be constructed from meager geological or geophysical observations with physics-based models. Before one can discuss efforts to model the physics of earthquakes, and especially of large earthquakes, one must appreciate the relevant phenomenology which must perforce form the targets of modeling efforts.

The extraordinary simplicity and universality of the familiar Gutenberg–Richter (G-R) power-law relation for the frequency of occurrence of earthquakes with a given energy has been a magnet for the statistical physics community, especially since power law relations also characterize the properties of magnetism, melting, etc., near critical points. The scale-independence of an empirical power law implies that the underlying physics is also to be found in scale-independent processes, and this course has been followed with much visibility and success in the model of self-organized criticality (1–8) and its application to the development of power-law relations for earthquakes.

The G-R power-law relation for earthquakes—the distribution of the number of earthquakes with seismic energy radiated greater than E,

$$N_{\text{cum}} \sim E^{-b/\beta} \qquad [1]$$

where b is the usual coefficient in the magnitude–frequency relation and is a number close to 1 for any region world wide (9, 10), and β is the coefficient in the radiated energy vs. magnitude relation, which has been measured to be 1.5 (11, 12), and has been calculated to be 3/2 for all but the largest earthquakes (13).

While the arguments for self-similarity are persuasive, there are even more persuasive arguments that the power-law relation cannot be extended to the largest energies and that large earthquakes obey different statistics and, hence, are subject to a different set of physical interrelationships than are small ones. Expression 1 cannot be extended indefinitely to infinite energies; otherwise the exponent $b/\beta \approx 2/3$ would imply that an infinite amount of energy be available from the motion of tectonic plates for the generation of earthquakes (14). Thus, there must be a cutoff or rolloff to the distribution at its large energy end. It follows that the occurrence of large earthquakes must take place under a different set of rules than the small ones. Thus, while the system is undoubtedly self-organizing, it is not self-organizing to a critical state.

There is also a power-law seismic moment–frequency relation with a similar exponent (15, 16). In the moment–frequency form, Eq. 1 describes the distribution of the product of the integrated final slip in the earthquake over the area of the rupture surface. Although the moment is written in energy units, it should not be considered to be anything other than a measure of slip, and thus this distribution is a constraint on the slip. By an argument similar to the above, we can show that the integrated slip rate on all earthquakes in the region cannot exceed the slip rate between the tectonic plates. Thus the moment distribution, too, must have a rolloff or cutoff.

It has been expressed frequently that the G-R law provides a basis for estimating seismic risk by extrapolating the statistics of small earthquakes to estimate the probability of occurrence of large ones (see ref. 17, for example). From the argument above, an extrapolation of this type can seriously overestimate the frequency of occurrence of large earthquakes. If the real distribution has a cutoff, its extrapolation may provide a finite estimate of the probability of occurrence of very large earthquakes that may never occur.

Because the G-R power-law distribution cannot be appropriate for large earthquakes, the properties of models of

The publication costs of this article were defrayed in part by page charge payment. This article must therefore be hereby marked "*advertisement*" in accordance with 18 U.S.C. §1734 solely to indicate this fact.

Abbreviations: G-R, Gutenberg–Richter; SAF, San Andreas fault.

seismicity on isolated faults that describe self-organization leading to a critical point may be irrelevant to our task. Because our concern is with the problems of large earthquakes, we try to understand why large earthquakes, and possibly others as well, fail to follow the power-law relation. We describe the phenomenological basis for developing an understanding of the physical processes that lead to the occurrence of large earthquakes.

We take as the basis for most of our discussions of phenomenology, observations of earthquakes in Southern California, which are the most extensive local data base we have, and thus the most studied of any history of instrumental seismicity. The magnitude–frequency relations for Southern California are reasonably well-established for the 60 yr of the Southern California catalog. The magnitude distribution of earthquakes in the Southern California catalog with aftershocks removed not only shows that the expected log-linearity for small magnitudes extends, most remarkably, up to the largest earthquakes (Fig. 1), excluding aftershocks. The 60-yr distribution of Fig. 1 does not show any hint of a deviation from linearity of the log-frequency vs. magnitude relation around $M = 6.4$ that has been proposed by a number of authors (13, 18–22) to correspond to a transition between two-dimensional and one-dimensional fracture shapes in a seismogenic zone of finite thickness. Despite the reasonableness of the proposal that it is the thickness of the seismogenic zone, which is of the order of 15 km in Southern California, that provides this characteristic dimension, contrary to recent assertions (21), the sharp cutoff to the distribution near $M = 7.5$ and the absence of a rolloff at smaller magnitudes does not support the simplistic proposal. A similar conclusion has been reached from a study of the energy–frequency distribution (23).

Excluding aftershocks, the statistics of the smallest earthquakes, which are by inspection the most numerous, is Poissonian (24); this does not imply that the less frequent stronger earthquakes are also randomly occurring events.

Large Earthquakes

Despite the presence of a cutoff to the distribution in Fig. 1 for the most recent 60 yr, we know that earthquakes with magnitudes greater than $M = 7.5$ occur in Southern California on a longer time scale, as for example the great Fort Tejon earthquake of 1857 on the San Andreas fault (SAF) in this region. Ten prehistoric earthquakes with large slips, and hence presumably with large magnitudes, have been identified by geochronometric methods between 671 ± 13 A.D. and 1857;

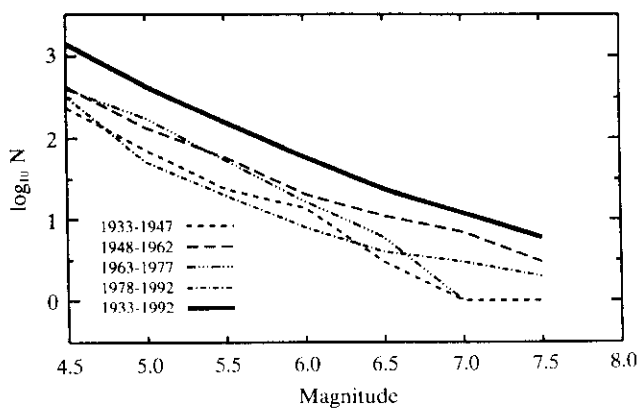

FIG. 1. Number of earthquakes in Southern California as a function of magnitude for the interval 1935–1994 in intervals of 0.5 magnitude units (upper curve). Lower curves are the subdivision into 15-yr intervals. Aftershocks have been removed from the distributions (from ref. 42).

the interval times range from roughly 50 to 330 yr, with a mean of about 135 yr (25, 26).

Because the form of the distribution of large earthquakes cannot depend on the power-law statistics of small earthquakes and appears to depend on events that have not happened within the time span of the catalog, we have no seismographic information to bear on this point. We approach the problem of the distribution of large earthquakes from a different point of view. Because the fracture length and the energy released in a large earthquake are roughly related, we assume that the distribution of fracture lengths also has a cutoff or rolloff. If it has a rolloff, then there is a finite probability that a fracture will occur whose length will extend completely across a region as large as Southern California. It has been argued that the fractures in the largest earthquakes are confined by relatively fixed barriers to the extension of growth (27) that may be associated with fault geometry. In this model, these characteristic fault segments have characteristic slips in large earthquakes. But a process of repeated slip between strong barriers must ultimately accumulate stress at the barrier edges, and the barriers in this model must ultimately break as well; under the constraint of a long-term average uniform slip rate at every point in a plate boundary, barriers cannot remain unbroken forever. Thus the stresses at the barriers must ultimately relax, either by fractures in even stronger earthquakes or by some (generalized) viscous relaxation. If the process is viscous, then the relationship between the time constants for stress relaxation and for loading the system becomes important. In most modeling exercises, the restricted view is taken that viscous stress relaxation is extremely slow and, hence, that even long-term stress relaxation can take place by brittle fracture.

If one barrier must ultimately break, does it follow that sooner or later *all* barriers within a given region must break in the same earthquake, if only we wait long enough? It is sufficient to apply this question to the faults that support the largest of the earthquakes, which are those that occur on the SAF. Hence our question really refers to earthquakes that have not happened in the catalog interval of the most recent 60 yr. If earthquakes on the SAF are stopped according to the same processes as the smaller earthquakes—namely, because of encounters with strong barriers with low stored prestress, then, since all points on an individual plate boundary such as the SAF must sooner or later break, sooner or later two adjacent barriers may reach a nearly threshold state at about the same time—i.e., their prestresses must be close to their strengths at the same time. If this is the case, then, on the model that a stress at the edge of a crack is scaled by the length of the crack, one barrier must surely be triggered into fracture by a rupture on an adjacent barrier and, hence, a superearthquake will be developed.

But this model is valid under the assumption that the earth is homogeneous. The barrier property of the characteristic earthquake model argues for a weaker region of the faults in the reaches between barriers and, hence, that the appropriate scaling distance for redistribution of stress is the size of the nucleation zone of these greatest earthquakes—i.e., the barrier dimension, rather than the length of the crack. Observational support for this point of view is to be found in the self-healing pulses observed in the dynamics of the rupture process described by Heaton (28). We argue in a companion paper (29) that a smaller scaling length is sufficient to prevent an earthquake from tearing through several barriers, if the barriers are widely spaced compared to the scaling distance for the size of the fluctuations in stress outside the edge of the crack and for a sufficiently large ratio between the fracture strengths of the barriers and the relatively smoother segments between them. The scaling distance is the size of the nucleation zone or it is the size of the self-healing pulse, and these two sizes may be the same (30).

Because the largest earthquakes do not fit the G-R distribution and are most likely limited in fracture length by barriers, the characteristic earthquake model is probably appropriate for their description. There is very likely a sharp cutoff to the distribution of earthquake sizes. If it were not for information derived from the spatial distributions of smaller earthquakes, we would be inclined to suppose that it would not be appropriate to describe smaller earthquakes by the characteristic earthquake model because the smaller events are dominated by the G-R distribution, and hence these events may be strongly influenced by the processes of self-organization. But to be able to draw a clearer opinion, we must describe the spatial distributions of earthquakes in Southern California.

Spatial Fluctuations

The epicenters of the earthquakes that define the G-R law for Southern California are widely distributed over the entire area (Fig. 2). If the G-R law and other features of the seismicity are properties of earthquakes in two dimensions, is it appropriate to try to simulate these features by modeling faulting in one dimension, as has been the vogue in recent years? If we are successful in simulating seismicity on a single fault, can these simulations be related to seismicity in two dimensions?

With regard to the G-R law, there is no convincing evidence that the hypocenters of small earthquakes, other than aftershocks, have a well-defined geometrical relationship to the mapped faults, or to buried faults for that matter. The seismicity on a number of mapped faults, including the SAF, is essentially nil over the 60-yr interval, an observation not inconsistent with the proposal above that the earthquakes on the faults that support large earthquakes have different statistical properties than the earthquakes on fault structures that support small ones. In the case of the SAF, there is an extraordinary absence of activity on the segment of the SAF that ruptured in the 1857 earthquake, down to magnitudes less than 3 (31). The Salton segment of the southernmost part of the SAF is also dormant (31, 32). Indeed, "no large earthquake ($M \geq 7.0$) has been documented in the historic record (since 1749) for the SAF south of Cajon Pass" (32). These observations imply, as already indicated, that efforts to synthesize a power-law distribution *on a single major fault* such as the SAF are inappropriate. An important feature of the seismicity in Southern California is that the major part of the SAF and other faults on which large earthquakes can occur are quiet at the present time and that very likely they will only slip in great earthquakes (33–35).

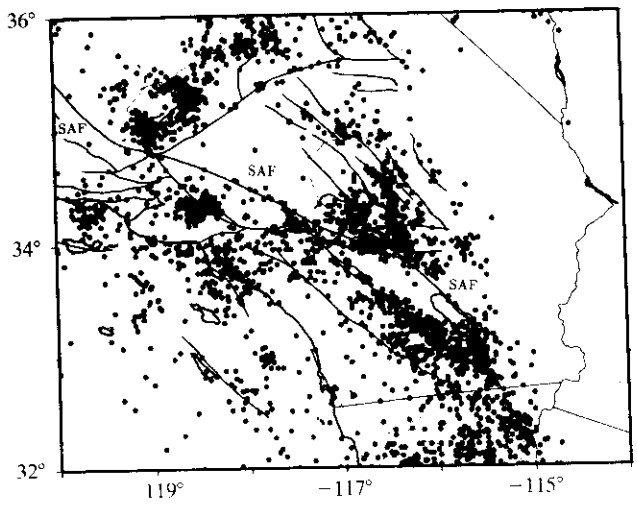

FIG. 2. Epicenters of earthquakes in Southern California with magnitudes greater than 3.5 in the inclusive interval 1935–1994. Aftershocks have not been deleted. Most of the clusters of epicenters are due to aftershocks of large earthquakes. The SAF is indicated.

Not only are the earthquakes that define the G-R distribution widely distributed in two dimensions but also the epicenters of the largest earthquakes of the past 80 yr with magnitudes near the cutoff in the instrumental distribution at $M = 7.5$ are also widely distributed two-dimensionally over Southern California, and all are located on faults other than the SAF. The 23 earthquakes with $M_w \geq 6.4$ since 1915 fall into two mutually exclusive categories: To the north and west of a line extending between the epicenters of the 1933 Long Beach and the 1993 Landers earthquakes, all of the focal mechanisms of the eight earthquakes are not strike-slip; while to the south and east of this line, all of the 15 earthquakes including the Long Beach and the Landers earthquakes have strike-slip focal mechanisms (36); most of the earthquakes in the southeastern region are located on the San Jacinto fault and its prolongation. The horizontal component of the slip on the nonstrike slip earthquakes in the northern part of the region is parallel to the plate motions. But since these earthquakes lie off the plate boundary, sooner or later the locked section of the SAF must also tear in a great earthquake with a component of slip parallel to the plate motions.

We have no way of knowing whether the absence of activity on the SAF, except for the largest earthquakes, is a condition that is likely to persist. The punctuation of activity on the SAF by relatively more frequent large earthquakes off the fault may be a steady process. Although it is possible that there might be a shift in style of seismicity from one that favors exclusivity of large earthquakes to one that favors a broad distribution of sizes on the SAF, some numerical simulations of seismicity on single faults with configurations of fracture thresholds that have been designed to favor the characteristic earthquake model have exhibited abrupt changes in size of earthquakes by factors that are much smaller than the range demanded by these speculations.

Large earthquakes on neighboring faults produce significant fluctuations in stress on the SAF and vice versa and influence the mode of self-organization under the conditions of stress redistribution. Simulations on a model of a single fault with spatially variable strengths, especially designed to simulate the influence on seismicity of strong barriers, lead to the strongest earthquake events that have a great regularity (37, 38). The large variability in the interearthquake times of the strongest earthquakes (26) on the SAF has, however, been modeled in a restricted sense by the study of seismicity on a pair of interacting faults; these have variations in the time intervals between large earthquakes by as much as the factor of 6 observed. While the demonstration of large variable interearthquake times through a model of a pair of interacting faults is not an adequate representation of interactive fault coupling on a model of the network of faults in Southern California, it is a genuine indication that simulations on single fault models are observed to be inadequate vehicles for the study of seismicity in a region with as complex a fault geometry as that of Southern California. Thus the modeling of fractures on the major units of the fault system must take into account coupling between the members of a two-dimensional web of faults through interactive stress transfer.

The modeling of seismicity on a network of faults as numerous as those in Southern California may not be a tractable problem, even with extraordinarily large computing resources. Although the time scale for the largest earthquakes on the SAF which is of the order of 135 years, with a variation that spans a factor of 6 [modeled with a truncated exponential distribution (29)], the time scale for the recurrence of earthquakes on the other faults of this region may be much longer. Sieh (39) has found that the last preceding earthquake on much of the fault complex that ruptured in the 1992 Landers ($M = 7.3$) event took place 6000 to 9000 yr before the present.

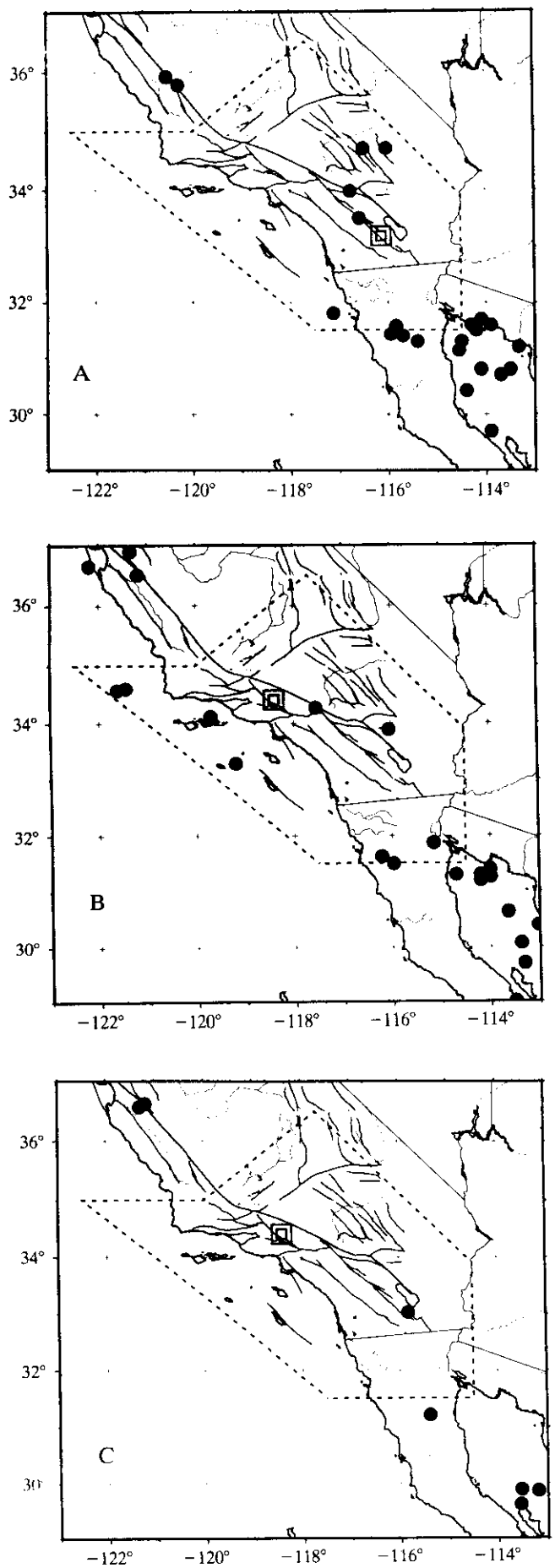

Assume the time scales for large earthquakes on faults other than the SAF are of the order of only 2000 yr. Assume, for the sake of argument, that $M = 7$ earthquakes occur 10 times as frequently as $M = 8$ earthquakes, using a factor taken from a convention that we have already argued against. Assume all of the $M = 7$ earthquakes do not take place on the SAF and all of the $M = 8$ events do take place on it. If we scale the rates of recurrence of individual earthquakes on the two classes of faults by a factor of 20, being the ratio between 2000 yr and 100 yr, we find that there are roughly 200 times as many fault segments that support $M = 7$ earthquakes as the SAF, which supports $M = 8$ earthquakes. We conclude that the SAF ruptures much more frequently than any other fault in the network, at least among the panoply of faults that support strong earthquakes, but that there are many such fault segments. The probability of a strong earthquake occurring on any specific fault other than the SAF is finite but small; the probability of occurrence of a strong earthquake with magnitude $M = 7$ is significantly higher than that of an earthquake with $M = 8$. The modeling demands are stupendous, especially in view of the fact that mapping has not yet identified most of the faults that support strong earthquakes of the Northridge or Landers types, in a network that we estimate to include as many as several hundred faults. A statistical model of rupture on a large network in two dimensions will be needed.

Small Earthquakes: "The G-R or Characteristic Earthquake Distribution, Which Is It?"

The title of this section reproduces the title of a paper by Wesnousky (40). We have proposed that the largest earthquakes are ruptures that take place on massively inhomogeneous faults. We return to the issue whether the smaller earthquakes, which fit the G-R distribution, belong to a distinct class of events from that of large ones, with an independent set of statistical rules, or whether there is a more complicated interaction. We offer the following speculations.

Consider the following extreme model. Aftershocks of individual strong earthquakes fit the Omori law in its simplest form $n \sim t^{-p}$ with $p \approx 1$. The aftershocks also fit the G-R distribution well with the usual exponent. Formally there is a small but finite probability of having an aftershock a very long time after a strong earthquake because of the infinite tail of the function. On this model, small earthquakes near New Madrid, MO, and Charleston, SC, today might be aftershocks of the earthquakes of 1811–1812 and 1886. If this is the case, the risk of strong earthquakes is small in the foreseeable future in these areas since aftershocks are windows to the past, rather than to the future. The rate of occurrence of the number of aftershocks in these regions appears to be more or less constant at the present time because of the long interval since these strong parents. Up to the present time, shocks in the vicinity of the Kern County, CA, earthquake of 1952 and the San Fernando earthquake of 1971 appear to be consistent with the Omori law, even 40+ yr after the Kern County event. In our description of the G-R distribution (Fig. 1), we have excluded aftershocks on a nominal basis through the use of a formula that looks for satellite earthquakes within a specified time and space window after a strong event *in the catalog*. If the Omori

FIG. 3. (*A*) Epicenters of earthquakes in Southern California with magnitudes between 5.1 and 6.3 from January 1, 1965, to April 9, 1968, which is the date of the Borrego Mountain ($M = 6.5$) earthquake; the epicenter of the ($M = 6.5$) earthquake is indicated by the double square. (*B*) Same as *A* for the interval April 9, 1968, to February 9, 1971; the latter is the date of the San Fernando ($M = 6.6$) earthquake. The epicenter of the San Fernando earthquake is shown by the double square. (*C*) Same as *B* for the 2 yr after the San Fernando earthquake, February 9, 1971, to February 8, 1973 (from ref. 42).

and G-R laws hold for a long time after the parent, then how many earthquakes in the Southern California catalog are in reality aftershocks of strong events that took place before the start of the catalog? If the Omori law is taken literally, then are all of the earthquakes that constitute the observations of the G-R distribution today aftershocks of past strong events(?). Since aftershocks depend on the existence of a mechanism for providing for a time delay between the main, strong shock and the aftershock, any model that purports to describe seismicity in a region such as Southern California and uses the G-R law as a paradigm must include a mechanism for time delays—i.e., some nonelastic stress transfer. Under this assumption, the G-R law does not tell us anything about future seismicity since aftershocks only refer to the past history of strong shocks.

However, today there are no significant aftershocks of the 1857 earthquake on the SAF. Thus at least for SAF earthquakes, the Omori law does not have an infinite tail, and there is a temporal cutoff for aftershocks. We speculate that the map of Southern California seismicity, which is dominated by the smallest earthquakes (Fig. 2), shows that some faults can produce long-term and others only short-term aftershocks. It is likely that we should not assume that all earthquakes in Southern California can be modeled under the same set of physical rules. Thus, we conclude that the relationship between the present-day small earthquakes that define the G-R law and future large earthquakes on the major faults is ill-defined; there exists the possibility that there is no relationship between present small and future large earthquakes.

Assume that the smaller earthquakes do not take place on the same fault structures as the larger ones. Then, except in unusual circumstances, the two populations of small and large earthquakes have independent distributions; we can assume that the smaller events fit the G-R law, and the larger ones have their own distribution, whatever that may be. If large mapped faults, or faults that are large enough to be mapped, are reserved for big earthquakes, then where do the small ones take place? The process zones at the tips of cracks are regions of highly deformed and/or broken material. As a fault grows, it must certainly grow through its own process zone. Thus we expect that the entire length of all faults must be surrounded by a zone of weakened material. Under an increasing tectonic stress, this zone will slip in small earthquakes. Irregular slip in large earthquakes on the nearby fault surface could cause fluctuations in stress that could trigger aftershocks in the adjoining process zone; aftershocks can thus occur along the entire length of a large earthquake, both in the process zone nearby and in the process zone beyond the ends of the crack by the more conventional mechanism of stress intensification. Thus small earthquakes with rupture lengths that are most frequently, but not necessarily, less than the thickness of the process zone occur in an elongated three-dimensional zone astride the fault. Hence, the distribution of small earthquakes on this model is characterized by the distribution of sizes of contacts where slips might take place in a three-dimensional space and might have different focal mechanisms, as well as different spatial locations, than the larger earthquakes, consistent with our conjecture.

If small and large earthquakes have different temporal distributions, why does the projection of the distribution for small earthquakes in Southern California extend almost perfectly into the magnitude range of the largest earthquakes in the past 60 yr, only to be truncated by an abrupt cutoff (Fig. 1)? Suppose that we divide Southern California into smaller seismic zones that each includes at least one fault that supports large earthquakes. Assume each zone will have its own G-R law for small earthquakes and that the exponent is the same for each. But the cutoff (or rolloff) will depend on the properties of the dominant fault in the zone, and especially its length, and we can expect that it will be different for each region. The sum of the seismicity distributions over all zones will give the seismicity for all of Southern California; the spatially cumulative distribution will have the usual power-law relation for small earthquakes with the usual exponent; but the rolloff for the spatial sum distribution will reflect the distribution of cutoffs (or rolloffs) for the zones. Because the summation seismicity has a sharp cutoff (Fig. 1), then either the distributions for each of the zones must have the same cutoff, which seems very unlikely, or the distributions at the large magnitude ends must vary widely, with some of the zones having a rate for large earthquakes that is greater than the extrapolation of the seismicity from the simple power-law relation, and some less than it. Thus the properties of the large earthquakes differ significantly from the G-R law for small earthquakes in each zone, and hence the small and large earthquakes interact differently. On the last model, the sharp cutoff in Fig. 1 is a coincidence.

Of course, there is always the argument that the distribution in Fig. 1 is based only on two earthquakes in the magnitude range 7.25–7.75 and, hence, the uncertainties are so large that the apparent sharp cutoff is a statistical fluctuation itself. In either case, one cannot say much about the validity of extending the G-R curve out to the largest magnitudes.

Space–Time Fluctuations

We have argued that the G-R law, which describes small earthquakes, excluding aftershocks, over a 60-yr period in Southern California, cannot be used directly to predict large earthquakes. However if the distribution is temporally variable or it is not Poissonian, fluctuations in the magnitude–frequency law might give possible indications of forthcoming large earthquakes. Fluctuations are indeed found on a time scale of 15 yr, in the magnitude range of 4.8–6.2 approximately, that are significant at the 2σ level (Fig. 1). Jones has also identified that there was a significant increase in the rate of occurrence of earthquakes with $M \geq 5$ in Southern California by a factor of two over the interval 1986–1992 in comparison with the rate over the 40 yr preceding 1986 (41). On the time scale of the order of 1–10 yr, there is an increase in the rate of occurrence of earthquakes with magnitudes greater than 5.1 before all of the strongest earthquakes in California with magnitudes $M \geq 6.8$ (42). It is doubtful whether these fluctuations in seismicity might be useful for earthquake prediction on the above time scale, because their space scale is so large, being of the order of the size of Southern California. No detailed exploration has been made as yet to see if similar fluctuations are to be found for smaller magnitudes, at shorter distances, and over shorter time intervals before strong earthquakes with magnitudes less than 6.8.

We have listed above nonuniform properties of earthquake occurrence that includes observations that (*i*) the rate of occurrence of the strongest earthquakes differs from the extrapolations of the G-R law for small earthquakes, (*ii*) there is long-term spatial quiescence at all magnitudes on the faults that support the largest earthquakes, (*iii*) there are fluctuations in the interval times between the strongest earthquakes on the SAF, and (*iv*) there are temporal fluctuations of intermediate-magnitude seismicity. We mention briefly the phenomenology of fluctuations that are coupled in space and in time. Kanamori (43) has given an excellent review of space–time-coupled fluctuations: quiescence or reduced activity has been identified prior to 41 very strong earthquakes worldwide out of a list of 52 earthquakes, over a time scale of a few months to as much as 30 yr, and over distance scales that are usually of the order of the dimensions of the fracture of the strong earthquake. Wyss and Habermann (44) have identified 17 cases of earthquakes that preceded by seismic quiescence on time scales of the order of 1 to 6 yr and distance scales of the order of the size of the fracture length in the strong earthquake. These examples include several earthquakes in Southern California.

Of particular interest is the case history of quiescence before both the Landers and the Big Bear earthquakes (45). A 75% to 100% reduction in the seismicity of small earthquakes took place within a space of dimensions of 10–20 km adjoining or astride the faults and extending for 4.5 yr and 1.6 yr before these earthquakes.

In a small number of cases of Japanese earthquakes, a contemporaneous local reduction and a distant increase of seismicity have been noted (46). Knopoff *et al.* (42) have described an increase in intermediate-magnitude seismicity to distances of the order of several hundred km before all 11 documentable earthquakes with magnitudes ≥6.8 in California over a time scale of the order of 1–10 yr as noted; the increase in activity ceases abruptly after selected strong earthquakes. Although stress redistributions are expected on the scale size of the fractures, these latter observations (42) are notable in two respects: (*i*) The precursory episode of increase of distant earthquakes terminates abruptly. (*ii*) The distances spanned by the precursor earthquakes is much larger than the classical scale size of the fracture in the strong earthquakes, thereby implying a much larger range of interactions than possible from standard elastic models of fracture. An example of remote prior increase in activity and subsequent rapid extinction associated with the smaller San Fernando earthquake (M = 6.6) of 1971 is shown in Fig. 3. The epicenters of earthquakes with magnitudes between 4.7 and 6.3 between 1965 and the date of the earthquake in 1972 are shown in two 3-yr stages; a remarkable decrease in the number of such earthquakes in the following two years is seen to extend over distances from the epicenter of the San Fernando earthquake, which are at least an order of magnitude larger than the size of its fracture dimensions (42). There does not appear to be any change in the level of activity before and after the Borrego Mountain earthquake (M = 6.5) 3 yr earlier.

In most cases, the anomalous precursory seismicity is widespread in two dimensions, and arguments for or against intermediate-term clustering in space and time, as well as any attempt to understand the mechanism for such clustering, must depend on the construction of a model of regional faulting that consists of a two-dimensional network of faults.

Stress Fluctuations and the Fracture Process

If the self-organization of seismicity is a response to the redistribution of stress by earthquake fractures, the final stress field after a fracture represents an initial state for the next fracture on the same fault segment and in its neighborhood; the stress field depends as well on the increase of stress by the tectonic load and the changes due to subsequent fractures in the neighborhood. Thus, the conditions of the fracture in the dynamic episode of "fast time" is a strong determinant of the times and locations of future earthquake events. The details of the rupture in an individual fracture depend on a number of parameters that include the friction on the fault, the degree of spatial inhomogeneity of the fracture threshold, and the aforementioned spatial distribution of prestress. Some information that bears on these points can be inferred from observations of earthquake occurrence. We cite a part of the list.

(*i*) From the focal mechanisms of small earthquakes in the neighborhood, we learn that the stress field along large parts of the extent of the SAF is oriented so that the principal compressional stress is normal to the fault (47). This orientation is a rotation from the expectation for an elastic continuum in which the component of the stress field on the SAF should be a shear field parallel to the tectonic load stress. This observation implies that much of the fault has a low fracture strength or coefficient of static friction, and, hence, that the strength of much of the SAF has not been restored to a fully healed value after the most recent major rupture.

(*ii*) The stress drops in Southern California earthquakes are highly variable quantities, ranging by a factor of from 300 to 400, from values less than 1 bar to more than 300 bars, as determined from the ratio between the seismic energy radiated and the seismic moment E_S/M_o, this ratio itself being proportional to the ratio σ/μ of the stress drop to the shear modulus, *for a homogeneous earth and fracture model.* On the high side, a value of about 300 bars has been reported for the Landers earthquake (48). Low values are found for small earthquakes on the San Jacinto fault (49). This quantity has been tabulated for almost 500 earthquakes worldwide (49–53), including 22 in Southern California, and for these, the ratio E_S/M_o is also highly variable. Kanamori *et al.* (50) propose that the faults in Southern California that undergo more frequent rupture, such as the SAF and the San Jacinto fault, tend to have much lower stress drops than do the faults that support less frequent events, implying that the healing process is gradual. On this interpretation, only small amounts of stress are stored in the fault zone in the time interval between SAF and San Jacinto fault earthquakes, over the time scale of repetition, and is a result that is not inconsistent with the observation of Zoback *et al.* (47) (see above).

(*iii*) Bullard (54) suggested that the frictional heat developed in great earthquakes should be enough to melt rocks in the vicinity of major earthquake faults in some tens of millions of years (and hence that earthquakes should no longer occur on old fault structures), and hence one ought to see an elevated heat flow along the major faults of the world. Measurements of heat flow along the SAF and several other major faults of Southern California indicate that the heat flow along the faults is not greatly elevated over the regional average (55–58), suggesting that the friction during sliding is low. There are at least two explanations: either the faults have been weakened significantly by the dynamics of the rupture event itself, or they have been weak for some time both before and during the ruptures (56).

In the first case, which is the proposal that the fault is weakened due to the dynamics of the event in fast time, melting during sliding was proposed early, but this model can be rejected because it implies high friction and a high level of residual heat. Brune *et al.* (59) have proposed that the heat flow paradox can be explained by assuming that a dynamical mode of slip on the fault exists that involves interface separation of fault contacts that has a traveling wave property in the wake of the rupture front, thereby reducing the sliding friction. It is not known if this model can be successful if the fault has strong inhomogeneity; the nature of the propagation of interface waves of separation in the presence of inhomogeneities of stress drop has not been studied.

The second alternative asks whether an inhomogeneous distribution of strength thresholds, frictions, and stress drops along the fault can be consistent with the heat flow paradox, as well as with seismological observations. In Kanamori's (43) asperity model, most of the deformational energy released in an earthquake is accumulated at a localized high strength node or asperity before the earthquake. The asperity is bounded by zones of very low strength; slip generated at the asperity then spreads easily through the region of low strength. In this model the average stress drop can be small because the regions of low stress drop can be large; the fracture length is large, being the sum of the lengths of the adjoining regions and the central asperity; thus the ratio of energy to moment can be low. High heat will be generated only in the zones of high stress drop, which are the asperities, and the heat flow has an average over the fault that is constrained by the friction on the low-friction patches that adjoin the site of nucleation.

Support for a model of inhomogeneous fracture is to be found in the following observations:

(*iv*) Heaton (28) has observed self-healing pulses of slip in large earthquakes; these are propagating patches of slip that

imply a reduction in the scale length of fracture, as indicated above; the best-documented example of self-healing patches of slip is the inversion for the slip in the Landers earthquake (60). It can be shown that self-healing slip pulses of constant duration require a critical scaling dimension for their generation. Cochard and Madariaga (30) have argued persuasively that the critical scale size is given by the dimensions of a nucleation zone, which we equate with an asperity. In this model, the pulse generated at the asperity breaks into a region of lower stress drop, wherein its velocity of growth attenuates, slip begins to diminish, and ultimately a velocity-dependent friction that is intrinsic to the healing process causes ultimate cessation of motion.

(v) The earthquakes studied by Heaton (28, 60) show significant irregularities of the slip distributions in the rupture plane, which indicate the presence of significant inhomogeneity of stress drop and/or fracture threshold in the plane. The slip at the surface in the Landers earthquake of 1992 has been studied in detail in the field (60–62) and over the entire plane by inversion of the seismic signal (60, 63, 64). Of particular interest is the presence of time delays of about 1–3 sec between termination of rupture on one strand of the fault and initiation of rupture on a neighboring strand (60, 63, 64). These time delays between rupture of successive strands of the large fracture can be accounted for by inhomogeneity of the fracture threshold or the stress drop, or both, as well as by a slip-weakening in slow time, over the time interval of the time delay, of the strength in the high-stress drop barriers.

Summary

We summarize these observations on the seismicity of Southern California as follows. Not all faults in Southern California behave in the same way statistically. For example, the SAF today supports large earthquakes only and does not support small ones. Hence an effort to apply a universal model that yields the G-R statistical law is doomed to failure.

The G-R law is valid for small earthquakes but not for large ones. The G-R law is a manifestation of seismicity over the entire area of Southern California. Thus efforts to model the power-law character through a process of self-organization on a single fault is misdirected. The power law is probably a manifestation of the distribution of little faults and/or aftershocks in two dimensions—i.e., it is a manifestation of the geometry of faulting in Southern California.

Although we do not know what the distribution for large earthquakes is, the distribution for large earthquakes on faults other than the SAF is likely to show large spatial fluctuations. Large earthquakes on the SAF occur more frequently than large earthquakes on any other major fault in Southern California; the SAF is the most rapidly slipping element of the fault network but may be slipping under conditions of low average stress drop—i.e., a small energy-to-moment ratio.

The temporal distribution of earthquakes must be dependent on the limitations of fracture size. What stops the growth of a fracture is the encounter of a growing crack with a barrier region, which is a zone of large stress drop. If the large stress drops are localized, the earthquake ruptures are confined, and the characteristic earthquake model is appropriate. Localization is possible where significant changes in the geometry of faulting are encountered, such as at sites of step-overs (echeloning) or bifurcations (fault junctions). Under the constraint of uniform average rate of moment release, strong barrier sites must themselves break or the stresses at these sites must relax. Not only is geometry on a network of faults likely to be important for the modeling enterprise, but also the geometry of individual faults is going to lead to fluctuations in strength, in rapidity of restoration of strength (suturing) after a big earthquake. These geometrical fluctuations are likely to lead to nonuniformity of slip. Temporal fluctuations in seismicity imply the importance of time-dependent stress transmission processes, such as those associated with creep. Probably the most alluring proposal for intermediate-term earthquake prediction is the idea that local quiescence of small earthquakes develops near the site of a future strong earthquake and that intermediate magnitude activity increases at distance from the future earthquake. The most likely candidate for modeling the fluctuations in stress drops and fracture thresholds is an asperity model for individual earthquakes and a barrier model that accounts for the complexity of the fault network.

This research was supported by a grant from the Southern California Earthquake Center. This paper is publication number 4621 of the Institute of Geophysics and Planetary Physics, University of California, Los Angeles, and is publication number 322 of the Southern California Earthquake Center.

1. Bak, P. & Tang, C. (1989) *J. Geophys. Res.* **94,** 15635–15637.
2. Nakanishi, H. (1990) *Phys. Rev. A* **41,** 7086–7089.
3. Nakanishi, H. (1991) *Phys. Rev. A* **43,** 6613–6621.
4. Christensen, K. & Olami, Z. (1992) *J. Geophys. Res.* **97,** 8729–8735.
5. Christensen, K. & Olami, Z. (1992) *Phys. Rev. A* **46,** 1829–1838.
6. Christensen, K., Olami, Z. & Bak, P. (1992) *Phys. Rev. Lett.* **68,** 2417–2420.
7. Olami, Z., Feder, H. J. S. & Christensen, K. (1992) *Phys. Rev. Lett.* **68,** 1244–1247.
8. Olami, Z. & Christensen, K. (1992) *Phys. Rev. A* **46,** 1720–1723.
9. Gutenberg, B. & Richter, C. F. (1944) *Bull. Seismol. Soc. Am.* **34,** 185–188.
10. Gutenberg, B. & Richter, C. F. (1954) *Seismicity of the Earth* (Princeton Univ. Press, Princeton, NJ).
11. Gutenberg, B. & Richter, C. F. (1956) *Ann. Geofis.* **9,** 1–15.
12. Gutenberg, B. (1956) *Q. J. Geol. Soc. London* **112,** 1–14.
13. Kanamori, H. & Anderson, D. L. (1975) *Bull. Seismol. Soc. Am.* **65,** 1073–1095.
14. Knopoff, L. & Kagan, Y. (1977) *J. Geophys. Res.* **82,** 5647–5657.
15. Kanamori, H. (1977) *J. Geophys. Res.* **82,** 2981–2987.
16. Hanks, T. C. & Kanamori, H. (1979) *J. Geophys. Res.* **84,** 2348–2350.
17. Turcotte, D. L. (1990) *Global Planet. Change* **3,** 301–308.
18. Rundle, J. B. (1989) *J. Geophys. Res.* **94,** 12337–12342.
19. Romanowicz, B. (1992) *Geophys. Res. Lett.* **19,** 481–484.
20. Romanowicz, B. & Rundle, J. B. (1993) *Bull. Seismol. Soc. Am.* **83,** 1294–1297.
21. Pacheco, J. F., Scholz, C. H. & Sykes, L. R. (1992) *Nature (London)* **355,** 71–73.
22. Okal, R. & Romanowicz, B. A. (1994) *Phys. Earth Planet. Inter.* **87,** 55–76.
23. Sornette, D., Knopoff, L., Kagan, Y. & Vanneste, C. (1996) *J. Geophys. Res.*, in press.
24. Gardner, J. K. & Knopoff, L. (1974) *Bull. Seismol. Soc. Am.* **64,** 1363–1367.
25. Sieh, K. E. (1978) *J. Geophys. Res.* **83,** 3907–3939.
26. Sieh, K., Stuiver, M. & Brillinger, D. (1989) *J. Geophys. Res.* **94,** 603–623.
27. Schwartz, D. P. & Coppersmith, K. J. (1984) *J. Geophys. Res.* **89,** 5681–5698.
28. Heaton, T. H. (1990) *Phys. Earth Planet. Inter.* **64,** 1–20.
29. Knopoff, L. (1996) *Proc. Natl. Acad. Sci. USA* **93,** 3830–3837.
30. Cochard, A. & Madariaga, R. (1994) *Pure Appl. Geophys.* **142,** 419–445.
31. Sieh, K. E. & Williams, P. L. (1990) *J. Geophys. Res.* **95,** 6629–6645.
32. Jones, L. M. (1988) *J. Geophys. Res.* **93,** 8869–8891.
33. Raleigh, C. B., Sieh, K. E., Sykes, L. R. & Anderson, D. L. (1982) *Science* **217,** 1097–1104.
34. Lindh, A. G. (1983) *U.S. Geol. Survey Open File Rep.* **83–63.**
35. Sykes, L. R. & Nishenko, S. P. (1984) *J. Geophys. Res.* **89,** 5905–5927.
36. Press, F. & Allen, C. R. (1995) *J. Geophys. Res.* **100,** 6421–6430.
37. Knopoff, L. (1993) *Proc. Am. Philos. Soc.* **137,** 339–349.
38. Knopoff, L. & Ni, X. X. (1995) in *Impact, Waves and Fracture*, eds. Batra, R. C., Mal, A. K. & MacSiphigh, G. P. (Am. Soc. Mech. Eng., New York), pp. 175–187.

39. Sieh, K. (1996) *Proc. Natl. Acad. Sci. USA* **93,** 3764–3776.
40. Wesnousky, S. G. (1994) *Bull. Seismol. Soc. Am.* **84,** 1960–1970.
41. Jones, L. M. (1994) *Bull. Seismol. Soc. Am.* **84,** 892–899.
42. Knopoff, L., Levshina, T., Keilis-Borok, V. I. & Mattoni, C. (1995) *J. Geophys. Res.* **101,** 5779–5796.
43. Kanamori, H. (1981) *Earthquake Prediction: An International Review*, eds. Simpson, D. W. & Richards, P. G. (Am. Geophys. Union, Washington, DC), pp. 1–19.
44. Wyss, M. & Habermann, R. (1988) *Pure Appl. Geophys.* **126,** 319–332.
45. Wiemer, S. & Wyss, M. (1994) *Bull. Seismol. Soc. Am.* **84,** 900–916.
46. Mogi, K. (1969) *Bull. Earthquake Res. Inst., Tokyo Univ.* **47,** 395–417.
47. Zoback, M. D., Zoback, M. L., Mount, V., Eaton, J., Healy, J., *et al.* (1987) *Science* **238,** 1105–1111.
48. Kanamori, H., Thio, H.-K., Dreger, D., Hauksson, E. & Heaton, T. (1992) *Geophys. Res. Lett.* **19,** 2267–2270.
49. Kanamori, H., Mori, J., Hauksson, E., Heaton, T. H. & Hutton, L. K. (1993) *Bull. Seismol. Soc. Am.* **83,** 330–346.
50. Vassiliou, M. S. & Kanamori, H. (1982) *Bull. Seismol. Soc. Am.* **72,** 371–388.
51. Kikuchi, M. & Fukao, Y. (1988) *Bull. Seismol. Soc. Am.* **78,** 1707–1724.
52. Houston, H. (1992) *Geophys. Res. Lett.* **17,** 1413–1417.
53. Choy, G. L. & Boatwright, J. L. (1995) *J. Geophys. Res.* **100,** 18205–18228.
54. Bullard, E. C. (1954) in *The Earth as a Planet*, ed. Kuiper, G. P. (Univ. of Chicago Press, Chicago, IL), pp. 57–137.
55. Henyey, T. L. & Wasserburg, G. J. (1971) *J. Geophys. Res.* **76,** 7924–7946.
56. Lachenbruch, A. H. & Sass, J. H. (1980) *J. Geophys. Res.* **97,** 6185–6222.
57. Lachenbruch, A. H. & Sass, J. H. (1988) *Geophys. Res. Lett.* **15,** 981–984.
58. Lachenbruch, A. H. & Sass, J. H. (1992) *J. Geophys. Res.* **97,** 4995–5015.
59. Brune, J. N., Brown, S. & Johnson, P. A. (1993) *Tectonophysics* **218,** 59–67.
60. Wald, D. J. & Heaton, T. H. (1994) *Bull. Seismol. Soc. Am.* **84,** 668–691.
61. Sieh, K., Jones, L., Hauksson, E., Hudnut, K., Eberhart-Phillips, D., Heaton, T., Hough, S., Hutton, K., Kanamori, H., Lilje, A., Lindval, S., McGill, S. F., Mori, J., Rubin, C., Spotila, J. A., Stock, J., Thio, H., Treiman, J., Wernicke, B. & Zachariasen, J. (1993) *Science* **260,** 171–176.
62. Spotila, J. A. & Sieh, K. (1995) *J. Geophys. Res.* **100,** 543–559.
63. Campillo, M. & Archuleta, R. J. (1993) *Geophys. Res. Lett.* **20,** 647–650.
64. Cohee, B. P. & Beroza, G. C. (1994) *Bull. Seismol. Soc. Am.* **84,** 692–712.

Proc. Natl. Acad. Sci. USA
Vol. 93, pp. 3830–3837, April 1996
Colloquium Paper

This paper was presented at a colloquium entitled "Earthquake Prediction: The Scientific Challenge," organized by Leon Knopoff (Chair), Keiiti Aki, Clarence R. Allen, James R. Rice, and Lynn R. Sykes, held February 10 and 11, 1995, at the National Academy of Sciences in Irvine, CA.

The organization of seismicity on fault networks

L. KNOPOFF

Department of Physics and Institute of Geophysics and Planetary Physics, University of California, Los Angeles, CA 90024-1567

ABSTRACT **Although models of homogeneous faults develop seismicity that has a Gutenberg–Richter distribution, this is only a transient state that is followed by events that are strongly influenced by the nature of the boundaries. Models with geometrical inhomogeneities of fracture thresholds can limit the sizes of earthquakes but now favor the characteristic earthquake model for large earthquakes. The character of the seismicity is extremely sensitive to distributions of inhomogeneities, suggesting that statistical rules for large earthquakes in one region may not be applicable to large earthquakes in another region. Model simulations on simple networks of faults with inhomogeneities of threshold develop episodes of lacunarity on all members of the network. There is no validity to the popular assumption that the average rate of slip on individual faults is a constant. Intermediate term precursory activity such as local quiescence and increases in intermediate-magnitude activity at long range are simulated well by the assumption that strong weakening of faults by injection of fluids and weakening of asperities on inhomogeneous models of fault networks is the dominant process; the heat flow paradox, the orientation of the stress field, and the low average stress drop in some earthquakes are understood in terms of the asperity model of inhomogeneous faulting.**

Homogeneous Faults

Our interest is in the prediction of large earthquakes since these are of the greatest societal concern. If large earthquakes are periodic, the problem is trivial. Since large earthquakes at the same site are not periodic (1, 2), we must inquire into the causes of the dispersion of interval times and especially to see if patterning is likely to develop. If patterns of seismicity emerge, then these can be used as templates for studies of likelihood of occurrence of strong earthquakes that take into account the small amount of information that is currently available concerning these events.

The physical causes of nonperiodicity of earthquakes must be rooted in interactions, since the absence of interactions would imply that the events earthquakes are simple relaxation oscillators. The only serious model for interactions that has been proposed is the redistribution of elastic stress by fractures. Thus, efforts to simulate evolutionary seismicity have focused on the development of fractures in an environment of fluctuations of the elastic stress field produced by earlier fractures: The stress field locally is lowered by fractures that occur when certain thresholds are reached, is restored by tectonic plate motions in the interval between earthquakes, and can be increased or decreased by the occurrence of fractures nearby and by stress relaxation from nonelastic processes. Do identifiable patterns of fractures arise under these conditions of fluctuating stresses?

Many of the simulation studies to date have taken as their paradigm the Gutenberg–Richter (G-R) power-law distributions of earthquake energies and moments and have attempted to do so by understanding the self-organization of fractures on a single, uniform earthquake fault. While these studies give insights into the process of self-organization of a complex system of small and large events, they are inappropriate to study the organization of large earthquakes on several accounts. First, the G-R law is appropriate only for small earthquakes and cannot be applicable to the description of large earthquakes (3). Second, the small earthquakes of Southern California do not take place on the plate boundary which is the San Andreas fault (SAF), or on some of the other major faults of Southern California but rather take place on a complex two-dimensional network of secondary and higher order faults (3). A third point concerns the current scale of computing of the simulations: Since the computational lattice size must correspond to events larger than the largest possible earthquakes, then the smallest plausible earthquake that is simulated well on the present-day lattice models corresponds to a magnitude 5 earthquake roughly. These smallest model earthquakes are close to the upper limit of applicability of the G-R law (3), and smaller earthquakes are not well modeled computationally today.

Large earthquakes are so rare in any given region, that we are unable to provide an appropriate statistical paradigm for their study. One goal of simulation studies must be the development of paradigms that are physically plausible.

Before discussing recent progress toward our goal of studying simulated seismicity on a network of faults (3), we first summarize some of the relevant results in the modeling of seismicity on a single fault as a preliminary step toward the more difficult problem. The focus on simulations of the power-law part of the distribution has led a number of authors to suggest that a scale-independent physics regulates the self-organization. The simplest scale-independent fault model is a homogeneous one, in which it is assumed that the structure of a given seismic region does not play an important part in the earthquake process at any scale, and that the seismicity is dominated by the mechanics of the self-organization due to the stress redistribution on a homogeneous landscape of structure (4–11). The total stress on the fault in scalar one- and two-dimensional (antiplane) elastostatic fractures does not decrease with time; thus, ultimately the stress in the system must exceed the fracture strength everywhere and a fracture must occur that is larger than any given size. If we require that the largest earthquakes be of finite length and that their growth stops by the same mechanism as the smaller ones, then these quasistatic models must ultimately develop a fracture whose length is greater than the largest that is geophysically possible.

Thus, an event must develop that is equal to the size of any finite computational lattice; at this point, the fracture interacts with the boundaries, and the system is no longer homogeneous: the evolutionary development of fractures is subsequently influenced by the interaction with the boundaries, by the

Abbreviations: G-R, Gutenberg–Richter; SAF, San Andreas fault; B-K, Burridge–Knopoff; 1D, one-dimensional.

inappropriate modeling of the transfer of stress from the fault regions outside it into the lattice segment. A throughgoing or lattice-wide fracture is not stopped by the same mechanism as that which stops the smaller fractures whose spans lie wholly within the lattice. There are thus two arguments against the applicability of homogeneous lattice models of self-organization: first, it is not possible to prevent the "runaway" or lattice-wide event, which is not stopped by the same mechanism as the smaller earthquakes, and second, there is no mechanism for discriminating between small and large earthquakes, as demanded by the finiteness of the energy budget for earthquakes (3). The same arguments apply against the development of scaling on an otherwise homogeneous system in the tensor (in-plane) case as well.

The dynamics of the fracture process represents an escape from the tyranny of the resolute increase of stress. A redistribution argument based on conservation laws no longer applies in this case, since the stresses are no longer solutions to Laplace's equation but are solutions to the elastic wave equation. The loss of energy in elastic wave radiation reduces the amount of energy available to promote further slip. However, dynamics does not provide an escape from the failure of a homogeneous system to develop an internally derived scale size that separates large from small fractures; absence of scaling is a powerful argument that self-organization of dynamic fractures on a single homogeneous fault must also lead to the abyss of the lattice-wide event.

We illustrate these remarks by a consideration of the self-organization of dynamic fractures on a single homogeneous fault model with periodic edge conditions through the vehicle of the Burridge–Knopoff (B-K) (12) spring-block model in one dimension. We do not elaborate on the dynamic B-K model, which has been discussed in detail elsewhere, except to remark that, in order that changes in the stress due to fracture be redistributed via elastic wave transmission, we guarantee that the (supersonic) dispersion, due to the local influence of the transverse springs in some dynamic versions of this model (13, 14), is moderated by fine-tuning a radiation damping term (15) that is equivalent to introducing a local viscosity as a frictional damping of the slip (12). It can be shown that the tunable radiation term merely represents a scaling of the size of the fracture with respect to the lattice spacing. Laboratory measurements of the nature of sliding friction in the range of slip velocities that occur in earthquakes have not been made: in our model, we do not invoke a velocity-dependent sliding friction; instead, the strength of the bonds at the crack edges drops instantly to the dynamic friction at the instant that the critical threshold stress is reached (15). Although the B-K models do not generate redistributed stresses that are scaled by the crack length, nevertheless these B-K models with critical radiation damping generate slip pulses whose ranges are of the order of $a(l/k)^{1/2}$ where a is the lattice spacing and l and k are the transverse and longitudinal spring constants and hence appropriate to simulations of self-healing pulses (16) in large earthquakes wherein slip is concentrated mainly near the growing edge of a crack. This model is more appropriate to the modeling of large earthquakes than small ones.

For arbitrary initial conditions on the homogeneous one-dimensional (1D) dynamic B-K fault model, the system quickly organizes itself into fractures with a power-law distribution of sizes (17). The events with power-law distribution of fracture sizes is only a transient state. Power-law transiency in the self-organization of other nonlinear systems has also been identified recently (18). Ultimately, a runaway event takes place that spans the entire lattice and hence has an infinite length on the periodic lattice. After the first runaway, subsequent seismicity displays only periodic runaways to the exclusion of smaller events, but this is a consequence of the smoothness of the stress after each runaway; other scenarios after the first runaway are possible, but they too lead to further runaways, and so on indefinitely.

In the transient state, the power-law distribution for the sequence of seismicity is not Poissonian but is rather a distribution that is dominated by (almost) periodic localized clusters. There is an intense clustering of repetitive events of almost the same size at the same locations, at almost equal time intervals (Fig. 1). These persistent clusters disappear after some time and others appear elsewhere. Such persistence is due to the smoothness of the stress across the extent of a fracture in this model (19). If the stress is smooth after fracture, the restoration of stress by the external loading mechanism brings the extent of a previous fracture to the uniform critical threshold at the same time, and hence local recurrence dominates this phase. Because of the nearest-neighbor property of the 1D B-K model, any changes in the stress can only take place at the edges of the fractures. Thus, the length of a fracture differs from its immediate predecessor only at its edges, and hence the persistence of a cluster is approximately scaled by the length of the fractures. The power-law distribution that results from this model describes the number of clusters of a given length weighted by the number of repetitions within the cluster. Thus, the spatial localization is evanescent, and the pattern has an overriding imprint of a periodicity imposed by the coupling of the smoothness of the postfracture stress and the homogeneity of the threshold fracture strength. The probability that any point along this fault will experience a large earthquake is the same for all points along the fault over the long term; over the long term, there can be no spatial localization.

A rolloff that is observed in the distribution (17) does not define a characteristic length; the scale size that is implied is an artifact of the fact that the count is terminated at the time of the first lattice-wide event; events that are slightly less than lattice-wide in size are undercounted compared with expectations for a larger lattice. The magnitude that corresponds to the rolloff corresponds to the parameter that mimics the seismic radiation; the larger the energy loss in the parameterized radiation, the longer the time to inevitable runaway.

Even if long-range forces are taken into account, the self-organization of fractures on a homogeneous landscape must ultimately develop a dynamic crack that is larger than any given size. A similar conclusion is reached if one introduces a weakening of strength into continuum quasistatic models with long-range redistribution of stress (20).

The Influence of Geometry

We turn to inhomogeneous faults or fault zones as systems with intrinsic scale sizes to explore the differences between large

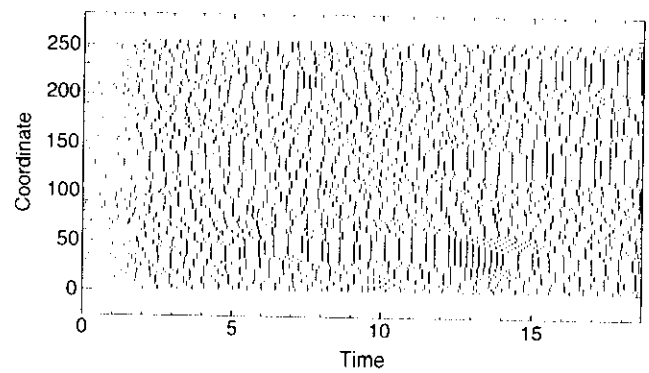

FIG. 1. Portion of the slip history of the transient phase on a homogeneous 1D B-K model with periodic end conditions. Vertical strokes define the linear extent of a fracture; fractures with greater length release more energy. Evanescent persistent clusters can be identified. After a long time, this pattern is replaced by lattice-wide periodic fractures. [Reproduced with permission from ref. 17 (copyright 1994, American Institute of Physics).]

and small earthquakes. We assume that the inhomogeneities on faults mirror the nonplanarity of geometry. The simplistic view of the physics of the resting or sliding of a single block on an inclined plane and the simplistic mathematics of planar fractures have obliged us to parameterize friction on a plane: in both cases, the complexity of the interface between the block and plane is ignored because it is physically or mathematically convenient to do so. The usual models of the development of fractures on planar fault surfaces with parameterized friction, including the continuum models of Kostrov (21), Burridge and Halliday (22), and successors, as well as the discrete nearest-neighbor models of B-K type (19), have relatively smooth distributions of stress after fracture; on the other hand, real earthquake fractures have very irregular poststress distributions, in view of the large numbers of aftershocks that occur close to the rupture surface.

There are several scales of nonplanar geometric features: (*i*) topographic irregularities on fault surfaces and the presence of fault gouge that are the cause of friction on faults; (*ii*) larger-scale geometrical fluctuations of faults such as bends, stepovers, bifurcations, etc., of faults; (*iii*) the dendritic nature of the network of secondary faults associated with plate boundaries and a possibly tegular character of the space between elements of the network; and (*iv*) the influence of the curvature of the earth and the distances between triple junctions of the tectonic plates. We have no contribution to make to this discussion on the influence of this last item on the organization of earthquakes worldwide.

While there is much to be said concerning the dynamics of friction at the smallest scales, limitations of space do not allow for a full discussion of recent efforts at modeling the dynamics of sliding of blocks with irregular contacts (23–25) or of the development of a fluid dynamics and deformation mechanics of granular materials (26–31).

We concentrate attention on the issue of larger scale irregularities in fault geometry. The two problems of the irregularity on the small and the large scales differ by virtue of the size of the dimensions of the irregularities scaled by the size of the slip. On the large scale, the dimensions of the irregularities are large compared with the slips, which are a number of meters in the largest earthquakes. The offset between the two more or less parallel sections of the SAF in Southern California is about 100 km. Whereas there is strike-slip motion on the parallel sections, the link between them, such as the connection between the two parallel sections of the SAF, must have some thrust component of motion. The continuum mechanics, especially from the viewpoint of iterative seismicity, is difficult and has not yet been worked out.

We make the assumption that there is a correspondence between irregularities in the large-scale fault geometry and spatial fluctuations in the fracture strength on a planar model; in other words, we make the usual, unjustifiable assumption about planarity. While we do not know the precise nature of these relationships, for the purpose of modeling assume that the fracture threshold is high where a fault has a relatively complex geometry (see list above) and that the threshold will be low when the fault is relatively straight and parallel to the regional shear stress, because it should be relatively more difficult to prolong propagation of a fracture that arrives at a region of complex fault geometry; King (32, 33) has presented persuasive arguments why the strength of these regions of complex geometries cannot persist and that stresses stored in them due to repeated fractures that stop there or nearby should relax on the long time scale. We do not consider these issues of long-term stress relaxation in this paper. We apply these considerations of inhomogeneity to the B-K model and preserve other properties of the B-K model including the homogeneity of the elastic parameters and the periodicity of the boundary conditions. As in the case of a homogeneous distribution of thresholds of fracture strengths, this system also rapidly enters upon an apparently steady state condition (15, 34), although it is hardly stationary on a short or intermediate time scale. Despite the seeming stochastic character of the space–time patterns in an example of large, correlated spatial fluctuations of fracture strength along the fault (Fig. 2) with a fractal distribution, there is a large-scale imprint of systematic pattern development, if not one of multidimensional chaos, not unlike the large-scale spatial localization with small-scale irregularity that appears in other nonlinear systems. In the example, the small fractures occur relatively frequently where the fracture thresholds are low. Large events are located where fracture strengths are large, with longer time intervals between events. Because of the correlations between fracture strengths in the model, a region of large fracture strength can store large amounts of potential energy that will be released in large earthquakes; sites with large fracture stresses require a greater time for restoration of the stress to the fracture threshold from plate tectonic sources than do those with small thresholds. The larger events have greater stress drops than do the small ones in these models with fractal distributions of thresholds, a result that is not wholly consistent with observation, thus suggesting that this fractal barrier model is inappropriate for the description of large earthquakes. In order that these cracks grow dynamically, they must deliver enough stress at their edges to overcome the local difference between the strength and the prestress. A region with a large, increasing change of strength will usually represent a barrier to crack growth. There is an anisotropy: fractures entering a region of increasing friction will have decreasing rates of growth and may stop; a crack leaving the same region but growing in the opposite direction will speed up; events that initiate in regions of high strength and high stress drop will occasionally extend into regions of low stress drop but the reverse is less likely.

Does a system with spatially varying thresholds develop runaways? The extent of the fracture is defined by its encounter with a barrier—i.e., a site with a sufficiently large difference between fracture threshold and prestress. Whether a given fracture breaks through a barrier or is stopped by it depends on the amount of stress available at the crack tip. In quasistatic models, the stress at the crack tip is proportional to the product of the average stress drop and the instantaneous length of the slipping region. Thus, a runaway must sooner or later occur on a quasistatic model because the longer a crack, the greater the size of the barrier that the crack can break through. But if dynamic slip is localized near the edge of a crack, the stress at the edge of a slipping patch of a dynamic crack is scaled by the size of the patch, which may or may not be the final length of the crack. From an elementary theory, except for reasonable dimensionless factors, the scale size of a dynamic crack is

$$L \approx uc/\dot{u},$$

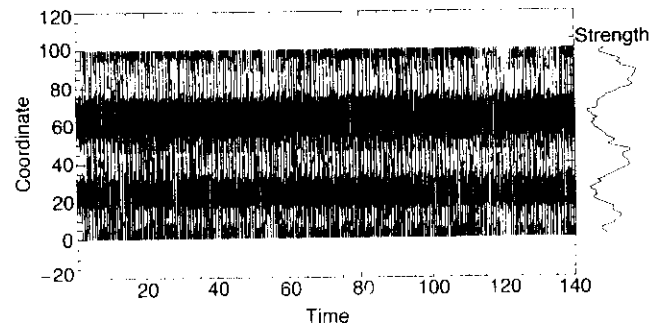

FIG. 2. Portion of the slip history on an inhomogeneous 1D B-K model with periodic end conditions. The fractal distribution of fracture thresholds is shown on the right. Where fracture strengths are low, small earthquakes occur frequently.

where u is the mean slip, $\dot{u}$ is the mean slip velocity, and c is the speed of the edge of the crack, which we take to be the shear wave velocity. For the largest earthquakes such as Landers or San Francisco, the scale size is of the order of 15 km, a distance that is more appropriate to the thickness of the seismogenic zone than is the length of the crack, by factors of 5 and 30 in the two cases. Thus, the stress at one edge of the largest earthquakes does not depend on the conditions at the remote, opposite edge but depends instead on some local property. We remark in passing that the range of aftershocks beyond the edge of an earthquake fracture can be expected to be scaled by L (35), which is more appropriately 15 km than the total length of the fracture. Conversely, the relatively short range of aftershocks in great earthquakes implies the presence of a moving patch of slip as the mode of rupture and is a condition observed for a number of earthquakes (16). If the scale size of rupture is independent of the length of the rupture in the largest earthquakes, then the stress at the edge does not increase with increasing length of rupture, and hence a sufficiently strong barrier will stop crack growth. If there are several such barriers in a region, then the breaking of one of these will not cause the others to fail. Hence, there will be no runaway in this case. Because of the nearest-neighbor coupling of stresses in the B-K model and the short range of stress interactions on the ruptured segment, this model is not likely to develop runaways in the presence of a nonuniform distribution of fracture strengths. Since large fluctuations in fracture thresholds serve to prevent runaways, and vanishingly small ones do not, we expect that there should be a transition between the cases of small fluctuations in barrier strengths, which allow for runaways, and those of large fluctuations, which allow for localization.

The distribution of earthquakes that is found on these inhomogeneous models is very sensitive to the distribution of fracture thresholds. A spiky distribution of fracture strengths, intended to simulate a sparse distribution of barriers on a single fault, leads to a very different display of space–time seismicity, from the preceding case (Fig. 3). In the example, the ratio of threshold fracture strengths in the spikes to that of the broad and almost flat valleys between them is very large. The space–time patterns show much greater regularity than in the preceding example. However, the notable interruptions from one seemingly stable pattern to another equally seemingly stable pattern, occur at times that are episodic and not apparently predictable, even on a deterministic model such as this one. These instabilities are triggered by the breaking of the strong barriers that form the borders to the deep, broad valleys of low strength, in contrast to models with infinite barriers at the edge of the lattice. Even the site with the greatest strength must break because of the constraint that the long-term average slip velocity be uniform at all lattice sites. The barrier earthquakes are usually strong, since these are the sites of large storage of deformational potential energy. The opening of the barrier gates transfers a large stress from one low strength valley to another and changes the stress distribution in the adjoining valley, thereby triggering a new mode of repetitive fractures in the valley. We suppose that in models with inhomogeneous thresholds the relaxation of the stresses in the barriers are important events, whether the thresholds are spiky or not. To assume that barriers are unbreakable with infinite thresholds leads to evolutionary histories that are not reliable.

In some cases, the valley with low fluctuations appears to be smooth and fractures are throughgoing from one barrier spike to the next barrier spike. But if the valley is sufficiently long, seismicity in the valleys breaks up into shorter fracture segments; these cases would appear to be consistent with a long model with homogeneous fracture strengths as described above (17). The factors that determine whether the seismicity in the valleys will be of one type or the other are the ratio between the fracture strengths of the peaks and valleys, which determines the strength of the stress impulse that is sent into a valley from a rupture at a peak, and the ratio between the length of the valley and the scale size for the B-K Green's function $a(l/k)^{1/2}$, which determines how far into the valley the stress impulse can travel.

In the models of this section, we have found it possible to generate a series of large or barrier events that belong to a different class than small or valley events. Some of the valleys break only in long fractures, while others break in a broad distribution of events having the G-R distribution, which is schematically a pattern not unlike seismicity in Southern California, although there are significant differences. The models are sensitive to the choice of geometry, but generally these models favor the characteristic earthquake model for large events on some of the faults of the system and the statistical model for smaller events on other faults of the system. The large events are stopped by significant barriers associated with major geometrical features of long faults. In these models, the smaller events are dominated by processes of self-organization on relatively smooth faults, since we have not allowed for their occurrence on individual faultlets that are not directly linked to major faults nearby.

By the arguments above, I have tried to suggest that the G-R law is not a characteristic of faults that support large earthquakes. If this is the case, what is the structure that supports the G-R law? Although the scale independence implied by the G-R law may arise due to self-organization on the scale independent, homogeneous system, this system has the defects already enumerated, that it does not develop localization, it does not provide for a discrimination between small and large earthquakes, and it does not prevent runaways. An orthogonal point of view is that the G-R distribution is a consequence of the geometry of the fault network, as are the properties of the largest earthquakes. On the geometrical model, we suppose that the power law distribution of earthquake sizes is due to seismicity on a myriad of isolated and noninteractive faults having a power-law distribution of sizes and strewn over the entire space. The failure of the SAF and several of the other faults to observe the regularity of the G-R law suggests therefore that the faults that support large earthquakes have different physical properties and geometry than do the smaller ones, a conclusion already suggested by the phenomenology. If the G-R law is an image of a power-law distribution of sizes of small faults or fracture surfaces, why is the G-R distribution universal? One possible answer is to propose that the formation of the fault surfaces of small dimension that support small earthquakes is linked to the process of slip on the larger, irregular faults, which may induce the formation of these secondary fractures. Under this model, the universality of the G-R law is a consequence of the universality of the fracture process of a three-dimensional structure under the influence

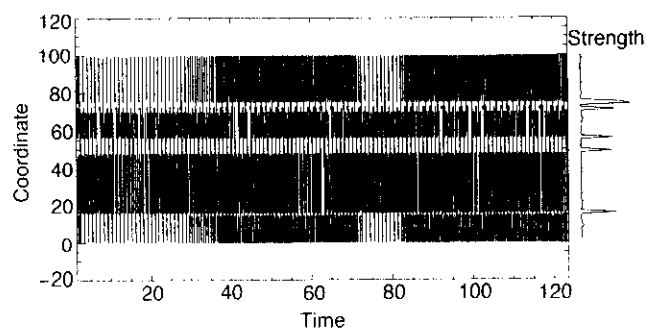

FIG. 3. Same as Fig. 2, but with a spiky distribution of fracture thresholds as shown on the right. Episodic shifts in periodicity are associated with fractures that breach the barriers. [Reproduced with permission from ref. 25 (copyright 1995, American Society of Mechanical Engineers).]

of a hierarchy of fractures of various sizes. Such a model has been proposed by Turcotte (36, 37) to explain the distribution of fragments in granular assemblages and in the present context can be assumed to describe the evolution of a fault network, whether dendritic or not, under some process of aggregation, such as diffusion-limited aggregation, in the process of development of regional fault structure.

Two Coupled Faults

The model of Fig. 3 favors characteristic earthquakes that are dominated by intervals of local periodicity, interrupted by episodic instabilities. The periodicity is, of course, not appropriate to the seismicity of Southern California. We consider whether the regularity of the large events is modified by exploring models of seismicity on a network or web of faults. In the discussion in this section, we describe only the interactions between two parallel faults. There is still much to be done before we can simulate a region as complex as Southern California.

Consider, as a simple model of fault interaction, the problem of two 1D scalar B-K fault models, coupled so that a fracture event on one fault reduces the stress on the other (Fig. 4); hence, both faults cannot tear in the same earthquake. This coupled system may be considered to be a skeletal model of the interaction between the San Jacinto fault (SJF) and the SAF in the southern part of the Southern California region, if we exclude the influence of all other faults in the region. We endow each model fault with its own set of fracture thresholds. The dissipation on each fault is tuned to the transverse spring constant.

We consider a distribution of thresholds on each fault that is intended to simulate several strong barriers that are separated by valleys with low threshold strength (Fig. 5). The barriers are staggered on the two faults; the valleys on the upper fault have slightly lower thresholds than on the lower fault and have rather higher thresholds at the barriers. Seismicity is notably different from the single fault model of Figs. 2 and 3, especially in the development of notable episodes of local quiescence on the faults. The principal difference from the case of a spiky distribution of thresholds on a single fault (Fig. 3) is the disappearance of local periodicity. The history is much less predictable.

The seismicity on the two faults is almost Babinet complementary: where one set of sites is active, the sites on the parallel fault are usually inactive (Fig. 5). (Quiescence does not disappear if the angular distribution of redistributed stresses at the ends of the fractures are taken into account.) The complementary quiescence and activity are due to the differences in fracture thresholds between the two faults: The fault that is the stronger of the pair at a given coordinate will in general be locked against slip, and fractures will take place on the weaker of the pair and its neighboring elements because of the correlations in fracture thresholds. Due to the coupling, stress on the stronger element of a pair does not build up because of the unloading when its weaker sibling ruptures. These results suggest that the dormancy of the SAF is complementary to the activity on the SJF but that at some time in the future, activity and quiescence will interchange between the two.

Because of the inexorable motion of the driving blocks, locked segments on the two faults cannot remain in the locked state indefinitely; the (diagonal) region between two locked segments on opposing faults stores increasingly more potential energy as tectonic motion continues, and this region must eventually lose its energy by fractures at one or the other of the locked segments. When one of the two locked segments breaks, it induces an extended episode of quiescence on weak segments on the companion fault. Around time 1720, activity on the upper fault is almost totally absent over the entire length but only temporarily so. Activity on the lower fault is similarly

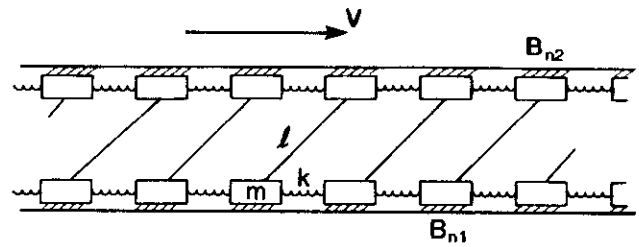

FIG. 4. Two 1D B-K model faults, coupled so that a fracture on one fault lowers the stress on the other. The two anvils have constant relative velocity. During sliding of any particle, there is a friction proportional to slip velocity with coefficient $2(ml)^{1/2}$, where m is the mass of any particle and l is the constant of the transverse coupling springs.

absent over much of its length around time 1960, again only temporarily.

Because the barrier locations are staggered between the two faults, the zones of quiescence are found to alternate spatially from one fault to the other, from region of strength to region of strength. It is notable that the extended absence of activity at the barrier on the upper fault at coordinate 200 between times 1300 and 1800 is matched by relatively frequent ruptures of the barrier at coordinate 175 on the lower fault. At about time 1800, activity on barrier upper 200 resumes and activity at barrier lower 175 ceases until time 2000.

Although the sum of the slip rates at a given coordinate is a constant for the entire region, the slip rates on the individual faults are not constant over time at a given coordinate. The slip rates can change abruptly; some active faults may become dormant, only to resume their activity later. These results are inconsistent with contemporary models that estimate seismic risk using the assumption that the present slip rate on a single fault of system is likely to be unchanged in the future (38).

The largest events occur where the barriers break and successive events at a given barrier release about the same amount of energy. Slip in the greatest earthquakes at a given site is not simply periodic: the interval times show significant variation. A cumulative distribution of the interval times is fit well by a truncated exponential distribution (Fig. 6): there are no interval times less than a certain critical value; the upper end of the distribution is terminated by the values for the extended lacunae, which are evidently inconsistent with the exponential distribution.

A comparison between the numerical distribution for intervals between large events on the model and the intervals between great earthquakes on the more northerly SAF measured at Pallett Creek (1, 2) suggests that the distribution at the latter site may also be truncated; it cannot be confirmed that the decay is exponential because of the small number of data. Lacunae are not be expected here since there are no long faults parallel to the SAF in this region to absorb the strain. It is likely that the fluctuations in interval times at Pallett Creek are due to interactions with large earthquake events in the neighborhood that generate stress transfer among ruptures on a more complex network of faults.

Without detailed information about the stress and strength distributions on the network, which is evidently not now possible for the faults of Southern California, we have no way at present to predict either the onset of lacunarity where appropriate or the interval time to the next great earthquake. It is doubtful that the time series of seismicity can be considered to be stationary if the effects of localization due to barriers are taken into account appropriately.

Intermediate Time Scale

Thus far, we have considered models with a time scale of seismic events that is set by the ratio between the elastic stress

drop at a lattice site and the stress loading rate. This time scale is appropriate to the long time scale of earthquake recurrence, which is of the order of 100 years in the case of the SAF and longer in the case of the other faults in its neighborhood. On the shorter time scale of intermediate-term precursory processes, let us say on a time scale of 1–10 years, we wish to identify clustering of smaller earthquakes before larger ones, a problem not adequately described by the above models. We modify the above models in two ways. First, we ask whether there is any physical mechanism that is competitive with brittle fracture to load or unload a fault on this time scale or shorter. In this section, we consider the diffusion of water in and out of fault zones and the nonelastic processes of slip weakening prior to fracture, which are mechanisms that are indeed important on the intermediate time scale; identification of precursory patterns of activity that make use of models of self-organization that are based on simple brittle-fracture processes only (39–41) must be modified to take the important influences of fluids and slip weakening into account. Second, we must be able to compute in detail over shorter time intervals, and hence we must forego the opportunity to study long-term evolutionary seismicity; here we describe computational schemes that explore precursors before each strong earthquake individually.

Because the normal stress on faults increases with depth below the earth's surface, brittle fracture on faults becomes increasingly difficult even at shallow depths in the crust; without the agency of water to reduce strength, faults would become locked, and yielding would not be localized on discrete fault surfaces. Hubbert and Rubey (42) proposed that the introduction of water into a fault would lower the friction and permit sliding to take place. Sibson (43–47) has described how water can be introduced into a fault zone from below the seismogenic zone before a large earthquake and how it can be removed after a large earthquake; removal allows for reestablishment of friction and hence for renewal of the earthquake process.

The introduction of fluids into a fault zone not only lowers the normal stress on the fault zone but also causes the normal stress on nearby faultlets to increase—i.e., as the walls of a major fault are pushed apart, other nearby faults should be squeezed together. Thus, activity of small earthquakes in the neighborhood of a fluidizing or fluidized fault should decrease—i.e., quiescence should be initiated. But why does not a fluidized fault rupture immediately upon lowering of the normal stress? To allow for a time delay between the onset of quiescence and occurrence of a strong earthquake, we assume that the fault is inhomogeneous and that while parts of it are fluidized, other parts remain locked in frictional contact; this is the asperity model of earthquakes.

In the barrier model (48) of the preceding sections, the growth of elastic fractures may stop at regions of low ratio of stress drop to strength. In the asperity model (49), a central, strong brittle zone or asperity is surrounded by a weak zone such as a crack that has a low shear strength or low friction because of the continuing presence of fluids, a structure that is inherently inhomogeneous. On a 1D fault, the asperity separates two disconnected, fluid-filled cracks. In the asperity model, unstable sliding is prevented by the asperity sutures; large scale sliding takes place when the asperities break. This model is not unlike the "bed-of-nails" model (50) proposed to understand porous flows in rocks at low pressures and the "fiber bundle model" (51, 52) designed to understand failure of braided cables or ropes. Neither of the latter statistical models have the correlations implicit in the present context; the issues in the present case involve the spatiotemporal development of conditions for occurrence of large earthquakes due to self-organization of the stress field.

An instability due to a decrease of friction with an increase of slip or slip rate for rocks close to their breaking point has been known for some time (53) and is a property of most solid materials. The instability associated with a lessening of strength as the critical state of fracture approaches has been studied more recently in experiments on stress corrosion, subcritical crack growth, and slip-weakening (54–59) and has been used in studies of self-organization on extended single faults (60–63). The presence of water vastly accelerates the rate of weakening of strength of fault materials and especially so at elevated temperatures because the weakening follows an activation process; it is the accelerated weakening that makes this process competitive in the intermediate time scale.

We combine the slip-weakening physics with the asperity model. We first consider a planar 1D array of fluid-filled preexisting cracks, separated by asperities (64). The crack lengths and the asperity widths are random variables, which we choose to have power law distributions. The cracks are subjected to an in-plane shear (mode II) stress. We solve the problem of the stress field in the complete long-range formulation. Cracks develop accelerated growth at their tips under the influence of the external shear stress, thereby causing the width of the asperities at their edges to decrease; cracks grow only along their own fault lines. The velocity of growth is a very strong function of the stress intensity factor at the crack tip, which we specify as $v_{tip} \sim e^{\sigma}$ or $v_{tip} \sim \sigma^n$ with n large (54–55). As the crack lengths increase, and as the widths of asperities at the edges of cracks decrease, the stress intensity factor at crack tips increases, and hence the velocities of the tips increase. When the velocity of the tip of a crack approaches the S-wave velocity, the crack begins to radiate seismic energy (60, 61) and, in the quasistatic approximation we use, the asperity disappears at this instant and an earthquake event occurs. The stress is now redistributed to the ends of the new crack, which has linear dimensions equal to the sum of the lengths of the two cracks and the now-vanished asperity; the suddenly increased stress intensity factors at the tips may cause further asperities to be consumed. For a finite array, in most cases only a few foreshocks, and in most cases no foreshocks, precede a strong event that releases prestress energy accumulated in the nucleation volume of the asperities; the large event transfers stress to great distance, being the extent of the fluidized zone. A homologous distribution of the few foreshocks over many simulations is in agreement with the inverse Omori law observed, also homologously, in large earthquakes worldwide (65, 66). It is to be expected that faults that are fluidized over much of their length, except for asperity contacts, should have normal stresses that are perpendicular to the fault structures, as observed (67), except at the asperities. This inhomogeneous model of faulting has bearing on the problem of the heat flow paradox. Lachenbruch and Sass (68) have remarked that the (average) stress drop in strong earthquakes is low (69) and that the heat flow across the SAF is not much above background (70, 71); these features combine to suggest that the fault is weak, a result inconsistent with field and laboratory measurements on whole rocks. There has been some discussion of the possibility of reducing the friction to very low values through a process of interface separation during the dynamics of rupture on relatively homogeneous materials (72); the asperity model suggests that the friction is low over much of the inhomogeneous fault before the rupture was initiated.

Consider now a network of faults (73). Suppose that fluids are introduced from below the seismogenic zone into the network when the region is at a sufficiently high state of stress. Let the width of the fluidized band of faults be small compared with their length. Seismic activity develops over the entire region in a series of local events of intermediate magnitude on individual faults of the network by the mechanism above. At a later time, a large earthquake having low average stress drop and great length develops on one of the faults. The large event not only extinguishes activity on its own fault but also lowers the stress on nearby faults and thus extinguishes activity on

them as well; activity on the entire region now ceases. If the fault network is studded with occasional asperity contacts in the fluidized state, the redistribution of stress may take on a filamentary geometry, as observed in experiments on granular assemblages, the grains having mainly free surfaces and only occasional bridging contacts (74–76).

If, however, an asperity having a dimension of let us say a few tens of kilometers does not break completely through, then a high stress drop earthquake will occur; because of failure to connect to the fluidized regions, these events will not cause significant changes in activity at distances of the order of several hundred kilometers. The agency of extended regions of fluid penetration into fault networks may help to understand the observations of an increase in intermediate-magnitude activity on a time scale of several years before a strong earthquake and its subsequent, rapid extinction on a distance scale of many times the classical dimension of rupture of a large earthquake that has been recently noted as part of the phenomenology of strong earthquakes in California (77). Reactivation takes place on the tectonic time scale.

If the faults of the network are somewhat farther apart in comparison with the length of the zone of activation, faults at intermediate distance may become reactivated after an episode of quiescence by the stress corrosion mechanism (73); the stress-corrosion reactivation time scale is much shorter than the tectonic reactivation time scale on an individual fault zone. Reactivation on a time scale of decades is consistent with some patterns of seismicity in Japan and is consistent with a greater width of the fault network in Japan than in California.

Summary

Because of scale independence, homogeneous fault models develop power-law distributions of seismicity that reproduce well the G-R distribution for small events. Unfortunately, the seismicity is only a transient state; for any finite fault, sooner or later seismicity interacts with inhomogeneities at the boundaries that leave an imprint on future seismicity that is characteristic of the nature of the boundaries. We have therefore considered inhomogeneous fault models, with geometrical fluctuations of fracture strengths, to guarantee that large events are localized and do not interact with boundaries and to guarantee that large earthquakes will not obey the power-law distribution. Inhomogeneous fault models favor the characteristic earthquake model for large events—namely, those that are limited by the strongest inhomogeneities—while the smaller earthquakes may continue to be described by power-law distributions. However, we find that the character of the seismicity is extremely sensitive to the geometrical distributions of inhomogeneities of fracture thresholds.

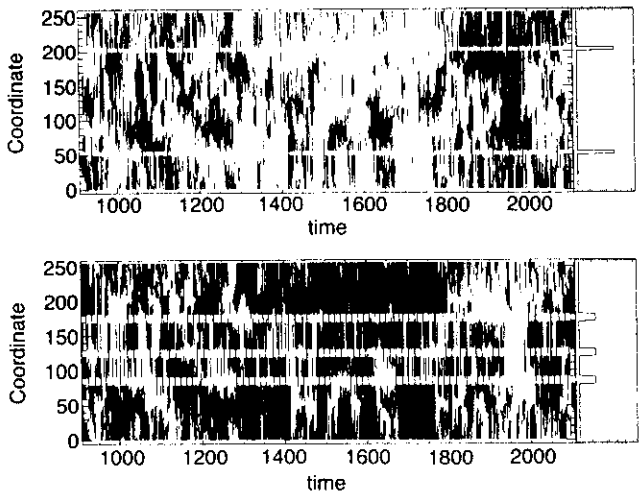

FIG. 5. Distribution of seismicity for a part of the time sequence for two faults coupled as in Fig. 4. The distribution of fracture thresholds is shown on the right. Periodic end conditions on both faults. Seismicity is largely complementary, with quiescence on one fault matched by activity on the other at the same coordinate and time. Around time 1600, the fault with stronger barriers becomes quiet over almost its entire length, which is matched by activity over almost the entire length of the other. Around time 1920, the pattern is almost completely reversed. Noteworthy is the interval from times 1300 to 1800, when the barrier at coordinate 200 on the upper fault does not tear; after time 1800, it tears frequently.

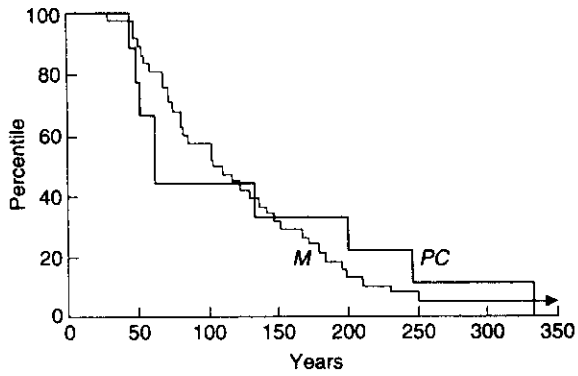

FIG. 6. Cumulative distribution of interval times for fractures of the strong barrier at coordinate 200 on the upper fault of the model (M), compared with the distribution of interval times for great earthquakes at Pallett Creek (PC). The model curve is well fit by a truncated exponential distribution except for the instabilities at the lacunae, such as that between times 1300 and 1800 (see Fig. 5). Time scales of the two curves have been adjusted to have a common median.

Most models of the seismicity of the largest events on single inhomogeneous faults show little dispersion of interval times. To generate significant dispersion of interval times, we have explored the nature of seismicity on a pair of parallel faults, whose stress redistribution patterns influence the occurrence of earthquakes on one another. Model simulations show that the instabilities of seismicity on a single fault have a different character in the coupled cases; seismicity now displays complementarity behavior as well as episodes of lacunarity. The distribution of interval times for the strongest earthquakes is a truncated exponential. We conclude that the popular assumption that the average rate of slip on individual faults is a constant is not likely to be valid.

Intermediate-term precursory activity in Southern California is simulated well by an asperity model that assumes that faults are fluidized and hence are weak over much of their length. Accelerated weakening of strength, coupled with the infusion of fluids from below the seismogenic zone, can account for local precursory quiescence for an increase of intermediate-magnitude activity at long range and the abrupt extinction of the latter by the occurrence of strong earthquakes with low average stress drop; the range of interaction can be many times the dimensions of the zone of brittle fracture in a large earthquake. The model of a fluidized fault network, sutured by occasional asperities, can explain the heat flow paradox, the orientation of the stress field near the SAF, and the low average stress drop in some strong earthquakes.

This research was supported by a grant from the Southern California Earthquake Center. This paper is publication no. 4622 of the Institute of Geophysics and Planetary Physics, University of California, Los Angeles, and is publication no. 323 of the Southern California Earthquake Center.

1. Sieh, K. E. (1978) *J. Geophys. Res.* **83,** 3907–3939.
2. Sieh, K., Stuiver, M. & Brillinger, D. (1989) *J. Geophys. Res.* **94,** 603–623.

3. Knopoff, L. (1996) *Proc. Natl. Acad. Sci. USA*, 3756–3763.
4. Bak, P. & Tang, C. (1989) *J. Geophys. Res.* **94,** 15635–15637.
5. Nakanishi, H. (1990) *Phys. Rev. A* **41,** 7086–7089.
6. Nakanishi, H. (1991) *Phys. Rev. A* **43,** 6613–6621.
7. Christensen, K. & Olami, Z. (1992) *J. Geophys. Res.* **97,** 8729–8735.
8. Christensen, K. & Olami, Z. (1992) *Phys. Rev. A* **46,** 1829–1838.
9. Christensen, K., Olami, Z. & Bak, P. (1992) *Phys. Rev. Lett.* **68,** 2417–2420.
10. Olami, Z., Feder, H. J. S. & Christensen, K. (1992) *Phys. Rev. Lett.* **68,** 1244–1247.
11. Olami, Z. & Christensen, K. (1992) *Phys. Rev. A* **46,** 1720–1723.
12. Burridge, R. & Knopoff, L. (1967) *Bull. Seismol. Soc. Am.* **57,** 341–371.
13. Carlson, J. & Langer, J. S. (1989) *Phys. Rev. Lett.* **62,** 2632–2635.
14. Carlson, J. M. & Langer, J. S. (1989) *Phys. Rev. A* **40,** 6470–6484.
15. Knopoff, L., Landoni, J. A. & Abinante, M. S. (1992) *Phys. Rev. A* **46,** 7445–7449.
16. Heaton, T. H. (1990) *Phys. Earth Planet. Inter.* **64,** 1–20.
17. Xu, H. J. & Knopoff, L. (1994) *Phys. Rev. E* **50,** 3577–3581.
18. Wacker, A., Bose, S. & Schöll, E. (1995) *Europhys. Lett.* **31,** 257–262.
19. Abinante, M. S. & Knopoff, L. (1995) *Phys. Rev. E* **52,** 5675–5678.
20. Rice, J. R. (1993) *J. Geophys. Res.* **98,** 9885–9907.
21. Kostrov, B. V. (1996) *J. Appl. Math. Mech.* **30,** 1241–1248.
22. Burridge, R. & Halliday, G. S. (1971) *Geophys. J. R. Astron. Soc.* **25,** 261–283.
23. Lomnitz-Adler, J. (1991) *J. Geophys. Res.* **96,** 6121–6131.
24. Pisarenko, D. & Mora, P. (1994) *Pure Appl. Geophys.* **142,** 447–466.
25. Knopoff, L. & Ni, X. X. (1995) in *Impact, Waves and Fracture*, eds. Batra, R. C., Mal, A. K. & MacSiphigh, G. P. (Am. Soc. Mech. Engrs., New York), pp. 175–187.
26. Scott, D. R., Marone, C. J. & Sammis, C. G. (1994) *J. Geophys. Res.* **99,** 7231–7246.
27. Chester, F. M. (1994) *J. Geophys. Res.* **99,** 7247–7261.
28. Herrmann, H. J. (1992) *Physica A* **191,** 263–276.
29. Knight, J. B., Jaeger, H. M. & Nagel, S. R. (1993) *Phys. Rev. Lett.* **70,** 3728–3731.
30. Ehrichs, E. E., Jaeger, H. M., Karczmar, G. S., Knight, J. B., Kuperman, V. Y. & Nagel, S. R. (1995) *Science* **267,** 1632–1634.
31. Tillemans, H.-J. & Herrmann, H. J. (1995) *Physica A* **217,** 261–288.
32. King, G. (1986) *Pure Appl. Geophys.* **124,** 567–585.
33. King, G. & Nabelek, J. (1985) *Science* **228,** 984–987.
34. Knopoff, L. (1993) *Proc. Am. Philos. Soc.* **137,** 339–349.
35. Chen, Y.-T. & Knopoff, L. (1986) *Geophys. J. R. Astron. Soc.* **87,** 1005–1024.
36. Turcotte, D. L. (1986) *J. Geophys. Res.* **91,** 1921–1926.
37. Turcotte, D. L. (1992) *Fractals and Chaos in Geology and Geophysics* (Cambridge Univ. Press, Cambridge, U.K.).
38. Working Group on California Earthquake Probabilities (1995) *Bull. Seismol. Soc. Am.* **85,** 379–439.
39. Kossobokov, V. G. & Carlson, J. M. (1995) *J. Geophys. Res.* **100,** 6431–6441.
40. Pepke, S. L., Carlson, J. M. & Shaw, B. E. (1994) *J. Geophys. Res.* **99,** 6769–6788.
41. Shaw, B. E., Carlson, J. M. & Langer, J. S. (1992) *J. Geophys. Res.* **97,** 479–488.
42. Hubbert, M. K. & Rubey, W. W. (1959) *Bull. Geol. Soc. Am.* **70,** 115–205.
43. Sibson, R. H. (1981) in *Earthquake Prediction: An International Review*, eds. Simpson, D. W. & Richards, P. G. (Am. Geophys. Union, Washington, DC), pp. 593–603.
44. Sibson, R. H., Moore, J. McM. & Rankin, A. H. (1975) *J. Geol. Soc. London* **131,** 652–659.
45. Sibson, R. H. (1992) *Earth-Science Rev.* **32,** 141–144.
46. Sibson, R. H. (1992) *Tectonophysics* **211,** 283–293.
47. Sibson, R. H. (1994) *Geol. Soc. Spec. Publ.* **78,** 69–84.
48. Aki, K. (1979) *J. Geophys. Res.* **84,** 6140–6148.
49. Kanamori, H. (1981) in *Earthquake Prediction: An International Review*, eds. Simpson, D. W. & Richards, P. G. (Am. Geophys. Union, Washington, DC), pp. 1–19.
50. Gangi, A. F. (1978) *Int. J. Rock Mech. Min. Sciences Geomech. Abstr.* **15,** 249–257.
51. Newman, W. I. & Gabrielov, A. M. (1991) *Int. J. Fract.* **50,** 1–14.
52. Newman, W. I., Gabrielov, A. M., Durand, T. A., Phoenix, S. L. & Turcotte, D. L. (1994) *Physica D* **77,** 200–216.
53. Griggs, D. T. (1940) *Bull. Geol. Soc. Am.* **51,** 1001–1022.
54. Atkinson, B. K. (1982) *J. Struct. Geol.* **4,** 41–56.
55. Atkinson, B. K. (1984) *J. Geophys. Res.* **89,** 4077–4114.
56. Dieterich, J. H. (1978) *Pure Appl. Geophys.* **116,** 790–806.
57. Dieterich, J. H. (1979) *J. Geophys. Res.* **84,** 2161–2168.
58. Dieterich, J. H. (1981) *Geophys. Monogr. Am. Geophys. Union* **24,** 103–120.
59. Ruina, A. (1983) *J. Geophys. Res.* **88,** 19359–10370.
60. Cao, T. & Aki, K. (1984) *Pure Appl. Geophys.* **122,** 10–24.
61. Cao, T. & Aki, K. (1986) *Pure Appl. Geophys.* **124,** 487–513.
62. Dieterich, J. H. (1986) *Geophys. Monogr. Am. Geophys. Union* **37,** 37–47.
63. Dieterich, J. H. (1988) *Pure Appl. Geophys.* **126,** 589–617.
64. Yamashita, T. & Knopoff, L. (1989) *Geophys. J. R. Astron. Soc.* **96,** 389–399.
65. Kagan, Y. Y. & Knopoff, L. (1978) *Geophys. J. R. Astron. Soc.* **55,** 67–86.
66. Jones, L. M. & Molnar, P. (1979) *J. Geophys. Res.* **84,** 3596–3608.
67. Zoback, M. D., Zoback, M. L., Mount, V., Eaton, J., Healy, J. *et al.* (1987) *Science* **238,** 1105–1111.
68. Lachenbruch, A. H. & Sass, J. H. (1992) *J. Geophys. Res.* **97,** 4995–5015.
69. Kanamori, H. & Anderson, D. L. (1975) *Bull. Seismol. Soc. Am.* **65,** 1073–1095.
70. Brune, J. N., Henyey, T. L. & Roy, R. F. (1969) *J. Geophys. Res.* **74,** 3821–3827.
71. Lachenbruch, A. H. & Sass, J. H. (1980) *J. Geophys. Res.* **85,** 6185–6222.
72. Brune, J. N., Brown, S. & Johnson, P. A. (1993) *Tectonophysics* **218,** 59–67.
73. Yamashita, T. & Knopoff, L. (1992) *J. Geophys. Res.* **97,** 19873–19879.
74. Dantu, P. (1967) *Ann. Ponts Chausées* **4,** 144.
75. Travers, T., Ammi, M., Bideau, D., Gervois, A., Messager, J. C. & Troadec, J. P. (1987) *Europhys. Lett.* **4,** 329–332.
76. Liu, C.-h., Nagel, S. R., Schecter, D. A., Coppersmith, S. N., Majumdar, S., Narayan, O. & Witten, T. A. (1995) *Science* **269,** 513–515.
77. Knopoff, L., Levshina, T., Keilis-Borok, V. I. & Mattoni, C. (1996) *J. Geophys. Res.* **101,** 5779–5796.
78. Yamashita, T. (1995) *J. Geophys. Res.* **100,** 8339–8350.

JOURNAL OF GEOPHYSICAL RESEARCH, VOL. 101, NO. B3, PAGES 5779–5796, MARCH 10, 1996

Increased long-range intermediate-magnitude earthquake activity prior to strong earthquakes in California

L. Knopoff, T. Levshina, V. I. Keilis-Borok,[1] and C. Mattoni[2]
Institute of Geophysics and Planetary Physics, University of California, Los Angeles

Abstract. We study the space-time relationships between strong earthquakes in California and the intermediate-magnitude earthquakes that both precede and follow them. All 11 earthquakes in California with nominal magnitudes greater than or equal to 6.8 from 1941 to 1993 were preceded by an increase in the rate of occurrence of earthquakes having magnitudes greater than 5.1. Ten of the 11 earthquakes occurred when or shortly after the intermediate magnitude activity was greater than its 75th percentile. Three of these strong earthquakes are in a conventional space-time foreshock-aftershock relationship with others of the 11 strong events. The precursory activity is concentrated in regions having linear dimensions of the order of a few hundred kilometers; these dimensions are significantly larger than the estimated fracture lengths of the ensuing strong earthquakes. The correlations are ill defined for smaller earthquakes and are almost unidentifiable for earthquakes with magnitudes less than about 4.6. The precursors to the strong earthquakes appear over a time interval of the order of 5 to 10 years before the strong earthquake, although the onset was about 25 years before the San Francisco earthquake. In the case of the Loma Prieta and San Francisco earthquakes, the onset of increased activity appears to be relatively abrupt. The increased activity is either switched off abruptly to distances of the order of hundreds of kilometers shortly after the occurrence of a strong earthquake, or the strong events are themselves part of a precursory pattern of continuing high activity before a second strong earthquake that takes place soon thereafter, with subsequent extinction of activity after it. Thus the intermediate-magnitude precursors do not directly influence the time and location of the subsequent strong event, but the strong event has a strong influence on the stress field in the vicinity of intermediate-magnitude earthquakes to distances of the order of many times the scale size of the strong earthquake.

Introduction

A precursory increase of seismic activity at relatively large distances and over timescales of the order of a few years has been described frequently, either as an isolated phenomenon or together with other seismicity patterns [e.g., *Mogi*, 1969; *Wesson and Ellsworth*, 1973; *Sykes*, 1983; *Wesson and Nicholson*, 1988; *Keilis-Borok et al.*, 1988; *Keilis-Borok and Kossobokov*, 1990; *Sykes and Jaumé*, 1990]. Among these other seismicity patterns are those of precursory quiescence and clustering which have been reported in a number of instances over distance ranges both shorter and longer than those indicated for increased activity [e.g. *Mogi*, 1969; *Kanamori*, 1981; *Keilis-Borok et al.*, 1988; *Wyss and Habermann*, 1988; *Habermann*, 1988]. *Keylis-Borok and Malinovskaya* [1964], *Keilis-Borok et al.* [1988], and *Keilis-Borok and Kossobokov* [1990] identified premonitory patterns of seismicity over broad geographical areas whose dimensions were much larger than the rupture sizes of upcoming strong earthquakes; however, the precise locations of the earthquakes that contribute to these patterns were not identified. In this paper we discuss the space-time relationships in fluctuations in intermediate-magnitude seismic activity and the relationship of these fluctuations to the strongest earthquakes of California.

A marked increase in seismic activity prior to the 1989 Loma Prieta earthquake $M = 7.1$ has been identified by *Sykes and Jaumé* [1990] and *Bufe and Varnes* [1993]. We show the cumulative number of earthquakes with $M_S \geq 5.5$ in a 3°×3° region around the Loma Prieta

[1]Now at International Institute of Earthquake Prediction and Mathematical Geophysics, Russian Academy of Sciences, Moscow.

[2]Now at Department of Physics, Harvard University, Cambridge, Massachusetts.

Paper number 95JB03730.
0148-0227/96/95JB-03730$05.00

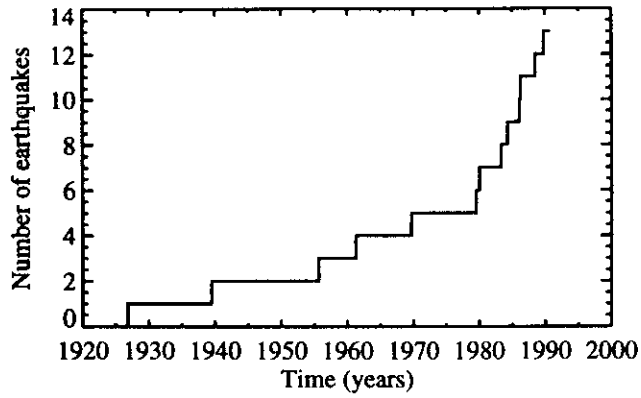

Figure 1a. Cumulative number of earthquakes with $M_L \geq 5.5$ in a $3° \times 3°$ region around the Loma Prieta epicenter from 1919 to 1989. Aftershocks have been deleted.

epicentral region for the 70 years before the earthquake (Figure 1). We have deleted obvious aftershocks from the list of earthquakes [*Gardner and Knopoff*, 1974]; we make adjustments for differences in the magnitude scales between the earlier Berkeley catalog and the later Preliminary Determination of Epicenters (PDE) catalog. An abrupt and significant change in the rate of occurrence takes place around 1979 (Figure 1). The rates differ roughly by a factor of 6. Intermediate-magnitude earthquakes in the interval 1919–1979 are widely distributed over the region, while the earthquakes in the interval 1979–1989 are concentrated in a smaller region approximately 1° on a side; the precursory earthquakes are not located on the San Andreas Fault itself.

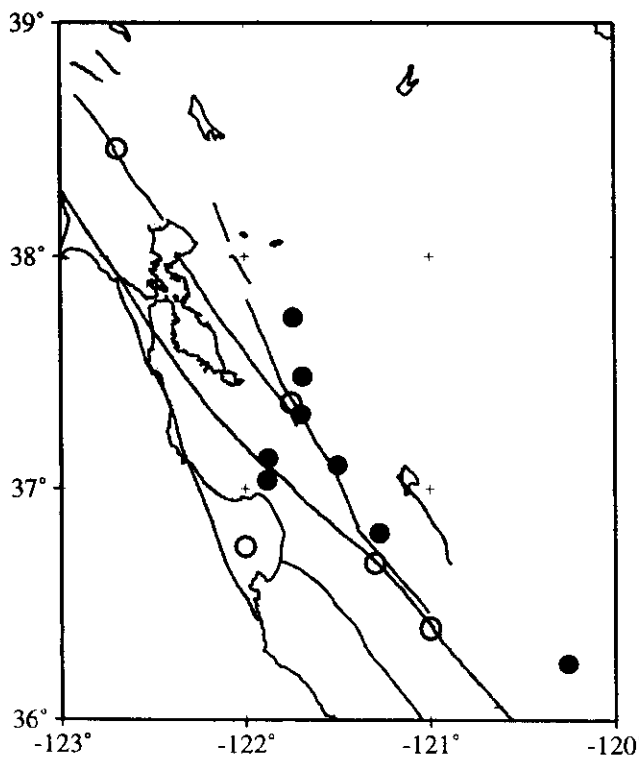

Figure 1b. Epicenters of the earthquakes in Figure 1a. Open circles are epicenters 1919 to 1978; solid circles are epicenters 1979 to 1989.

A similar increase in seismicity prior to the $M = 8.3$ San Francisco earthquake of 1906 has been noted in qualitative terms by *Ellsworth et al.* [1981]. We use the W.L. Ellsworth et al. catalog of earthquakes for almost the same region as Figure 1, for the period after 1855; we hesitate to link this catalog with that used in the preparation of Figure 1 because of the incompatibility of the historical basis for one and the instrumental basis for the other. A magnitude-frequency plot of the Ellsworth catalog shows deviation from log linearity for events with magnitudes less than about 5.5, implying an underreporting of earthquakes with smaller magnitudes; *Ellsworth et al.* [1981, p. 137] "estimate that the catalog is essentially complete down to M 5.5 after 1855 in the San Francisco Bay region". We assume it is complete over the region at this magnitude level. We plot the cumulative number-time distribution for the catalog for earthquakes with $M \geq 5.5$, in this case without removing aftershocks because of the lack of resolution of locations in the historical catalog (Figure 2). Again, a significant change in rate by about a factor of 2.5, sets in around 1880, or 25 years before the 1906 earthquake; the onset of the interval of increased seismicity prior to both the Loma Prieta and San Francisco earthquakes seems to be abrupt. The prolonged episode of low seismicity after 1906 and lasting until 1979 has already been noted. The $M = 6.7$ earthquake of 1868 was also preceded by a brief interval of increased seismicity and was followed by an abbreviated interval without earthquakes.

In this paper we explore the generalization whether a rather simple precursory pattern of increase of activity is to be found on a timescale of several years before each strong earthquake in the California area, and distributed over a region as large as several hundreds of kilometers from the strong earthquake.

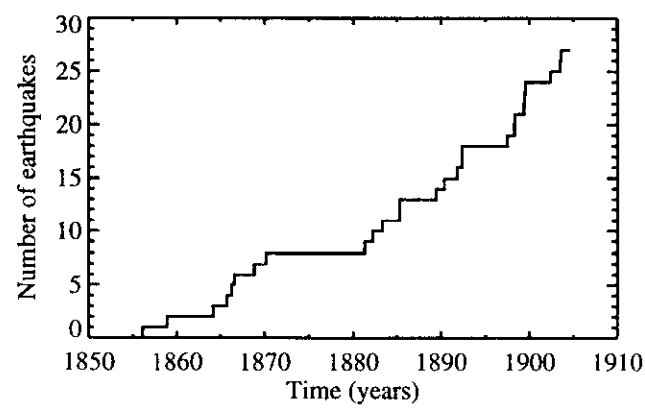

Figure 2. As Figure 1a for earthquakes in a 3° region around San Francisco from 1850 to 1906.

Regionalization and Catalogs

We consider the occurrence of earthquakes in three different regions of California and vicinity (Figure 3), which we call the southern, central, and northern regions, and which are located astride the plate boundaries of the Pacific Coast of California and Oregon. The northern region encompasses the seismically active area around Cape Mendocino and the complex plate boundary to its west and northwest. The southern region is essentially that spanned by the CalTech catalog but it excludes the region to the east of the Sierra Nevada. With one exception, the boundaries have been chosen to reflect gaps in the seismicity of the entire region for earthquakes with $M \geq 5.1$ over the interval 1965-1993 for the northern region, 1939-1993 for the central region, and 1933-1993 for the southern region. The southern and central regions are separated by a gap at the Carrizo Plain; the northern and central regions are separated by the gap in northern California centered near Point Arena; the northern boundary to the northern region is drawn at the gap in seismicity that starts at the southern edge of the Juan de Fuca Ridge. The southern boundary of the southern region is the southern edge of the CalTech catalog and lies about 1° south of the United States-Mexico political border. Magnitudes for intermediate-magnitude earthquakes south of this boundary are mostly unavailable from 1933 to 1965; in a few cases we give a qualitative discussion of the relevance of the earthquakes after 1965 in this region to our analysis. The Parkfield area of the San Andreas Fault system near latitude 36°N lies to the north of the Carrizo gap and thus is included in the central region rather than in the southern region, but this is not critical to the subsequent discussion.

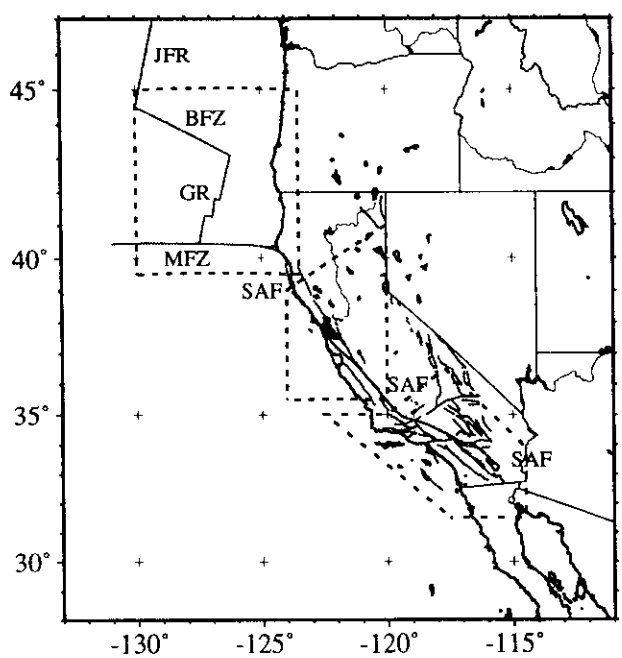

Figure 3a. Regional boundaries and fault map. The Juan de Fuca Ridge (JFR), Blanco Fracture Zone (BFZ), Gorda Ridge (GR), Mendocino Fracture Zone (MFZ), and San Andreas Fault (SAF) are indicated.

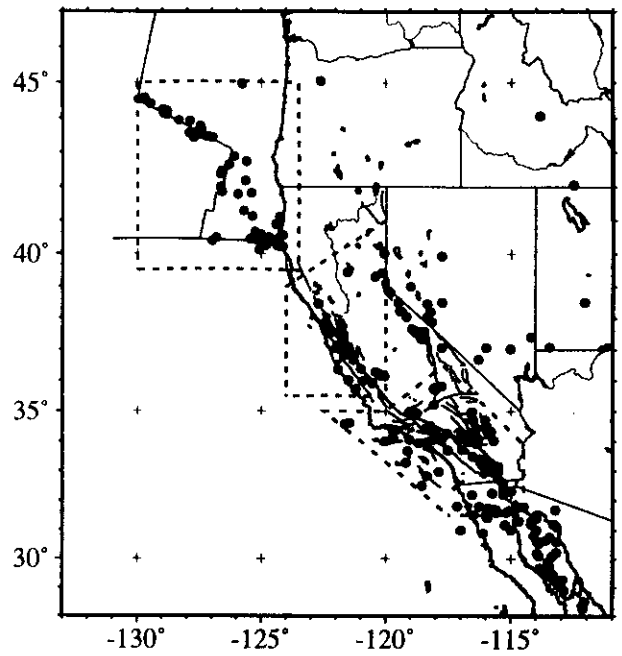

Figure 3b. Earthquake epicenters with $M \geq 5.1$ spanning the intervals 1933-1993 in the southern region and 1965-1993 for the other parts of the map.

We have used the CalTech catalog for southern California earthquakes (1935-1993) with modifications given by *Hutton and Jones* [1993], a combined catalog for the central region (1939-1993) that fuses the Berkeley, the U.S. Geological Survey (USGS), and the PDE catalogs that has been prepared by Y. Kagan, and the USGS/PDE catalog of earthquakes (1965-1993) for the other regions. These catalogs are complete during these periods for earthquakes with magnitudes $M \geq 4.7$, which is sufficient for the purposes of this paper. Aftershocks are eliminated from these catalogs by the use of an algorithm given by *Gardner and Knopoff* [1974]; an aftershock is defined as the smaller and later of a pair of events that are separated by time and distance intervals that depend on the magnitude of the earlier of the pair. Our analysis makes use of earthquakes prior to March 25, 1993. The Northridge earthquake of January 17, 1994, occurred while this paper was in preparation; we have extended our analysis of seismicity in the southern region to include earthquakes up to the latter date, and discuss this aspect of the seismicity in a separate section.

Unfortunately, the magnitude scales are not identical across all the catalogs. For southern California earthquakes, we use the revised magnitudes M_W listed in *Hutton and Jones* [1993] where available. For the other two catalogs and for the remainder of the southern re-

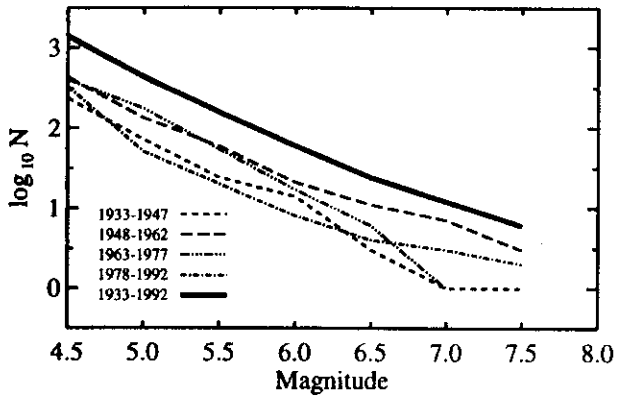

Figure 4. Differential magnitude-frequency relation for Southern California earthquakes with aftershocks removed from 1933 to 1992. Each data point is the number of events in the interval $M \pm 0.25$ where M increases in 0.5 increments. A division into four 15-year subcatalogs shows divergences that are significant at the 2σ level in the approximate magnitude range 4.6 to 6.2.

gion, we used M_S where available, which means, in effect, for earthquakes with magnitudes greater than 6.0. For the smaller earthquakes we used M_L where available and for those events for which M_L is not given, an adjustment for the differences between m_b and M_L was made.

Activity Before Earthquakes With Magnitudes $M \geq 6.8$

We define strong earthquakes to be those with magnitudes greater than or equal to a threshold of M_{th}. In this section we choose $M_{th} = 6.8$. To define the magnitudes of earthquakes over which fluctuations in activity occur, we construct the usual magnitude-frequency relationship for the southern California catalog with aftershocks removed (Figure 4); we observe the usual linear relationship to the largest magnitudes. However, there is a divergence among 15-year subcatalogs that is significant at the 2σ level in the magnitude range between 4.6 and 6.2, approximately; we focus our studies of fluctuations in seismicity in this magnitude range. We illustrate the fluctuations in seismicity in the three regions by displaying the number of earthquakes with magnitudes between 5.1 and 6.7 in the 5 years preceding a given time (Figure 5a, 5b, 5c); the times of these intermediate-magnitude events are indicated at the bottom of each diagram; a catalog of these intermediate-magnitude events is given in the appendix. To establish a terminology, we call the output of the smoothing filter, as in Figure 5, the windowed activity. (In all cases discussed in this paper, except for the Borrego Mountain and San Fernando earthquakes, the filter window is 5 years. If we had set the window width to zero, we would have obtained the "picket fence" at the bottom of Figure 5a, 5b, and 5c). The actual rate of occurrence of earthquakes in this magnitude range is called the activity. The times of the strong earthquakes in each region are indicated by long vertical lines.

Our use of a sliding window of finite width as a smoothing filter, such as the window of 5 years in this case, presents some problems for the interpretation of the results, as we describe below. The times in Figure 5 correspond to the end of the window interval. The magnitudes of the intermediate-magnitude earthquakes were chosen to range from the threshold magnitude that defines the strong earthquakes down to 1.7 magnitude units below it; this choice allowed us to explore in a consistent way variations in the activity within the mag-

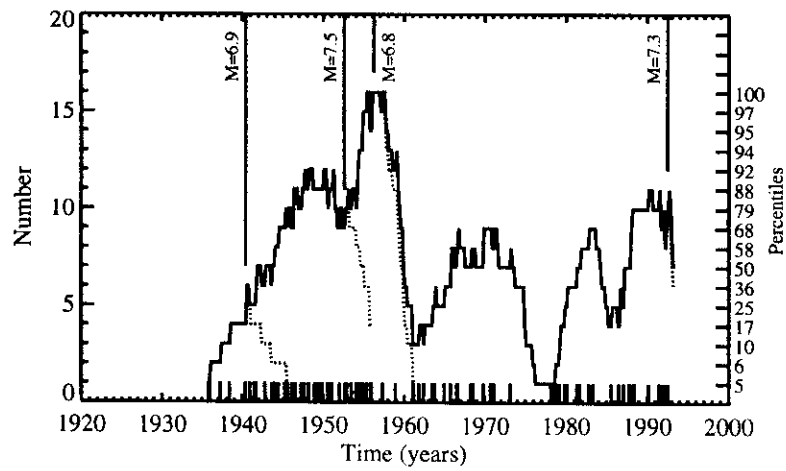

Figure 5a. Windowed activity in the southern region. Solid curve is the number of earthquakes with $5.1 \leq M \leq 6.7$ in a 5-year sliding window; the window slides by 4-month intervals. Dashed curve is the windowed activity under the assumption that no earthquakes occurred after each strong earthquake. If the solid and dashed curves overlay one another, no earthquakes actually occurred in the 5-year interval after the earthquake. Heavy vertical lines indicate times of strong earthquakes.

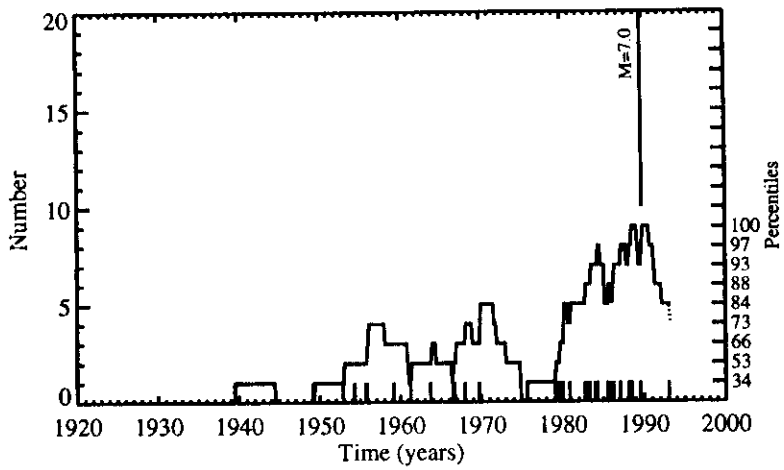

Figure 5b. Windowed activity in the central region.

nitude range of fluctuations identified in Figure 4 and their relation to strong earthquakes with different magnitudes. In the present case we have increased the upper limit of intermediate magnitudes to 6.7, a value that is indeed above the upper limit for statistically significant fluctuations in Figure 4, but there are few earthquakes in the interval 6.2 to 6.7 and our interpretation does not depend on this feature.

We consider the relationships between the activity and the strong events with $M \geq 6.8$ in the time intervals of the catalogs. The 1940 earthquake in the southern region occurs at the beginning of the useful part of the curve, so we do not know whether this earthquake was preceded by increased activity. We do not concern ourselves with this earthquake any further.

There is a closely spaced series of five earthquakes in this magnitude range in the northern region from 1991 to 1995; these are the $M = 6.9, 7.1, 7.1, 7.0$, and 6.8 events in 1991, 1991, 1992, 1994, and 1995, respectively (see appendix, Table A3). The first of the quintuplet preceded the second (the $M = 7.1$ offshore earthquake of August 17, 1991) by only a little over 1 month and was located nearby. We consider it to have been a foreshock of the second. The last two of this quintuplet are located sufficiently close to the focus of the Petrolia earthquake ($M = 7.1$, April 25, 1992) that they were probably aftershocks of it. The two sets of epicenters are widely separated. In order to avoid weighting our tabulations unduly by this concentration of events, we have arbitrarily chosen to count each of these clusters as a single event; we return to this point below. There are thus eight events in this magnitude range: four in the southern region (having deleted one), one in the central region and three in the northern region.

Seven of the eight events with $M \geq 6.8$ are preceded within 2 years by a windowed activity greater than or equal to the 75th percentile level for the specific regional distribution; that is, they take place during the roughly 25% of the time that the intermediate-magnitude windowed activity in the interval $5.1 \leq M \leq 6.7$ is at its greatest. All eight earthquakes occur when the windowed activity is high; strong earthquakes do not occur at times near minima in the windowed activity. The percentiles are calculated excluding values in the first 5

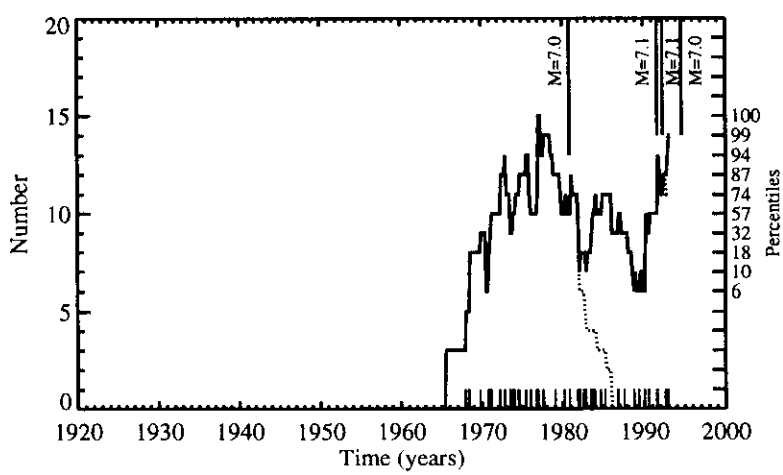

Figure 5c. Windowed activity in the northern region.

years following the start of the regional catalog, which represents a startup transient interval. A data point in the startup interval for the southern region that is plotted at 1938, for example, only includes actual catalog data for the abbreviated interval 1935-1938. A percentile measure to identify the occurrence of peaks in windowed activity is useful only if the fluctuations in the measure have large amplitudes and do not oscillate too frequently.

The windowed activity prior to the first of the pair July 13, 1991($M = 6.9$)/August 17, 1991 ($M = 7.1$) in the northern region, occurs at a time when the windowed activity is at the 57% level which, while not low, is not above the 75% threshold; the second of this pair occurs when the windowed activity is well above the 75% threshold (Figure 5c). Extension of Figure 5c with new data beyond its termination shows that all of the last triplet of the Petrolia earthquake and its two aftershocks, all of which have magnitudes greater than 6.8, occur at times when the windowed activity is above its threshold. As remarked, although literally 10 out of 11 events with $M \geq 6.8$ are preceded by a windowed activity above the 75% threshold, in view of the density of the last five events, we indicate that only 7 out of 8 have been so anticipated.

Activity After Earthquakes With Magnitudes $M \geq 6.8$

If peaks in activity are correlated with the occurrence of strong earthquakes, then reductions in activity must also be correlated with them in order that the system be reset before the next strong earthquake. Thus a test of the correlation of strong earthquakes with activity must involve both the increasing and decreasing phases of the activity.

To measure activity after a strong earthquake, we must circumvent an artifact of the windowing procedure. A precursory peak of windowed activity often extends beyond its corresponding strong earthquake (Figure 5). Part of the extension is caused by the finiteness of the window: The windowed activity at a time, let us say, 2 years after a strong earthquake includes a count of the number of intermediate-magnitude events that occurred less than 3 years before the strong earthquake, since the windowed activity is attributed to the time at the end of the sliding window. Of course, some of the windowed activity after a strong earthquake is also due to intermediate-magnitude events that occurred after it. The dotted lines in Figure 5 show the windowed activity calculated by deleting all intermediate-magnitude earthquakes that occurred after each strong earthquake. Thus we can evaluate the relative importance of the two influences: if the dotted curves lie close to the solid lines, the activity after the strong earthquake is small.

After the 1956 San Miguel earthquake in the southern region, after the 1989 Loma Prieta earthquake in the central region, and after the 1980 Eureka earthquake in the northern region, the activity was very quickly reduced to a very low level. We comment below about the seismicity in the southern region in the time interval after the Landers earthquake and before the Northridge earthquake of January 17, 1994.

After the July 1952 Kern County earthquake in the southern region, activity remained high. The Kern County earthquake is followed within about 4 years by the 1956 San Miguel earthquake. Part of the region remains in a highly active state after the Kern County earthquake.

Activity has remained high ever since the first of the northern quintuplet. The time interval since the last of these events in 1995 is too short for us to determine whether there is a falloff in activity after it or that it remains high.

Thus activity has either fallen abruptly or has remained high after every event. There does not seem to be any gradual decrease in activity.

Windowed activity has a pronounced peak of about the same shape in both the central and southern regions starting from 1980; there is a similar peak in the northern region that begins around 10 years earlier, and an incipient peak that begins around 1990, thereby suggesting that the two southernmost, if not all three regions, reach a peak of activity at about the same time. However, we have no data in the northern region before the start of reporting of PDE magnitudes in 1965 (which implies activity before 1970 in our definition), so we cannot evaluate correlations with activity in the other regions. Furthermore, the quiescence from 1935 to 1979 in the central region is in contrast with the presence of two strong peaks in the southern region; we speculate that the quiescence in the central region up to 1979 is a prolonged aftermath of the lowering of stress by the 1906 San Francisco earthquake. (A cross correlation among the pairs of curves of Figure 5 shows that the single peak of the central region (Figure 5b) is most strongly correlated with the strongest peak 35

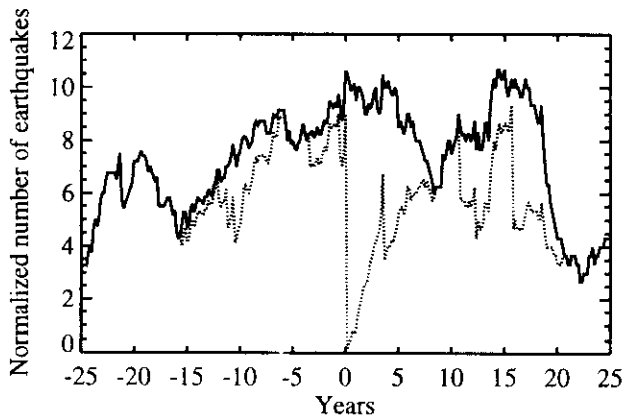

Figure 6. Stacked windowed activity before and after the strong earthquakes of Figures 5a, 5b and 5c. All strong earthquakes are assumed to occur at $t = 0$.

to 40 years earlier in the southern region. The isolated peaks in the central and northern regions are correlated as expected with a lag of 10 years.) A hypothesis of correlation over larger distances than our three individual regions is supported only by the most recent peak of windowed activity that appears in all regions. With regard to this most recent peak, it is arguable whether the Coalinga cluster near latitude 36° (see Figures 7g and 7h) represents a linkage between the southern and central regions that creates a single "superregion". At this time, we retain our regionalization as defined.

A more explicit representation of the correlations between the fluctuations in activity and the strong earthquakes is given by stacking the individual plots of windowed activity for all eight strong earthquakes, averaged over the time intervals for which we have data (Figure 6). The stacked curve rises from a minimum about 15 years before a strong earthquake to a maximum at the time of the strong earthquake, with a maximum-to-minimum ratio of about 2.5; thus an increase in activity before these strong earthquakes is a general property. The apparent symmetry of the curve in Figure 6 after $t = 0$ is due to at least three competing influences which are the contribution of windowed activity prior to the strong earthquake due to the finiteness of the window, as noted above, the continued activity after some earthquakes and the decrease in activity after others.

Spatial Distributions

We map the epicenters of the intermediate-magnitude earthquakes that contribute to the peaks in the windowed activity of Figure 5. Except where noted, the time intervals represented for the events on the following maps of activity before strong earthquakes start 5 years before the windowed activity crosses the 75th percentile threshold, and end at the time of the strong earthquake itself. We also map the intermediate-magnitude earthquakes for a time which is usually 5 years after the strong earthquake. We consider such maps in turn for each of the eight strong earthquakes with $M \geq 6.8$.

Southern Region

We consider first the pair of the Kern County, July 21, 1952, and the San Miguel, February 9, 1956, earthquakes in the southern region. Since a time 5 years before the crossing of the 75% windowed activity threshold for the Kern County earthquake overlaps the date of the 1940 earthquake in the Imperial Valley, we have mapped all epicenters between the 1940 and 1952 earthquakes (Figure 7a). The epicenters of the intermediate-magnitude earthquakes ($5.1 \leq M \leq 6.7$) in this time interval span much of the southern region, which is more than 5° in its longest dimension. The White Wolf fault, on which the Kern County earthquake occurred, lies along the periphery of the distribution. Most of these intermediate-magnitude events that occurred prior to the Kern County earthquake are located at some distance from the future fracture trace of the strong earthquake. In the last 5 years of the 12-year interval, that is from 1947 to 1952, the seismicity was concentrated in the southern part of the map (compare Figure 7b and 7c) a region 350 km in dimension. This feature may represent the development of a more localized *Mogi* [1969] doughnut prior to the Kern County earthquake; we have not observed similar localized reductions in activity prior to the other cases of strong earthquakes in this magnitude range.

As noted, activity in the southern region before and after the Kern County earthquake, even after removing aftershocks, did not diminish significantly but continued at a high level up to the time of the San Miguel earthquake. Figure 7d is a map of the intermediate-magnitude epicenters between the times of these two strong earthquakes. The majority of the earthquakes in this interval lie astride the international border and extend about 150 km to the north of the San Miguel epicenter; we do not have complete magnitude information for earthquakes to the south of the boundary to the region for this time interval, and hence we do not know whether the pattern of epicenters extends beyond the southern boundary, nor if this epicenter is at the periphery of the spatial pattern or not. In Figure 7e we show the epicenters of earthquakes in the first 5 years after the San Miguel earthquake; much of the activity remaining after the Kern County earthquake has been switched off after the San Miguel earthquake; about 5 years after the San Miguel earthquake, activity begins to revive (Figure 7f). In this case and several cases to follow, we see that activity is not switched off by a first strong earthquake; instead, a second strong earthquake follows after the first in less than roughly 5 years. Activity is then switched off by the second strong earthquake of the pair.

Figure 7g is a map of the intermediate-magnitude earthquakes in the southern region in the 7.3-year interval from February 28, 1985 to June 28, 1992, the latter being the date of the Landers earthquake. The earthquakes are again spread over a large, elongated part of the southern region, which is about the same as that for the Kern County and San Miguel earthquakes. The precursory pattern probably should include the three earthquakes south of the regional boundary to the southern region as defined. But since the southern boundary was defined by the southern California catalog prior to 1965, only earthquakes within the southern region as specified were used to define the peak in the activity before the Landers earthquake; the earthquakes outside the region may be of value to help identify switch-off or its absence. The Landers earthquake also was at the periphery of the area of increased activity prior to it and the fault break extended outside and to the north of the pattern.

The recency of the Landers earthquake makes it dif-

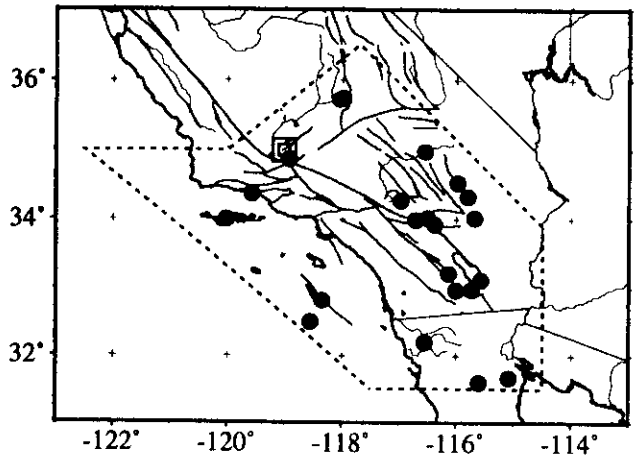

Figure 7a. Epicenters of intermediate-magnitude earthquakes $5.1 \leq M \leq 6.7$(dots) before and after strong earthquakes with $M \geq 6.8$ (squares). Regions are outlined by dashed lines. Twelve-year interval before the Kern County earthquake from May 19, 1940, to July 21, 1952.

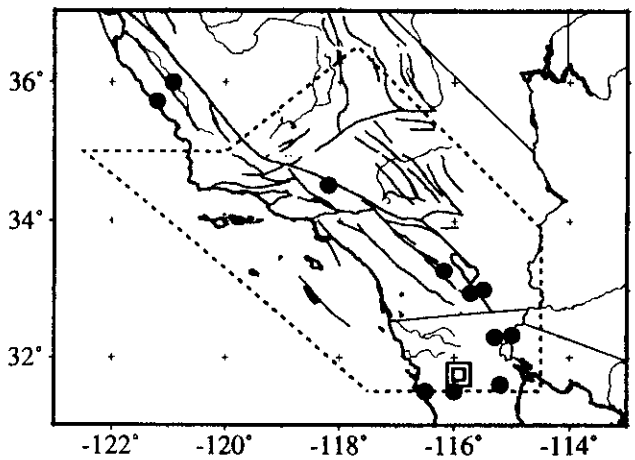

Figure 7d. 3.5-year interval between the Kern County July 21, 1952, and San Miguel February 9, 1956 earthquakes.

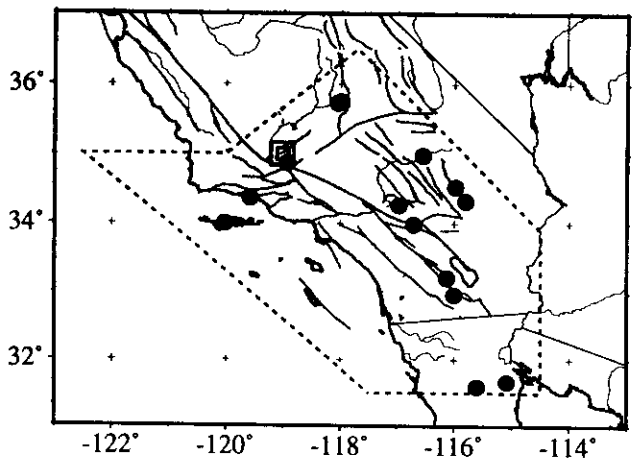

Figure 7b. Seven-year interval before the Kern County earthquake from May 19, 1940, to July 21, 1947.

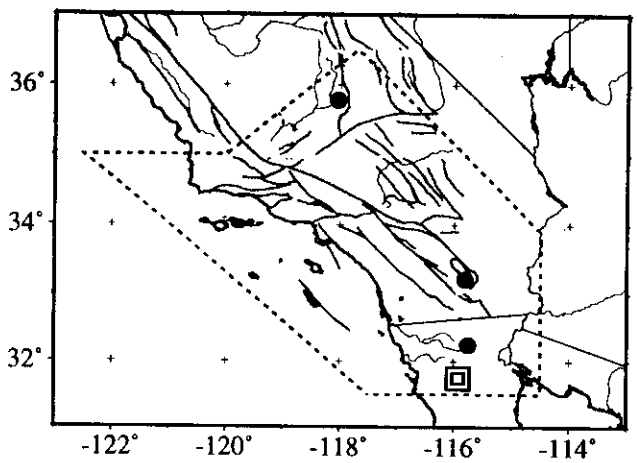

Figure 7e. Five-year interval after the San Miguel earthquake from February 9, 1956, to February 8, 1961.

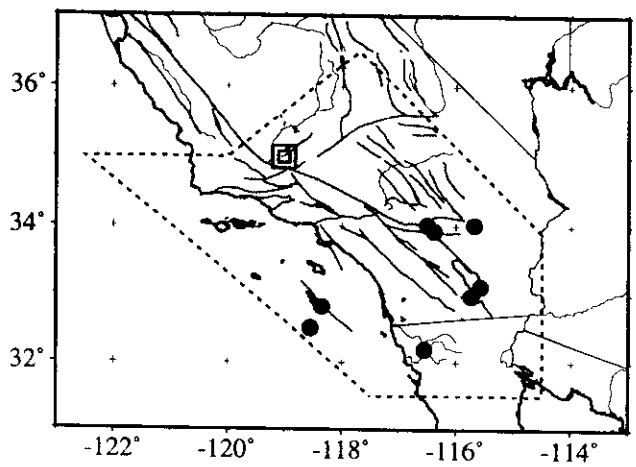

Figure 7c. Five-year interval before the Kern County earthquake from July 22, 1947, to July 21, 1952.

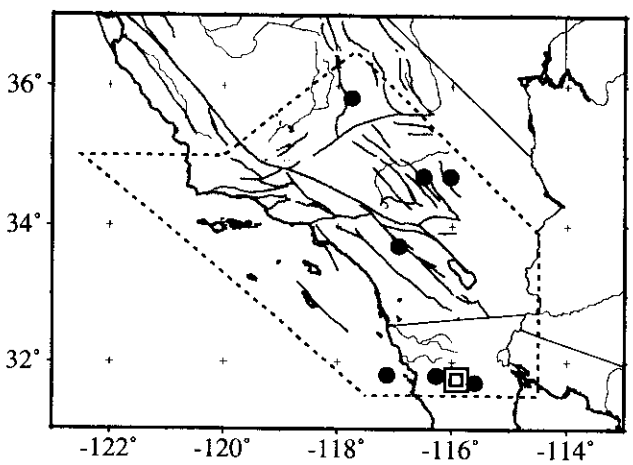

Figure 7f. Five-year interval after the San Miguel earthquake from February 9, 1961, to February 8, 1966.

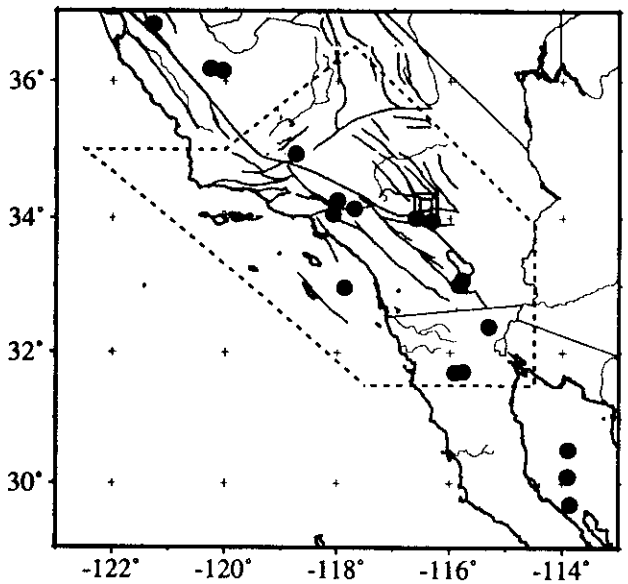

Figure 7g. 7.5-year interval before the Landers earthquake from February 28, 1985, to June 28, 1992.

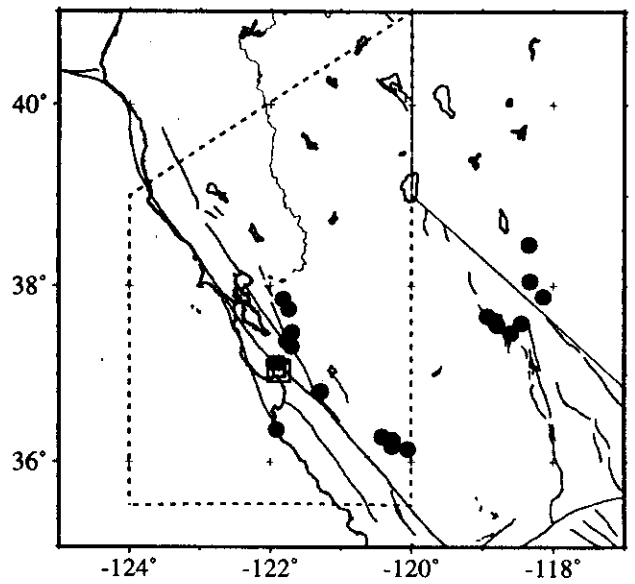

Figure 7h. Ten-year interval before the Loma Prieta earthquake from October 19, 1979, to October 18, 1989.

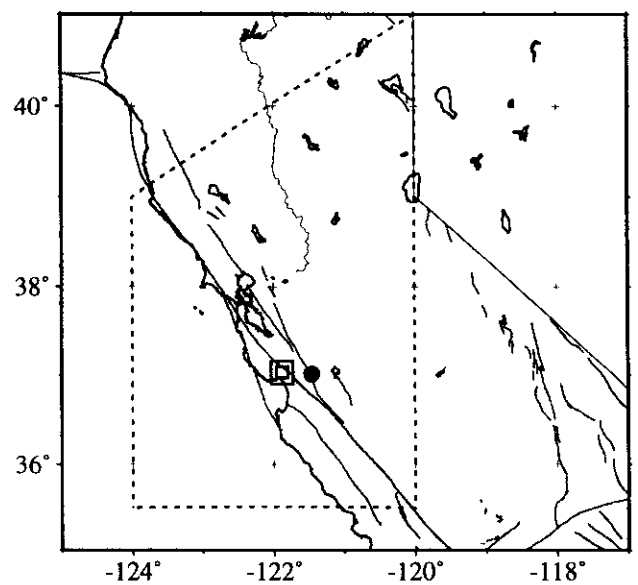

Figure 7i. 3.5-year interval after the Loma Prieta earthquake from October 18, 1989, to March 25, 1993.

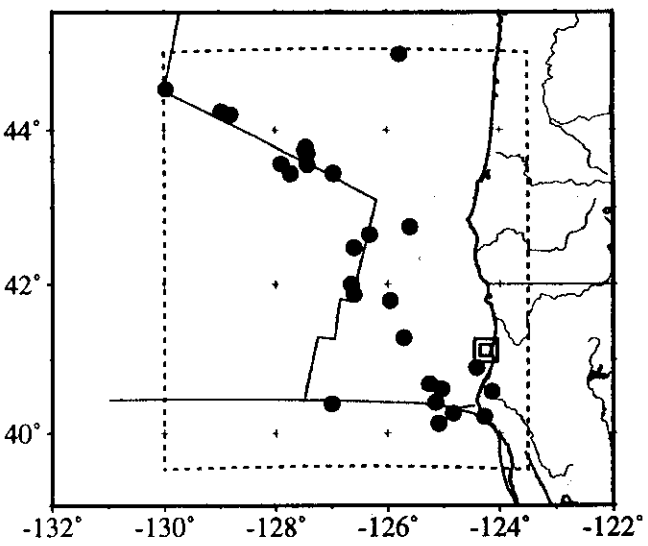

Figure 7j. Thirteen-year interval between November 9, 1967, and earthquake of November 8, 1980.

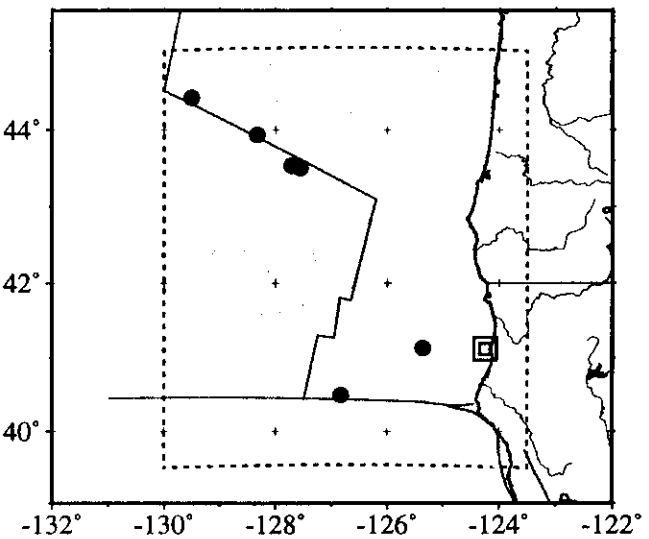

Figure 7k. Five-year interval between earthquake of November 8, 1980, and November 7, 1985.

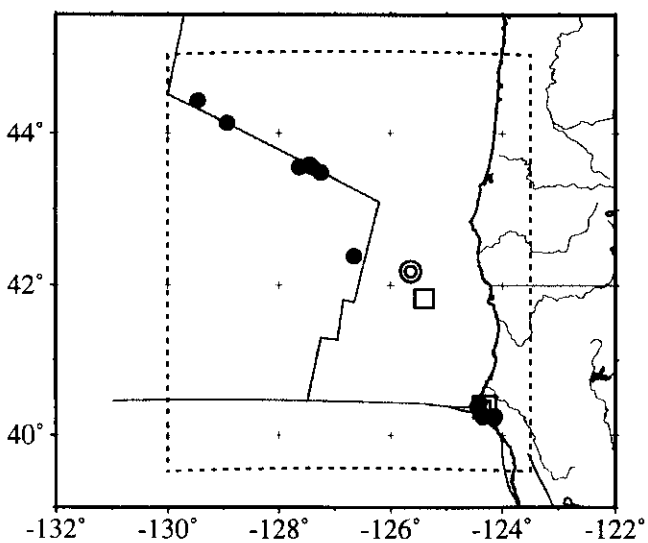

Figure 7ℓ. Six-year interval between April 26, 1986, and Petrolia earthquake ($M = 7.1$, double square) of April 25, 1992. Also shown are earthquakes of July 13, 1991 ($M = 6.9$, double circle), and August 17, 1991 ($M = 7.1$, double square).

ficult to determine the level of activity after it. In the 2.5 years between the Landers earthquake and the end of 1994, four earthquakes with $M \geq 5.1$ occurred in the region, other than aftershocks. Taken literally, this implies a high rate of activity after the Landers earthquake, and would imply that activity was not switched off abruptly by the Landers earthquake. One of these four events was the Northridge earthquake. Two of the remaining three earthquakes with $M \geq 5.1$ occurred in the interval between the Landers and Northridge earthquakes, implying that the activity was high after the Landers earthquake. There is thus a suggestion that the Landers and Northridge earthquakes are paired as suggested by *Levshina and Vorobieva* [1992], as were the Kern County and San Miguel earthquakes and hence that the Landers event was part of the precursory sequence that anticipated the Northridge earthquake. The Northridge earthquake is too recent an event for us to determine whether intermediate-magnitude seismicity after it has been switched off and that Northridge is the terminator of this sequence.

Central Region

The activity before the Loma Prieta earthquake has already been discussed at magnitude level $M = 5.5$ (see Figure 1). At the lower threshold for the intermediate-magnitude earthquakes of 5.1 that we consider here, several additional events are added to the map (Figure 7h). Except for the Coalinga events in the southeastern part of the region, the epicenters span a triangular region a little over 1° on a side with the Loma Prieta earthquake itself near the middle. The Mammoth Lakes/Western Nevada events, near longitude 118.5° lie outside the region, are not needed to define the peak in windowed activity, and were not used in the construction of Figure 5b. In the 3.5 years since the occurrence of the earthquake, the activity in the central region has been minimal (Figure 7i). Activity in the Mammoth Lakes/Western Nevada region is completely absent after the Loma Prieta earthquake at the threshold of $M = 5.1$. Both the nuclei of activity that are near the focus and near Mammoth Lakes appear to follow the model pattern of increase and extinction associated with the Loma Prieta earthquake.

Northern Region

Intermediate-magnitude epicenters for the 13 years prior to the Eureka, California, earthquake of November 8, 1980 ($M = 7.0$), fall in an elongated zone extending NW-SE over a distance of about 700 km in its long dimension (Figure 7j). The events include earthquakes on the major units of the plate boundary, namely the Mendocino Fracture Zone, the Gorda Ridge, and the Blanco Fracture Zone; there are also some intraplate earthquakes that extend from Cape Mendocino to the northern end of the Gorda Ridge, and give the structure a linear aspect. The Eureka earthquake is at the periphery of the zone of precursory activity. The map of epicenters with $M \geq 5.1$ which displays the activity in the 5 years after the Eureka earthquake, is given in Figure 7k. The annual rate of earthquakes in the 5 years after the Eureka earthquake (1980) is reduced by a factor of about 2 from that in the 13 years before it. This decrease is almost completely due to the cessation of activity from about latitude 43° southward, that is, along the Gorda Ridge and the Mendocino Fracture Zone and along the eastern part of the Blanco Fracture Zone. Activity was not reduced to zero because the western part of the Blanco Fracture Zone continued active at the same rate as before the 1980 earthquake. The maximum dimensions of the region of reduction is about 350 km.

We have already commented on the unusual outburst of strong earthquakes with $M \geq 6.8$ in the interval 1991 to 1995 in this region. There are also several strong events with magnitudes just below this threshold. Two strong aftershocks of the 1992 earthquake, both with $M = 6.6$, occurred within 18 hours of the main shock. In addition a $M = 6.6$ event in 1984 was the westernmost event on the Mendocino Fracture Zone shown in Figure 7k. The space-time interrelationships of the activity before and after the five strong earthquakes overlap on a timescale that is short compared with those that we have considered for the southern and central regions. Thus an interpretation on the basis of simple models that apply in the other two regions is much more difficult. The use of a strong earthquake threshold at $M = 6.8$ may also be questioned in this case; we have continued to use it in this discussion to make our analysis uniform from region to region.

Figure 7ℓ shows the seismicity in the 6 years before the Petrolia earthquake ($M = 7.1$, August which is the second of the pair (1992) of strong earthquakes within the northern region. Figures 7j, 7k,and 7ℓ show an almost complete preevent, postevent, and again preevent sequence; not enough time has elapsed since the 1995 earthquake, the last of the quintuplet, to determine whether the activity will drop or remain high. In the precursory episode before the 1992 Petrolia earthquake, seismicity along the Mendocino Fracture Zone was clustered very closely around the site of the subsequent Petrolia earthquake (1992); the two strong earthquakes with magnitudes 6.9 and 7.1 in this interval do not lie on the plate boundary segments; seismicity on the Blanco Fracture Zone continued unabated at about the same rate as in the preceding 20 years.

Summary Thus Far

Despite individual differences in the patterns of occurrence of earthquakes in all three regions, there is a common feature that can be discerned. The entire region becomes active before a strong earthquake. When strong earthquakes switch off the activity of

intermediate-magnitude earthquakes, they do so to distances of the order of 250 km or even larger. We note that the seismicity in the southern and central regions has a strong imprint of the more-or-less linear fault patterns that correspond to the geometry of the San Andreas Fault, whereas the plate boundaries in the northern region have a complex angular structure which carries the implication that the stress fields are likely to have an even more complex geometry than in the central and southern regions, and that the tensor character of stress redistribution by these earthquakes as an influence on self organization of the stress field may be more important in this region than to the south.

In summary, the rate of intermediate-magnitude occurrence is high at the time of all eight strong earthquakes with magnitudes greater than 6.8 and is above the 75% threshold before seven of the eight. No strong earthquakes occur when the activity is low. The linear dimensions of the cloud of epicenters in each activity peak is much larger than the classical fracture dimensions of the subsequent strong earthquake. The causal relationship between the precursors and the strong earthquakes which follow them is established by the relatively rapid switch off of the intermediate-magnitude activity immediately after some strong earthquakes; in the other cases for which activity following a strong earthquake remains high, a second strong earthquake occurs within a few years. The range of the switch off of activity is much larger than the classical fracture dimensions of the subsequent strong earthquake. The geometry is complex, especially in the case of the northern region, and its importance in the development of self organization has not been considered here.

We list the strong earthquakes we have used in this paper in Table 1. A quantitative measure of the reduction of activity after three of the strong earthquakes is given in the last column; the entry is the ratio of the average annual number of intermediate-magnitude earthquakes in the interval between the time of start of the window when the threshold is reached to the strong earthquake, to the number of intermediate-magnitude earthquakes in the 5 years after the earthquake. In the

Table 1. Strong Earthquakes $M \geq 6.8$

	Date	Time, UT	Location °N	°W	Magnitude	Reductions
		Southern Region				
Imperial Valley[a]	1940 May 19	0436	32.73	115.50	6.9	···
Kern County[b]	1952 July 21	1152	35.00	119.02	7.5	···
San Miguel[b]	1956 Feb. 09	1432	31.75	115.92	6.8	3.9
Landers[c]	1992 June 28	1157	34.20	116.44	7.3	···
(Northridge[c,d]	1994 Jan. 17	1231	34.56	118.76	6.7	···)
		Central Region				
Loma Prieta	1989 Oct. 18	0004	37.04	121.88	7.0	5.3
		Northern Region				
Eureka	1980 Nov. 08	1028	41.12	124.25	7.0	1.9
---[d,e]	1991 July 13	0250	42.18	125.64	6.9	···
---[d]	1991 Aug. 17	2217	41.82	124.40	7.1	···
Petrolia[d]	1992 April 25	1806	40.37	124.32	7.1	···
---[d,f]	1994 Sept. 01	1515	40.41	125.65	7.0	···
---[d,f]	1995 Feb. 19	0403	40.56	125.53	6.8	···
		Southern Region ($6.4 \leq M < 6.8$)				
Borrego Mountain[g]	1968 April 09	0228	33.19	116.13	6.5	···
San Fernando[g]	1971 Feb. 09	1400	34.41	118.40	6.6	5.6

[a]Reliable windowed activity determined only after this earthquake.
[b]Kern County and San Miguel precursor series coupled.
[c]Landers and Northridge precursor series presumed coupled.
[d]Precursor series coupled. Too recent to allow determination of windowed activity after earthquakes.
[e]In precursory pattern of 1991 August 17.
[f]Aftershocks of Petrolia earthquake.
[g]Borrego Mountain and San Fernando precursor series coupled.

case of paired strong earthquakes, the earthquakes "before" are counted from the time of the crossing of the threshold before the first of the pair to the time of the second of the pair; the earthquakes "after" are those in the 5-year interval after the second of the pair. The windowed activity decreases by a factor of between roughly 2 and 5 after the three cases of strong earthquakes with magnitudes $M_{th} \geq 6.8$.

The Kern County and Landers Earthquakes

We try to construct a generalization of the foregoing observations as follows: Strong earthquakes with magnitudes $M \geq M_{th}$ are preceded over a specified time interval and in a fixed region by an increase of the number of earthquakes in the magnitude range $(M_{th}-1.7) \leq M < M_{th}$, and in some cases by an abrupt decrease in the rate of occurrence of earthquakes in this magnitude range. We use this definition to test an assumption that there is a self similar or scaling principle involved in the fluctuations and their relation to the strong earthquakes. The Kern County and Landers earthquakes in the southern region are significantly stronger than any other events. It seems appropriate to study them separately. For the purposes of this section, we redefine strong earthquakes to be those with $M \geq M_{th} = 7.3$, which is the magnitude of the smaller of the two earthquakes. We use the same 5-year window as before, but raise the lower threshold that defines the intermediate-magnitude earthquakes to 5.6, to correspond to the definition above. With these parameters, we obtain precursory peaks in windowed activity before these two earthquakes as seen in Figure 8.

The spatial extent of increased intermediate-magnitude precursory activity is essentially the same as before, as expected, since many of the same earthquakes are used in the analysis of both the preceding section and this section. Again, activity in part of the region was extinguished before the Kern County earthquake; the remaining part was switched off by the subsequent $M = 6.8$ San Miguel earthquake.

There are two subthreshold peaks in Figure 5a near 1970 and 1983. These are mainly defined by earthquakes in the magnitude 5.1 to 5.3 range; these peaks are much less pronounced in Figure 8. Because of the suppression of these two peaks, the pattern of Figure 8 shows a much greater correlation of the peaks in activity as precursors of the strong earthquakes, with the activity being defined at a higher threshold magnitude level. In both the cases of strong earthquakes with $M_{th} = 6.8$ and 7.3, the precursors extend to large distance and are not concentrated in the neighborhood of the future strong earthquake. Because the data are partially overlapping in the two cases, the second set of results is evidently insufficient to provide verification and can only give qualitative support to the assumption.

Strong Earthquakes With Magnitudes $M \leq 6.7$

Above, we have identified correlations between fluctuations in activity both before and after only seven earthquakes. To enlarge the data set, we attempted to explore fluctuations in activity and their correlation with more abundant earthquakes with threshold magnitudes. Accordingly we selected for study the 12 strong earthquakes in the three regions with $6.4 \leq M \leq 6.7$, and set $M_{th} = 6.4$. These earthquakes in the southern region recur so frequently, that we were obliged to reduce our window interval to 2 years to avoid possible overlap among fluctuations; as above, we determine intermediate-magnitude activity in the range $4.7 \leq M \leq 6.3$. While the activity with these param-

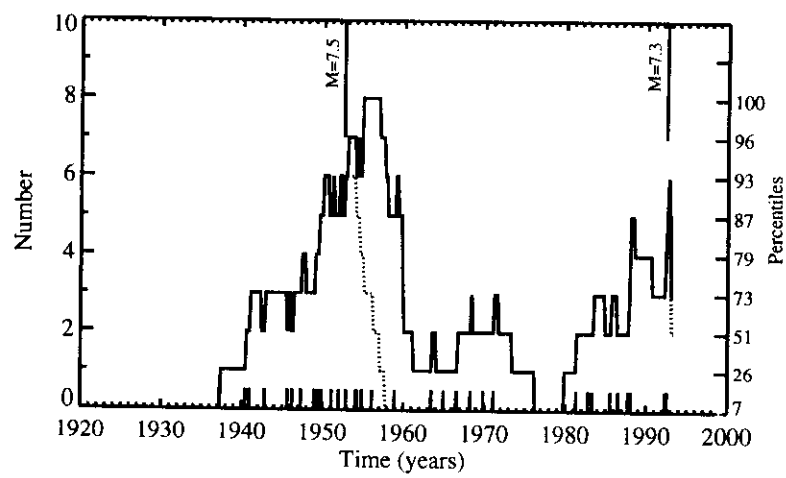

Figure 8. Windowed activity in the southern region. Solid curve is the number of earthquakes with $5.6 \leq M \leq 7.2$ in a 5-year sliding window. Dashed curve is the contribution from earthquakes occurring before the Kern County ($M = 7.5$) and Landers ($M = 7.3$) earthquakes. Heavy vertical lines indicate the times of these two events.

eters does indeed fluctuate with large amplitudes and relatively high frequency, it is not as strongly correlated with strong earthquakes in the $M_{th} = 6.4$ category as in the previous cases. The number of failures-to-correlate is larger, both in terms of peaks of activity above the 75% threshold that were not followed by strong earthquakes and, in one case, of a strong earthquake that was not anticipated by a peak. In the cases where prior peaks in activity are correlated with subsequent strong earthquakes, the reduction in activity after these strong earthquakes is significantly smaller than in the cases of strong earthquakes with magnitudes $M \geq 6.8$. We believe the general lowering of the "signal-to-noise" ratio for this type of diagnostic is due to use of a lower threshold for intermediate magnitude earthquakes of 4.7 that approaches the magnitude range where temporal fluctuations in the rate of occurrence are now no longer significant statistically, at least on the timescale of 15 years (see Figure 4).

The activity extending from before the April 9, 1968 Borrego Mountain earthquake ($M = 6.5$) to after the February 9, 1971, San Fernando earthquake ($M = 6.6$) (Figure 9a, 9b, and 9c) is a significant exception to the generally poorer identification of these correlations with decreasing M_{th}. This sequence of events also allows us to assess the importance of earthquakes in and near the Gulf of California, that lie outside the southern region.

The threshold for identification of a peak was set at 72%, a value that is closest to our convention of 75% and differs from it because of the discreteness of counting individual earthquakes. There are seven intermediate-magnitude earthquakes located in the southern region in the time interval from 2 years before the 72% threshold (determined for the interval 1935 to 1993) was crossed up to the date of the Borrego Mountain earthquake; activity in and around the Gulf of California is much higher. The activity between the 1968 and 1971 earthquakes both within the southern region and the Gulf to the south of it, is not reduced after the 1968 earthquake, although some activity within the southern region appears for the first time offshore in the interval between the two strong earthquakes. During the 2 years after the San Fernando earthquake, the activity fell to a

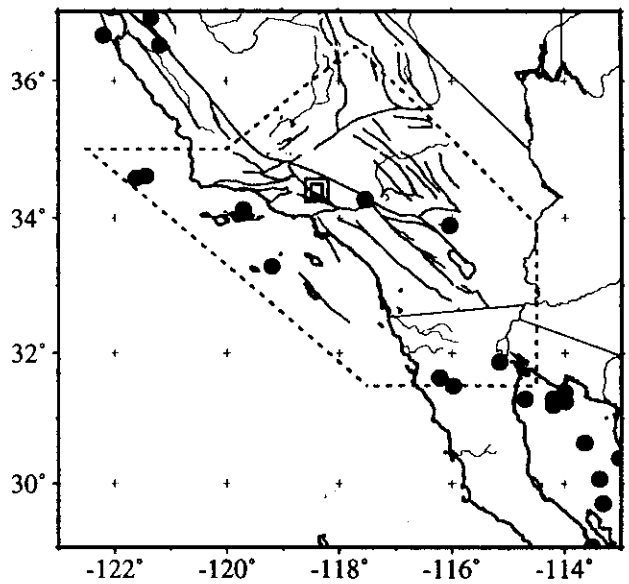

Figure 9b. Earthquake epicenters in the southern region in the range $4.7 \leq M \leq 6.3$ in the 3-year interval between the Borrego Mountain earthquake (April 9, 1968) and the San Fernando earthquake (February 9, 1971).

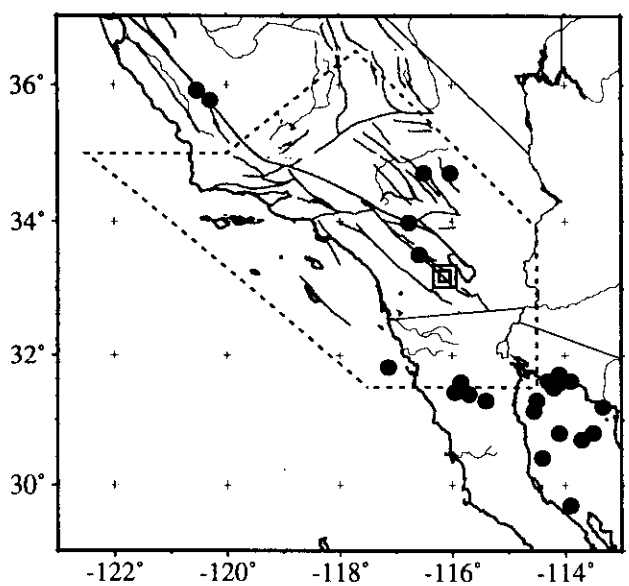

Figure 9a. Earthquake epicenters in the southern region in the range $4.7 \leq M \leq 6.3$ in the 3-year interval from January 1, 1965, to the Borrego Mountain earthquake, April 9, 1968.

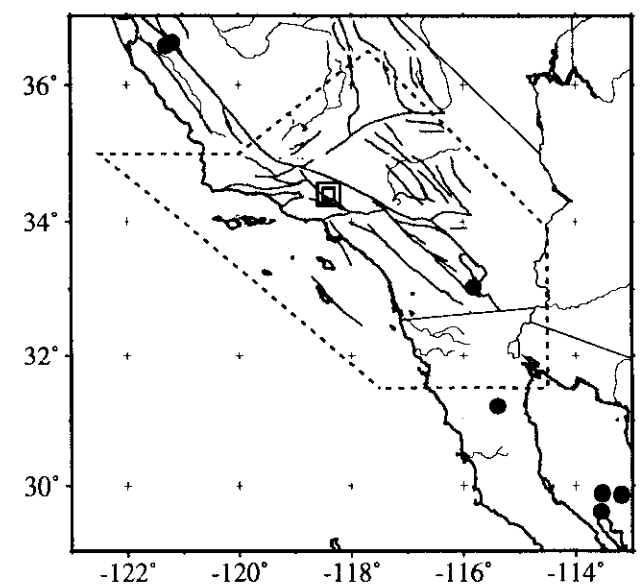

Figure 9c. Earthquake epicenters in the southern region in the range $4.7 \leq M \leq 6.3$ in the 2-year interval between the San Fernando earthquake of February 9, 1971, and February 8, 1973.

very low level both inside and outside the boundaries of the region. The decrease in activity immediately after the San Fernando earthquake extends to a distance of as much as 800 km! The San Fernando epicenter lies at the periphery of the distribution of precursory events. The annual rate of activity within the southern region was reduced by a factor of 5.6 after the San Fernando earthquake; the reduction was also large to the south of the southern region. We have included this pair of strong earthquakes in our listing in Table 1.

Parameter Range of Precursory Activity

Threshold for Strong Earthquakes

We discuss the sensitivity of the analysis to the choices of the parameters in this search for increases in precursory activity. The lower magnitude threshold that defines strong earthquakes is an important ingredient in our proposal that strong earthquakes are anticipated by an increase in temporal activity of intermediate-magnitude earthquakes that spans a larger part of the specific region. If the magnitudes we have used for the strong earthquakes are significantly in error, then strong earthquakes will be added to or deleted from the list, and the correlations with fluctuations in activity may not be as good as it is. Our results are relatively stable with regard to the choice of this threshold. There is a naturally occurring gap in the magnitude distribution for the time intervals of the catalogs at around $M = 6.5$ or 6.6. Unless there are significant errors in the magnitudes of the earthquakes by 0.2 or more, the population with magnitudes greater than 6.8 is not likely to be changed. If we had lowered our value of M_{th} from 6.8 to 6.7, then the Northridge earthquake would have been well correlated as a pair to the Landers event, as discussed above; our exclusion of the Northridge earthquake from the original discussion by our a priori choice of the higher threshold, or if the magnitude of this event had been slightly higher at $M = 6.8$, then our success rate would have been eight out of nine events instead of seven out of eight.

Definitions of Regions

We have carried out a number of tests that confirm what is to be expected from inspection of Figure 7. If the sizes of the regions are reduced so that fewer intermediate-magnitude earthquakes are included, then the correlations implied by Figure 5 disappear. We interpret this statement to mean that the interactions implied by the abrupt reductions in activity are indeed long range to distances that are a significant fraction of the extent of our three regions. We do not believe the increase in activity before strong earthquakes implies an interaction. We have searched for correlations at distance scales greater than the sizes of these regions, and while they are indeed observed, there is a tendency to introduce a greater number of "false alarms" into the analysis, for example, by attaching the Parkfield or Coalinga earthquakes to the southern region and deleting them from the central region. The conclusions about the peak in activity before Parkfield are not altered whether one includes the Mammoth Lakes earthquakes in the central region or not; if we had incorporated the eastern Sierra into the central region, our result regarding the anticipation of the Loma Prieta earthquake would have been strengthened. We have only the one example of the Loma Prieta earthquake to define the central region, and we cannot generalize.

Our principal concern in regard to the choice of boundaries to the regions, involves the question of the inclusion of the earthquakes in Mexico to the south of the boundary to the southern region. We have commented on this issue; since there was a significant reduction in activity south of the boundary after the San Fernando earthquake, we conclude that the natural boundary lies to the south of the one we have used.

Activity Windows

The correlations between the intermediate-magnitude precursory peaks of windowed activity and the subsequent strong earthquakes persist even if the durations of the activity windows are changed within reasonable limits. If the width of the window were to be reduced to a sufficiently small value, then our measure of windowed activity would be an irregular comb of delta functions of unit height, as are displayed at the bottoms of Figures 5 and 8. To determine the density of spikes on the comb, we would have to apply a smoothing window as we have done. If the width of the window were set too large, then we lose our ability to resolve the onset and prolongation of the active state; that is, we must choose a window that is shorter than the duration of the interval of increased activity. Since this time is about 10 years in the Loma Prieta case and is about the same in the other examples, the time constant of 5 years is probably an appropriate choice for these strong earthquakes. We have varied the widths of the windows over the range 2 to 10 years in the case of strong earthquakes with $M \geq 6.8$ and $M \geq 7.3$ and find that precursory activity can still be identified and correlated with strong earthquakes satisfactorily. The choice of a square window is not optimal; we do not report here results from a number of experiments in this direction.

Intermediate-Magnitude Threshold

In this paper the lower threshold of intermediate-magnitude windowed activity was chosen to be 1.7 magnitude units below that of the smallest of the strong earthquakes in each of the categories. If this threshold were significantly raised, then the number of precursory earthquakes would become so small that peaks of intermediate-magnitude windowed activity would not

be identifiable. At the other extreme, as this threshold is lowered, we lose our ability to identify precursory activity. In general, the correlations between the activity and strong earthquakes with $M_{th} = 6.8$ start to disappear when the lower intermediate-magnitude threshold is lowered below about 4.6, which, as remarked, we believe is due to the absence of resolvable fluctuations at this magnitude. Indeed, if the threshold is lowered to 4.0, the fluctuations become erratic and quite uncorrelated with the strong earthquakes. In general, a variation of ± 0.25 magnitude units in the lower threshold of intermediate-magnitude earthquakes leaves the correlations intact.

Activity threshold

In the results summarized above, the windowed activity threshold was set to be about 75% by a posteriori parameter fitting. For the northern region, the choice of the percentile windowed activity threshold is additionally complicated by the low degree of fluctuation in the windowed activity (Figure 5c). For example, the interval between the 32nd and 74th percentiles is strongly compressed and hence the interpretation is unstable in regard to the choice of this parameter; a reduction of the size of the northern region to exclude the seismicity on the Blanco Fracture Zone, improves the stability slightly. At bottom, the problem with regard to this parameter is the relatively low level of intermediate-magnitude seismicity in all regions. We do not have much hope of increasing the size of the data sets: We are limited by the geophysical constraints on the parameters we have discussed; namely, how much the lower magnitude threshold for intermediate-magnitude earthquakes can be lowered, the spatial restrictions of the bounds to the regions from the gaps in seismicity, and the temporal widths of the filter windows, constrained by the frequency of occurrence of strong earthquakes in California.

In summary, the correlations are not an artifact of special conditions arising from our analysis. They are found for a broad range of the parameters and are not fine-tuned to specific values of these parameters.

Aftershock Identification

We have performed an activity analysis similar to the above but without filtering out the aftershocks of earlier earthquakes. Our use of an aftershock rejection filter focuses our attention on activity at distances of the order of hundreds of kilometers and more from the strong earthquake, a distance range not heretofore investigated significantly. Without the use of aftershock rejection, we could not have observed what may be the most important part of these observations; namely, the sharp decline in intermediate-magnitude activity outside the "classical" aftershock region that takes place almost immediately after the strong earthquake. We have varied the parameters of the aftershock filter within small limits without damaging our conclusions.

Summary and Comments

We have shown that the rate of occurrence of intermediate-magnitude earthquakes increases significantly before all the strong earthquakes in the magnitude range $M \geq 6.8$. Intermediate-magnitude earthquakes with magnitudes less than 4.5 or so do not seem to participate in the process. The high activity for the precursory intermediate-magnitude events either drops significantly and abruptly after a strong earthquake, or it remains high until a subsequent strong earthquake occurs within a short time. Not infrequently, strong earthquakes may occur in pairs and that it is the second member of the pair that switches off the intermediate-magnitude activity; in one example, these earthquakes have occurred at least as a quintuplet.

The precursory earthquakes involved in the increase of activity are distributed widely over broad geographical areas; these events almost fill the outlines of our geographical regions as defined. The same region is reactivated with precursors before every strong earthquake in the region. The size of the precursory does not appear to be significantly scaled by the magnitude of the subsequent strong event, at least for these strongest earthquakes. In most cases, the strong earthquakes occur at the periphery of the zones of intermediate-magnitude activity, implying the presence of well-demarked zones of quiescence outside the active areas. The precursors to the strong earthquakes appear over a time interval of the order of 5 to 10 years before the strong earthquake, although onset began about 25 years before the San Francisco earthquake. In the case of the Loma Prieta and San Francisco earthquakes, the onset of precursory activity appears to be relatively abrupt.

Intermediate-magnitude activity is best correlated with strong earthquakes in the range $M \geq 6.8$. It is less well defined for strong earthquakes with smaller magnitudes. We speculate that if it should turn out that fluctuations in activity are indeed associated with strong earthquakes having smaller magnitudes, then the areas over which precursory activity will be correlated will be smaller than the regions we have explored [*Keilis-Borok and Kossobokov,* 1990], that is, that scaling is involved in the process.

The dimensions of the active regions that are switched off by the strong earthquakes are many times larger than the classical fracture length of the strong event, and point to interactions in the switch off mechanism that have very long range. This range is from 250 to 450 km in distance from these strong earthquakes, and in the case of the San Fernando earthquake, the range of reduction of activity is much larger. Within our present ability to resolve temporal relationships, the decrease in activity appears to be contemporaneous with the strong earthquake, without substantial lag; thus the reductions

in activity appear to be causally related to the occurrence of the strong earthquakes and to remarkably large distances. There is no evidence to suggest that the precursor earthquakes directly influence the time and location of the subsequent strong earthquake.

The choice of parameters in this program is arbitrary; some flexibility in their choice is possible. However, if the parameters are changed too much, the correlations disappear. Of greater concern to us has been our use of discrete thresholds for magnitudes and times, and fixed regional boundaries. We hope that future developments will include the construction of a diagnostic model that is less dependent on discrete choices of parameters; a modification of this program to include adjustable parameters lies beyond this first thrust into the identification of these correlations.

This paper has not been an essay on earthquake prediction nor have we attempted to construct a physical model of the phenomenology we have described. This paper has been concerned with the phenomenology of earthquake occurrence in and around California; we have searched for precursory activity in the space-time-magnitude parameter space of the earthquake history of California. Nevertheless, the phenomenological findings in this paper have implications for the physics of the evolution of seismicity in California. Evidently the fluctuations in activity are related to fluctuations in the stress field associated with earthquake occurrence. The scale size of these events, even at the magnitude 5.5 level is so small that the redistribution of the stress field by the intermediate-magnitude earthquakes is not significant at distances of the order of hundreds of kilometers. Thus the presence of precursor earthquakes distributed over large distances are an indicator that the stress field is greater than a critical threshold for fracture and this elevation is widespread over large distances, that is, the precursory seismicity is a qualitative stress gauge. If the stress fields due to intermediate-magnitude earthquakes do not directly serve as triggers of future strong earthquakes at distances that are orders of magnitude larger than their scale size, the converse does not seem to hold, which raises serious questions regarding the physical processes that are involved. How can a strong earthquake with fracture dimensions of 30 to 75 km effectively reduce the stress at distances of the order of hundreds of kilometers by, as we estimate, as much as perhaps 10 bars, and do so relatively rapidly? Clearly, models based on the stress redistributions to be expected due to the introduction of cracks into an elastic continuum are inappropriate. We are seeking answers to the question by studying nonelastic processes, such as the role of possible fluctuations of stresses due to the presence of fluids in the fault network of the seismogenic slab. A discussion of these issues will be presented elsewhere.

Appendix

The following are catalogs of earthquakes in the three regions for earthquakes with magnitudes greater or equal to 5.1. Aftershocks have been removed.

Table A1. Earthquakes of the Southern Region with $M \geq 5.1$

Date	Time, UT	Location °N	°W	Magnitude
1935 Oct. 24	1448	34.10	116.80	5.1
1935 Dec. 20	0745	33.17	115.50	5.2
1937 March 25	1649	33.41	116.26	6.0
1938 May 31	0834	33.70	117.51	5.2
1940 May 18	0503	34.08	116.30	5.3
1940 May 19	0436	32.73	115.50	6.9
1940 Dec. 07	2216	31.67	115.08	6.0
1941 July 01	0750	34.37	119.58	5.5
1941 Sept. 21	1953	34.87	118.93	5.1
1942 Oct. 21	1622	32.97	116.00	6.6
1943 Aug. 29	0345	34.27	116.97	5.3
1943 Dec. 22	1550	34.33	115.80	5.3
1944 June 12	1116	33.99	116.71	5.2
1945 April 01	2343	34.00	120.02	5.1
1945 May 12	0733	31.60	115.60	5.2
1945 Aug. 15	1756	33.22	116.13	5.7
1946 March 15	1321	35.75	117.99	5.5
1946 March 15	1349	35.73	118.05	6.0
1946 July 18	1427	34.53	115.98	5.5
1947 April 10	1558	34.98	116.55	6.5
1947 July 24	2210	34.02	116.50	5.3
1948 Feb. 24	0815	32.50	118.55	5.3
1948 Dec. 04	2343	33.93	116.38	6.0
1949 May 02	1125	34.02	115.68	5.8
1949 Nov. 04	2042	32.20	116.55	5.7
1950 July 28	1750	33.12	115.57	5.4
1950 July 29	1436	33.12	115.57	5.5
1951 Jan. 24	0717	32.98	115.73	5.8
1951 Dec. 26	0046	32.82	118.35	5.9
1952 July 21	1152	35.00	119.02	7.5
1952 Aug. 23	1009	34.52	118.20	5.1
1952 Nov. 22	0746	35.73	121.20	6.0
1953 June 14	0417	32.95	115.72	5.5
1954 Feb. 01	0423	32.30	115.30	5.2
1954 Feb. 01	0432	32.30	115.30	5.6
1954 March 19	0954	33.28	116.18	6.4
1954 May 31	0806	31.60	115.20	5.2
1954 Oct. 17	2257	31.50	116.50	5.7
1954 Oct. 24	0944	31.50	116.00	6.0
1954 Nov. 12	1226	31.50	116.00	6.3
1955 April 25	1043	32.33	115.00	5.2
1955 Nov. 02	1940	36.00	120.92	5.2
1955 Dec. 17	0607	33.00	115.50	5.2
1956 Feb. 09	1432	31.75	115.92	6.8
1957 April 25	2157	33.22	115.81	5.2
1958 Dec. 01	0321	32.25	115.75	5.8
1961 Jan. 28	0812	35.78	118.05	5.3
1961 Oct. 19	0509	35.83	117.76	5.4
1962 May 27	0145	31.70	115.60	5.1
1963 June 11	1523	31.80	116.27	5.8
1963 Sept. 23	1441	33.71	116.93	5.1
1964 Dec. 22	2054	31.81	117.13	5.6

Table A1. (continued)

Date	Time, UT	Location °N °W	Magnitude
1965 Sept. 25	1743	34.71 116.50	5.2
1965 Sept. 26	0700	34.71 116.03	5.1
1966 June 28	0426	35.92 120.53	5.6
1966 Aug. 07	1736	31.80 114.50	6.3
1968 April 09	0228	33.19 116.13	6.5
1968 July 05	0045	34.12 119.70	5.3
1969 Oct. 22	2251	34.58 121.62	5.4
1969 Oct. 24	0829	33.29 119.19	5.1
1969 Nov. 05	1754	34.61 121.44	5.6
1970 Sept. 12	1430	34.27 117.54	5.2
1971 Feb. 09	1400	34.41 118.40	6.6
1973 Feb. 21	1445	34.06 119.04	5.3
1978 May 05	2103	32.21 115.30	5.2
1978 Aug. 13	2254	34.35 119.70	5.1
1979 Jan. 01	2314	33.94 118.68	5.2
1979 March 15	2107	34.33 116.44	5.3
1979 Oct. 15	2316	32.61 115.32	6.4
1980 Feb. 25	1047	33.50 116.51	5.5
1981 April 26	1209	33.10 115.63	5.7
1981 Sept. 04	1550	33.67 119.11	5.5
1982 Oct. 25	2226	36.29 120.41	5.6
1983 May 02	2342	36.25 120.26	6.3
1985 Aug. 04	1201	36.15 120.05	5.8
1986 July 08	0920	34.00 116.61	5.6
1986 July 13	1347	32.97 117.87	5.4
1987 Feb. 07	0345	32.39 115.31	5.4
1987 Feb. 14	0726	36.18 120.27	5.1
1987 Oct. 01	1442	34.06 118.08	5.9
1987 Nov. 24	0154	33.08 115.78	6.2
1987 Nov. 24	1315	33.01 115.84	6.6
1988 Jan. 25	1317	31.71 115.77	5.6
1988 June 10	2306	34.94 118.74	5.4
1990 Feb. 28	2343	34.14 117.70	5.3
1991 June 28	1443	34.26 118.00	5.4
1991 Dec. 03	1755	31.70 115.91	5.2
1992 April 23	0450	33.96 116.32	6.1
1992 June 28	1157	34.20 116.44	7.3
1992 July 11	1814	35.21 118.07	5.7

Table A2. Earthquakes of the Central Region with $M \geq 5.1$

Date	Time, UT	Location °N °W	Magnitude
1939 June 24	1301	36.40 121.00	5.5
1949 March 09	1228	36.02 121.48	5.2
1952 Nov. 22	0746	35.73 121.20	6.0
1954 April 25	2033	36.93 121.68	5.3
1955 Sept. 05	0201	37.37 121.75	5.8
1955 Nov. 02	1940	36.00 120.92	5.2
1959 March 02	2327	36.98 121.58	5.3
1961 April 09	0723	36.68 121.30	5.6
1963 Sept. 14	1946	36.85 121.63	5.4
1966 June 28	0426	35.92 120.53	5.6
1966 Sept. 12	1641	39.42 120.15	6.0
1967 Dec. 18	1724	37.01 121.79	5.2
1969 Oct. 02	0457	38.47 122.69	5.6
1969 Oct. 02	0620	38.46 122.69	5.7
1975 Aug. 01	2020	39.44 121.53	5.7

Table A2. (continued)

Date	Time, UT	Location °N °W	Magnitude
1979 Feb. 22	1557	40.01 120.07	5.2
1979 Aug. 06	1705	37.10 121.50	5.9
1980 Jan. 24	1900	37.85 121.82	5.5
1980 Jan. 27	0234	37.74 121.74	5.8
1980 Nov. 28	1821	39.31 120.43	5.2
1982 Oct. 25	2226	36.29 120.41	5.6
1983 May 02	2342	36.25 120.26	6.3
1984 Jan. 23	0540	36.37 121.91	5.4
1984 April 24	2115	37.32 121.70	6.2
1985 Aug. 04	1201	36.15 120.05	5.8
1986 Jan. 26	1921	36.81 121.28	5.5
1986 March 31	1156	37.48 121.69	5.7
1987 Feb. 14	0726	36.18 120.27	5.1
1988 Feb. 20	0840	36.80 121.30	5.3
1988 June 13	0146	37.38 121.77	5.4
1988 June 27	1843	37.13 121.88	5.7
1989 Aug. 08	0813	37.13 121.95	5.4
1989 Oct. 18	0004	37.04 121.88	7.0
1993 Jan. 16	0630	37.02 121.46	5.3

Table A3. Earthquakes of the Northern Region with $M \geq 5.1$

Date	Time, UT	Location °N °W	Magnitude
1965 May 31	0508	44.10 128.80	5.5
1965 June 14	0940	44.60 129.70	5.4
1965 June 20	1805	42.90 126.10	5.6
1967 Dec. 10	1207	40.50 124.70	5.6
1967 Dec. 28	0626	44.20 128.80	5.4
1968 May 08	1217	43.57 127.90	6.4
1968 May 09	0303	43.44 126.97	5.1
1968 June 26	0142	40.23 124.27	5.9
1969 Oct. 09	0745	43.71 127.43	5.5
1970 Sept. 13	2110	40.13 125.08	5.4
1970 Oct. 27	0238	40.40 127.00	5.1
1970 Nov. 26	0312	43.78 127.45	5.9
1971 Feb. 27	0032	40.27 124.83	5.2
1972 March 01	0929	40.67 125.25	5.2
1972 April 08	0624	42.65 126.32	5.6
1972 Oct. 25	0102	43.44 127.73	5.2
1973 June 16	1444	44.98 125.77	5.1
1973 Oct. 12	0554	43.74 127.47	5.2
1974 Jan. 05	1554	42.48 126.60	5.1
1974 July 03	0501	40.42 125.14	5.1
1974 Sept. 12	0520	41.86 126.60	5.1
1975 June 07	0846	40.57 124.14	5.2
1976 Jan. 10	0859	43.55 127.43	5.4
1976 Sept. 30	1736	43.45 126.97	5.1
1976 Nov. 26	1119	41.29 125.71	6.4
1976 Dec. 09	0951	44.53 129.96	5.5
1976 Dec. 19	1901	42.75 125.60	5.4
1976 Dec. 23	0939	41.78 125.95	5.3
1977 July 28	1522	44.24 128.97	5.4
1977 Sept. 07	0311	42.00 126.65	5.1
1979 Feb. 03	0958	40.89 124.41	5.2
1980 March 03	1417	40.60 125.03	5.1
1980 Nov. 08	1028	41.12 124.25	7.0
1980 Nov. 09	0409	40.50 125.34	5.2

Bulletin of the Seismological Society of America, Vol. 87, No. 4, pp. 789–798, August 1997

The Paradox of the Expected Time until the Next Earthquake

by D. Sornette and L. Knopoff

Abstract We show analytically that the answer to the question, (can it be that) "The longer it has been since the last earthquake, the longer the expected time till the next?" depends crucially on the statistics of the fluctuations in the interval times between earthquakes. The periodic, uniform, semi-Gaussian, Rayleigh, and truncated statistical distributions of interval times, as well as the Weibull distributions with exponent greater than 1, all have decreasing expected time to the next earthquake with increasing time since the last one, for long times since the last earthquake; the lognormal and power-law distributions and the Weibull distributions with exponents smaller than 1 have increasing times to the next earthquake as the elapsed time since the last increases, for long elapsed times. There is an identifiable crossover between these models, which is gauged by the rate of fall-off of the long-term tail of the distribution in comparison with an exponential fall-off. The response to the question for short elapsed times is also evaluated. The lognormal and power-law distributions give one response for short elapsed times and the opposite for long elapsed times. Even the sampling of a finite number of intervals from a Poisson distribution will lead to an increasing estimate of time to the next earthquake for increasing elapsed time since the last one.

Introduction

While small earthquakes after removal of aftershocks have a Poissonian distribution (Gardner and Knopoff, 1974), intermediate and large earthquakes in a given region are clustered in time (Kagan and Knopoff, 1976; Lee and Brillinger, 1979; Vere-Jones and Ozaki, 1982; Grant and Sieh, 1994; Kagan and Jackson, 1991, 1994; Kagan, 1983; Knopoff *et al.*, 1996); "clustering" is taken to mean that the earthquakes do not have a purely Poissonian, memoryless distribution of time intervals. According to this interpretation, periodic earthquakes are the extreme limit of clustering and can be predicted exactly. More generally, if there is temporal clustering, the estimate of the probability of occurrence of a future earthquake in a given time interval is improved if there is a knowledge of the times of previous events, since clustering implies a memory. To express this property quantitatively, we relate the elapsed time since the last earthquake in a region to the conditional probability of occurrence of the next earthquake within a given time interval from the present. Davis *et al.* (1989) have posed a version of this problem in the form of the following question (hereafter referred to as Q.):

> (can it be that) "The longer it has been since the last earthquake, the longer the expected time till the next?"

The observation of Davis *et al.* for the log-normal distribution was that the answer to Q. is positive. Ward and Goes (1993) and Goes and Ward (1994) showed numerically that, in the case of the Weibull distribution, the response to Q. can be either yes or no, depending on the exponent in the distribution. The positive responses would seem to be counterintuitive, since it is to be expected that an earthquake should be more likely to occur with increasing time in response to an inexorable tectonic loading that brings a fault ever closer to its finite threshold of fracture.

The intuitive interpretation is of course consistent with simple relaxation oscillator models of the earthquake process, such as the slip- or time-predictable models. But these models should be reconsidered if the stress field is altered on a given fault segment due to redistribution derived from earthquakes on nearby fault elements; these interactions can cause fluctuations in the stress field, with consequent fluctuations in the interval times. Knopoff (1996) has proposed that the fluctuations in the interval times between great earthquakes on the San Andreas Fault (Sieh *et al.*, 1989) may be associated with stress interactions between the San Andreas Fault and other nearby faults.

Below, we give a rigorous statistical framework for the derivation of a quantitative response to Q. Statistical estimates of recurrence times will be found to be very sensitive to assumptions about statistical distributions. Our results confirm, quantify, and extend the numerical analyses of Davis *et al.* (1989), Ward and Goes (1993), and Goes and Ward (1994) by providing an analytic basis for the problem.

The Time to the Next Earthquake

Let $p(t)$ be the probability density of the time intervals between earthquakes. If the time (now) since the last earthquake is t, what is the probability density function $P(t')$ that we must wait an additional time t' until the next earthquake? From Bayes' theorem for conditional probabilities, cited in elementary statistics textbooks, the probability that an event A, given the knowledge of an event B, is simply the quotient of the probability of the event A without constraint and the probability of event B:

$$P(A|B) = \frac{P(A)}{P(B)}. \tag{1}$$

Applied to this problem, $P(A) = p(t + t')$, which is the probability that the next earthquake will occur at time t' from now, and $P(B) = \int_t^\infty p(s)ds$, which is the probability that no earthquake has occurred up to now. Thus,

$$P(t') = \frac{p(t + t')}{\int_t^\infty p(s)ds}, \tag{2}$$

which is normalized.

We calculate the expected time until the next earthquake $\langle t' \rangle$ as a function of the time since the last one.

(A.) *The answer to Q. is given by the sign of $d\langle t' \rangle/dt$, if $\langle t \rangle$ exists.*

From equation (2), the average expected time to the next earthquake is

$$\langle t' \rangle = \frac{\int_0^\infty t' p(t + t')dt'}{\int_t^\infty p(u)du}. \tag{3}$$

By a simple change of variable,

$$\langle t' \rangle = \frac{\int_t^\infty (u - t)p(u)du}{\int_t^\infty p(u)du}. \tag{4}$$

We integrate the numerator of (4) by parts and get

$$\langle t' \rangle = \frac{\int_t^\infty ds \int_s^\infty p(u)du}{\int_t^\infty p(u)du}. \tag{5}$$

The denominator and numerator of (5) are the familiar first cumulative integral and the less familiar second cumulative integral of $p(u)$. For simplicity, we write (5) as

$$\langle t' \rangle = -\frac{f(t)}{f'(t)}, \tag{6}$$

where $f''(t) = p(t)$; that is, $f(t)$ is the second cumulative integral of $p(u)$. Thus,

$$\frac{d\langle t' \rangle}{dt} > 0 \quad \text{if} \quad f(t)f''(t) - [f'(t)]^2 > 0. \tag{7a}$$

Equivalently,

$$\frac{d\langle t' \rangle}{dt} = -\frac{g''(t)}{[g'(t)]^2} > 0 \quad \text{if} \quad g''(t) < 0, \tag{7b}$$

where we have set $f(t) = e^{-g(t)}$. The signs are appropriately reversed in the case $g''(t) > 0$. Equation (7b) especially favors an appreciation of the behavior at large values of elapsed time t.

If $p(t)$ is finite at $t = 0$, we can find yet a third version of (5), which is useful for small t. A straightforward expansion for small t shows that

$$\lim_{t \to 0^+} \frac{d\langle t' \rangle}{dt} = p(0)\Delta - 1, \tag{7c}$$

where

$$\Delta = \int_0^\infty ds \int_s^\infty p(u)du = \langle t \rangle.$$

The result of the integration follows directly from (5); $\langle t \rangle$ is the average (unconditional) time of recurrence between two earthquakes. Let $\tau \equiv 1/p(0)$, where τ is the estimate of the waiting time until the next earthquake made immediately after the occurrence of the preceding earthquake. We call τ the instantaneous estimate of t'. Thus, $d\langle t' \rangle/dt$ can be rewritten in the simple form

$$\lim_{t \to 0^+} \frac{d\langle t' \rangle}{dt} = \frac{\langle t \rangle}{\tau} - 1. \tag{7d}$$

- If the instantaneous estimate τ of the waiting time is smaller than the average waiting time $\langle t \rangle$, the time to the next earthquake increases with increasing time since the last one for small t: this reflects the fact that the average waiting time $\langle t \rangle$ is formed by contributions from the distribution over all time, and a value of $\langle t \rangle$ larger than τ indicates contributions from the distribution that are larger than τ at nonzero times; in this case, $\lim_{t \to 0+} d\langle t' \rangle/dt > 0$.
- If $\langle t \rangle < \tau$, the reverse is true, shorter and shorter timescales are sampled on the average as time increases, and the time to the next earthquake decreases with increasing time since the last one for small t.

In particular, if $p(0) = 0$, then $\lim_{t \to 0+} d\langle t' \rangle/dt = -1$, and the time to the next earthquake decreases with increasing time since the last one for small t; if, however, $p(0) = \infty$, then $\lim_{t \to 0+} d\langle t' \rangle/dt = \infty$, and the time to the next earthquake increases with increasing time since the last one for small t.

The generalization of (7c) to times other than $t = 0$ is the criterion (7a), when the mean $\langle t \rangle$ exists. When it does not exist, as, for example, when the tails of the distributions decay slower than t^{-2}, we must compare $P(t')$ as given by (2), with $p(t')$.

Exponential Distribution

In order to develop some intuition, we first consider the exponential distribution, which is the familiar case of Poissonian statistics,

$$p(t) = \frac{e^{-t/t_0}}{t_0}, \quad t \geqq 0,$$

where t_0 is the mean interval time between earthquakes. From equation (2),

$$P(t') = \frac{e^{-t'/t_0}}{t_0}. \tag{8}$$

Not unexpectedly, the estimate of the time of occurrence of the next earthquake does not depend on the elapsed time: the average time from now to the future earthquake is t_0, no matter what the value of t. This case is memoryless; indeed, it is the only distribution that has no memory. The expected time to the next earthquake is $\langle t' \rangle = t_0$; there is no need to invoke the machinery of (7) to derive $d\langle t' \rangle/dt = 0$. The Poisson distribution is the unique case $g''(t) = 0$, which gives the same result.

The exponential distribution is the fixed point of the transformation $p(t) \rightarrow P(t')$; that is, it is the solution to the functional equation

$$P(t') = p(t'). \tag{9}$$

To verify that (8) is the solution to (9), differentiate (2) with respect to t and substitute in (9). We get

$$-p(t)p(t') = \frac{dp(t + t')}{dt}. \tag{10}$$

Take the Laplace transform of (10) with respect to t', with $1/t_0$ the transform variable. The result (8) follows. Thus the exponential distribution is the fixed point of (2).

We restate these results: Except for the Poisson distribution, all statistical distributions must have an average time from now to the future earthquake that depends on the time since the last earthquake. If the long-time tail of the function $f(t)$, defined as the integral of the integral of the distribution $p(t)$, falls off at a rate that is faster than exponential, the expected time to the next earthquake is reduced, the longer the elapsed time since the last, and vice versa. The Poisson distribution is the crossover between the two states. The exponential case has neither a positive nor a negative response to Q., since the time since the last earthquake has no influence on the time of the next.

Other Conditional Distributions

We calculate the expected time to the next earthquake for several examples of statistical distributions $p(t)$ with memory. We illustrate the results in Figure 1 by displaying the average time to the future earthquake t' plotted against the time since the last earthquake t for selected distributions $p(t)$; whether the values are greater or less than 1 gives the answers to Q. The details of the calculations are given in the Appendix.

The analytical results are summarized in Table 1. The times in the table are scaled by a characteristic time t_0 for a given distribution; the precise definition of t_0 for each distribution is given in the Appendix. In general, t_0 is of the order of the mean time between earthquakes, if it is not so exactly. In most cases, we can give an answer A. that is valid over the entire range of elapsed times since the last earth-

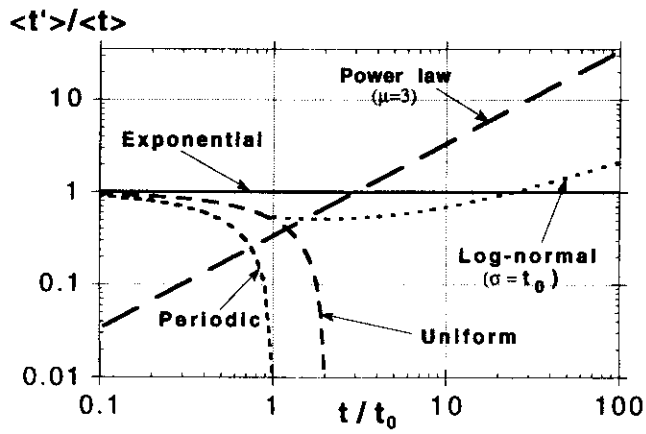

Figure 1. Expected time of the next earthquake as a function of the elapsed time since the last one. The response to Q. is given by the value of the curve with respect to 1.

Table 1
Response to Q.

Distribution	Short Times	Long Times
Exponential	0	0
Periodic	−	
Uniform	−	
Gaussian		−
Semi-Gaussian	−	−
Lognormal	−	+
$\frac{1}{4}\sqrt{x}e^{-\sqrt{x}}$	−	+
Weibull ($m > 1$)	−	−
Rayleigh ($m = 2$)	−	−
Weibull ($m < 1$)	+	+
Power law	−	+
Truncated power law	+	−

quake. In some cases, we can only give the answer for the limits of short and long time since the last earthquake. The table is arranged to favor the limiting responses, even though we may have the complete solution. In the case of the exponential distribution, the response is neutral, as we have already discussed. In the cases of the periodic and uniform distributions, the response is only meaningful for times up to t_0; in the case of the Gaussian distribution, the response is meaningful for long elapsed times, as we discuss in the Appendix. In the cases of the Weibull distribution with $m > 1$ and the semi-Gaussian distribution, the response can be proved to be negative for both short and long elapsed times and can be inferred to be negative for all elapsed times. For the Weibull distribution with $m < 1$ and the power-law distribution, the response is positive for both short and long elapsed times and can be inferred to be positive for all elapsed times. For the lognormal, power-law, and truncated power-law distributions, there is one response for short elapsed times and the opposite response for long elapsed times, with the implications of a crossover and hence neutral response at an intervening time scaled by t_0; the lognormal and truncated power-law distributions have opposite responses to each other in the long and short time regimes.

Since the truncated and ordinary power-law distributions give opposite results for long elapsed times, it follows that the answers to Q. are unstable with respect to the presence or absence of a cutoff in the distributions. It is by definition problematical that a presumed existence of a cutoff can be identified from a finite set of observations of interval times: there is no guarantee that a presumed cutoff will not disappear with a future observation of a longer interval between earthquakes. Thus a positive response to the question for long elapsed times since the last earthquake is only conjectural; that is, it is only as strong as one knows the distribution to times longer than have been observed, which is impossible. Of course, the distribution can always be postulated *a priori*, as in the numerical examples of Davis *et al.* (1989) and Ward and Goes (1993), but the postulate does not ensure that it represents nature.

Estimate of t_0

Suppose that we do not know *a priori* the characteristic time t_0 of time intervals between successive earthquakes. We then have to estimate it from a finite suite of observations of interearthquake time intervals. Assume that $(n-1)$ observations of time intervals $t_1, t_2, \ldots, t_{n-1}$ are made precisely; we ignore here the additional problem of the uncertainties in the time intervals that occur for historical earthquakes; this can be treated by standard statistical methods (Sieh *et al.*, 1989). Suppose that the time since the last event is t. Then, in the case of the Poisson distribution $p(t) = e^{-t/t_0}/t_0$, the standard maximum likelihood method gives the estimate of t_0 as the value that maximizes

$$\frac{1}{t_0^n} e^{-(t + \sum_{j=1}^{n-1} t_j)/t_0};$$

that is,

$$t_0 = \frac{1}{n}\left(t + \sum_{j=1}^{n-1} t_j\right). \tag{11}$$

Thus, even for the Poissonian case, the use of the information that no event has occurred since t gives an estimate of the average recurrence time t_0 for the next event that increases with t! The Poisson distribution is memoryless only if its parameter t_0 is known *a priori*.

The calculation (11) can be generalized for the other distributions discussed above. Our previous results must thus be reconsidered if the parameters of the distributions are themselves not known precisely but are estimated using presently available information. This does not pose any difficulty in principle, but must be addressed case by case. This simple calculation demonstrates the sensitivity of the "prediction" to the assumptions concerning what is really known and what is only inferred from the data.

Summary

These observations can be summarized as follows:

- The Poisson or exponential distribution is memoryless and the expected time until the next event is independent of previous observations and of the elapsed time since the last earthquake. The exponential thus acts as a fixed point in the space of distributions of the transformation (2) and sits at the boundary between the positive and negative classes of memory, that is, at the boundary between positive and negative responses to Q. Any statistics of the fluctuations of recurrence times that is different from Poissonian entails the explicit assumption of a memory.
- Any distribution that falls off at large time intervals at a faster rate than an exponential, such as the periodic, quasiperiodic, uniform, and semi-Gaussian distributions, and the Weibull distribution with $m > 1$, has the property "the longer it has been since the last earthquake, the shorter the expected time until the next." The truncated power-law distribution for times close to the cutoff time also has this property.
- Any distribution that falls off at large time intervals at a slower rate than an exponential, such as the Weibull distribution with $m < 1$, the unbounded lognormal and power-law distributions, and the truncated versions of these distributions for times remote from the cutoff, has the property "the longer it has been since the last earthquake, the longer the expected time till the next."
- All distributions that have an instantaneous expectation time interval between earthquakes *smaller* than the average waiting time between earthquakes have the property of an *increasing* time to the next earthquake for an increas-

ing time since the last one, for short times since the last one. This includes the cases $p(0) = \infty$.

- All distributions that have an instantaneous expectation time interval between earthquakes *larger* than the average waiting time between earthquakes have the property of a *decreasing* time to the next earthquake for an increasing time since the last one, for short times since the last one. This includes the cases $p(0) = 0$.
- Caution should be exercised in the use of statistics of fluctuations of interval times deduced from data sets that describe only the distributions for short time intervals between earthquakes. This is because of the strong dependence of our result for long times, and in some cases for short times as well, on the properties of the tails of the distributions as well as on the values of the parameters of the distributions.
- The estimate of the time until the next earthquake depends on a precise estimate of the tail of $p(t)$ and is unstable with respect to presently available data for the recurrence of large earthquakes. Even a finite sampling of the Poisson distribution will lead to an estimate of the time to the next earthquake that increases with increased time since the last one.

Thus the positive response of Davis *et al.* (1989) to Q., "the longer it has been since the last earthquake, the longer the expected time till the next," is shown to arise from the use of a distribution that decays slower than an exponential and that is unbounded for large time intervals; the result is valid for other distributions as well. If a slowly decaying law itself undergoes a transition at even longer intervals to a more rapidly decaying law, as in the extreme case of a distribution with a cutoff, one can expect that eventually the next earthquake will become more and more probable. The response to the question (Q.) is also related, in part, to the finiteness of the number of observations of time intervals between earthquakes that gives the estimate of the distribution $p(t)$; the extrapolation of the estimate of the distribution to its asymptote for very large time intervals is exceedingly dangerous, since this procedure is likely to be based on few, if any, observations. The results of this exercise suggest that caution be used in the extrapolation of statistics deduced from short timescale data sets to long timescales.

Acknowledgments

This research has been partially supported by the NSF/CNRS under the U.S./France International Cooperation program. This article is Publication Number 4669 of the Institute of Geophysics and Planetary Physics, University of California, Los Angeles, and Publication Number 369 of the Southern California Earthquake Center.

References

Davis, P. M., D. D. Jackson, and Y. Y. Kagan (1989). The longer it has been since the last earthquake, the longer the expected time till the next?, *Bull. Seism. Soc. Am.* **79,** 1439–1456.

Gardner, J. K. and L. Knopoff (1974). Is the sequence of earthquakes in southern California, with aftershocks removed, Poissonian?, *Bull. Seism. Soc. Am.* **64,** 1363–1367.

Goes, S. D. B. and S. N. Ward (1994). Synthetic seismicity for the San Andreas fault, *Ann. Geof.* **37,** 1495–1513.

Grant, L. B. and K. Sieh (1994). Paleoseismic evidence of clustered earthquakes on the San Andreas fault in the Carrizo Plain, California, *J. Geophys. Res.* **99,** 6819–6841.

Kagan, Y. Y. (1983). Statistics of characteristic earthquakes, *Bull. Seism. Soc. Am.* **83,** 7–24.

Kagan, Y. Y. and D. D. Jackson (1991). Long-term earthquake clustering, *Geophys. J. Int.* **104,** 117–133.

Kagan, Y. Y. and D. D. Jackson (1994). Long-term probabilistic forecasting of earthquakes, *J. Geophys. Res.* **99,** 13685–13700.

Kagan, Y. and L. Knopoff (1976). Statistical search for non-random features of the seismicity of strong earthquakes, *Phys. Earth Planet. Interiors* **12,** 291–318.

Kagan, Y. Y. and L. Knopoff (1981). Stochastic synthesis of earthquake catalogs, *J. Geophys. Res.* **86,** 2853–2862.

Kagan, Y. Y. and L. Knopoff (1987). Statistical short-term earthquake prediction, *Science* **236,** 1563–1567.

Knopoff, L. (1996). A selective phenomenology of the seismicity of southern California, *Proc. Natl. Acad. Sci. U.S.* **93,** 3756–3763.

Knopoff, L., T. Levshina, V. I. Keilis-Borok, and C. Mattoni (1996). Increased long-range intermediate-magnitude earthquake activity prior to strong earthquakes in California, *J. Geophys. Res.* **101,** 5779–5796.

Lee, W. H. K. and R. R. Brillinger (1979). On Chinese earthquake history—an attempt to model incomplete data set by point process analysis, *Pure Appl. Geophys.* **117,** 1229–1257.

Sieh, K., M. Stuiver, and D. Brillinger (1989). A more precise chronology of earthquakes produced by the San Andreas Fault in southern California, *J. Geophys. Res.* **94,** 603–623.

Vere-Jones, D. and T. Ozaki (1982). Some examples of statistical estimation applied to earthquake data. I. Cyclic Poisson and self-exciting models, *Ann. Inst. Statist. Math.* **B34,** 189–207.

Ward, S. N. and S. D. B. Goes (1993). How regularly do earthquakes recur? A synthetic seismicity model for the San Andreas Fault, *Geophys. Res. Lett.* **20,** 2131–2134.

Appendix

We calculate the expected time to the next earthquake for several examples of statistical distributions $p(t)$ with memory.

Periodic Distribution

The simplest of the distributions with memory is the periodic distribution,

$$p(t) = \delta(t_0 - t).$$

By inspection, we have

$$P(t') = \delta(t_0 - t' - t), \quad \langle t' \rangle = t_0 - t.$$

Thus, $d\langle t' \rangle/dt = -1$ without invoking the generalized machinery. In this simplest of cases, the expected time of the forthcoming earthquake decreases as the elapsed time since the preceding earthquake increases. Extension to quasiperiodic cases can be made.

Uniform Distribution

The uniform distribution is

$$p(t) = \frac{1}{2t_0} \quad 0 \leqq t \leqq 2t_0,$$

where $2t_0$ is the maximum interval between earthquakes and t_0 is the mean. From equation (2), we get

$$P(t') = \frac{1}{2t_0 - t} \quad 0 \leqq t' \leqq 2t_0 - t. \qquad \text{(A1)}$$

$P(t')$ is independent of t'; that is, it is itself a uniform distribution, but its value is dependent on t. The probability that an earthquake will occur at any time in the future up to t_0 increases as the time since the last earthquake increases and becomes infinite as $t \to 2t_0$, which simply expresses the intuitive result that the event will occur with certainty before $2t_0$. It is easy to see that the average time to the future earthquake from the present is $\langle t' \rangle = \frac{1}{2}(2t_0 - t)$. The negative value of $d\langle t' \rangle/dt$ gives the answer (A.): the expected time to the next earthquake decreases with increasing time since the last earthquake. In Figure 1, we show the average time to the future earthquake plotted against the time since the last earthquake; both coordinates are normalized by the mean time between earthquakes, t_0. The linear relationship between $\langle t' \rangle$ and t is strongly curved on the log–log plot.

In Figure A1, we display the probability that the next earthquake will occur at time t' from now. We show the unconditional probability, that is, the probability as though we knew the distribution of intervals $p(t)$ but did not know the time of the last earthquake. We also show the (conditional) probability of an earthquake in the future knowing that the last earthquake took place at time $1.33t_0$ in the past. In the latter case, no earthquake can occur after $0.67t_0$ from now; according to (A1), the probability of occurrence of the future earthquake is higher by a factor of 3 than the unconditional probability and is independent of the time of the future earthquake.

(Semi)-Gaussian Distribution

The Gaussian distribution is

$$p(t) = \frac{1}{\sqrt{2\pi}\sigma} e^{-(t-t_0)^2/2\sigma^2},$$

where t_0 is both the mean and the most probable time interval of earthquake recurrence; the standard deviation is σ. The Gaussian distribution has a finite probability that the next earthquake will occur before the preceding one. The drawback is minor if $\sigma \ll t_0$, a condition that describes a nearly periodic distribution; we have considered the periodic case above. To restrict the problem to cases of positive t, we could

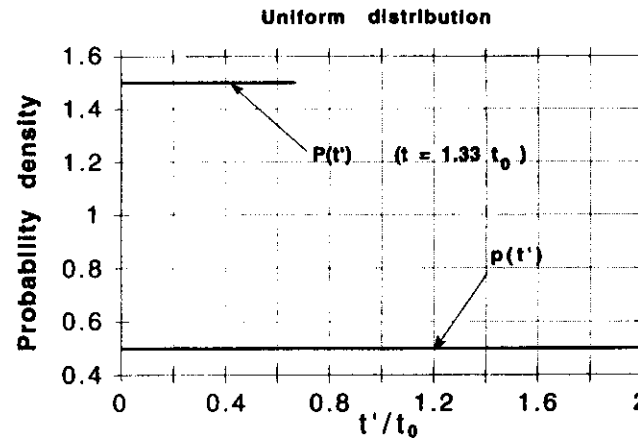

Figure A1. Uniform distribution: $p(t')$ and $P(t')$ for $t = (4/3)t_0$.

truncate the distribution at $t = 0$; however, this leads to messy mathematics; for large times, the drawback is minor.

For the simpler problem $t \gg t_0$, we use the approximation

$$p(t) = \frac{2}{\pi t_0} e^{-(t/t_0)^2/\pi}, \quad t \geqq 0,$$

which is the semi-Gaussian distribution; that is, it is a Gaussian centered at $t = 0$; the mean time interval of earthquake recurrence is t_0, and the most probable time for recurrence is of course zero for this distribution. Formally, equation (2) yields

$$P(t') = \frac{2}{\pi t_0} \frac{e^{-(t+t')^2/\pi t_0^2}}{\operatorname{erfc}\left(\frac{t}{\tau t_0}\right)}, \qquad \text{(A2)}$$

where $\operatorname{erfc}(x)$ is the usual complementary error function.

If the elapsed time since the last earthquake is very large, $t \gg t_0$, we can use the first term of the asymptotic expansion of the second cumulative integral that is

$$f(t) \sim \frac{e^{-t^2/\pi t_0^2}}{t^2}.$$

Then $g(t) \sim t^2 + O(\log t)$, $g''(t) > 0$ for large t, and from (7b),

$$\frac{d\langle t' \rangle}{dt} < 0$$

For short times, we use (7c) with $p(0) = 2/(\pi t_0)$ and $\Delta = t_0$ and get

$$\frac{d\langle t' \rangle}{dt} \approx \frac{2}{\pi} - 1 = -0.363.$$

Thus in both the short and long time limits, the expected time until the next earthquake decreases as the time since the last one increases.

Lognormal Distribution

The lognormal distribution is

$$p(t) = \frac{1}{\sqrt{2\pi}\sigma}\frac{1}{t}e^{-(\log t/t_0)^2/2\sigma^2} = \frac{1}{\sqrt{2\pi}\sigma t_0}e^{-1/2\sigma^2(\log t/t_0 + \sigma^2)^2 + \sigma^2/2}, \tag{A3}$$

which is similar in shape to the Rayleigh distribution (see below) near $t = 0$ but has a much more slowly decaying tail for large times. In this case, t_0 is the median time; the mean time is $\langle t\rangle = t_0 e^{\sigma^2/2}$; the most probable time is $t_0 e^{-\sigma^2}$. From (A3), we can write

$$g(t) = (\log\left(\frac{t}{t_0}\right) + \sigma^2)^2 + O[\log\log\left(\frac{t}{t_0}\right)],$$

whence

$$g''(t) \approx \frac{2}{t^2}\left(1 - \sigma^2 - \log\frac{t}{t_0}\right).$$

For $t \gg t_0$, $g'' < 0$, and hence $d\langle t'\rangle/dt > 0$. For $t \ll t_0$, $g'' > 0$, and $d\langle t'\rangle/dt < 0$; alternatively, we note that $p(0) = 0$, and hence from (7c), $dt\langle t'\rangle/dt < 0$, which is the same result. Thus the lognormal distribution has a crossover in response to Q.

We express these results graphically. For the case $\sigma = t_0$, we display $P(t')$ for times $t = 2t_0$ and $t = 5t_0$ (Fig. A2) together with the unconditional lognormal distribution $p(t)$. From Figure A2a, we see that $P(t')$ is significantly smaller than $p(t')$ for times comparable to the elapsed time t, but $P(t')$ is, as expected, larger than $p(t')$ at large times (see extension of Fig. A2a to long times in Fig. A2b). This is a small effect for $t = 2t_0$ but is much stronger for $t = 5t_0$ and all the more so if t increases even more. Thus, numerically as well as analytically, for early elapsed times t that are comparable to the peak of the distribution, the longer the elapsed time since the last event, the shorter the time until the next event; but for large elapsed times since the last earthquake, the longer the time since the last event, the longer the time until the next one. In the lognormal case, it is correct to state that "the longer it has been since the last earthquake, the longer the expected time until the next" but only for elapsed times greater than times of the order of the characteristic time. The lognormal distribution is an example of a case that has one answer to Q. for short times since the last earthquake and the opposite answer for long times. Of course, the crossover takes place at elapsed times that are of the order of the characteristic time t_0. Note that the probabilities for long times in the future are, as might be expected, very small. The lognormal case is an example of a distribution with a tail that decays slower than an exponential.

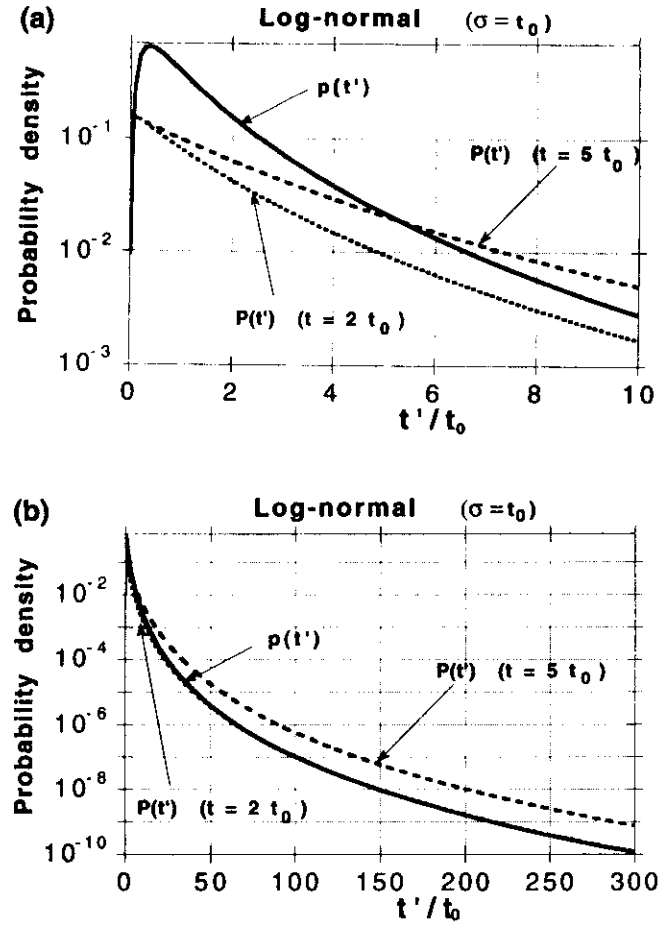

Figure A2. Lognormal distribution with $\sigma = t_0$: $p(t')$ and $P(t')$ for $t = 2t_0$ and $t = 5t_0$: (a) short times and (b) long times.

To illustrate more concretely the properties of a system that has a crossover response to Q., we concoct the distribution

$$p(t) = \frac{1}{4t_0}\sqrt{\frac{t}{t_0}}e^{-\sqrt{t/t_0}},$$

which probably has no redeeming virtue in nature but has the property that it has easily calculable integrals. It is evident that this distribution has both a long-time tail that decays slower than exponential, and the property $p(0) = 0$, as in the case of lognormal distribution. Thus we are guaranteed that there is a crossover in the response to Q. More precisely, the criterion function (7a) is $f(t)f''(t) - [f'(t)]^2 = \frac{1}{4}(x^3 + 4x^2 + 4x - 4)e^{-2x}$, where $x = \sqrt{t/t_0}$. The criterion has a crossover in sign between x small and large at $t/t_0 = 0.3532$. The lognormal distribution has similar properties.

Weibull Distribution

The Weibull distribution is

$$p(t) = mt_0^{-m}t^{m-1}e^{-(t/t_0)^m}, \quad 0 < t < \infty, \quad m > 0,$$

having a most probable value $(m - 1)^{1/m}t_0$, a mean $\alpha(m)t_0$ where $\alpha(m) = \int_0^\infty e^{-t^m}\,dt$, and median $(\log 2)^{1/m}t_0$. Values of m smaller than 1 correspond to $p(t)$ decaying slower than an exponential for large t and give the so-called stretched exponential distributions, while values of m larger than 1 lead to a decay that is faster than exponential. For large m, $p(t)$ approaches a delta function centered on t_0, that is, to the periodic distribution we have considered above. Ward and Goes (1993) and Goes and Ward (1994) have studied the degree of earthquake clustering as a function of m; in their notation, $v = 1/m$. Equation (2) yields

$$P(t') = mt_0^{-m}(t + t')^{m-1}e^{-[(t+t')^m - t^m]/t_0^m}. \quad \text{(A4)}$$

The first term of the asymptotic series for $f(t)$, which is the second cumulative integral of $p(t)$, is

$$f(t) \sim \frac{e^{-(t/t_0)^m}}{\left(\frac{t}{t_0}\right)^{3(m-1)}} = e^{-(t/t_0)^m - (3m-1)\log t/t_0}.$$

Evidently, $g(t) \sim t^m + O(\log t)$, and hence $g''(t) \sim m(m-1)t^{(m-2)}$. Thus if $0 < m < 1$, then $g''(t) < 0$, and $d\langle t'\rangle/dt > 0$ for large t, while if $m > 1$, then $g''(t) > 0$, and $d\langle t'\rangle/dt < 0$ for large t. For small t, $p(0) = 0$, $m > 1$, and it follows from (7c) that $d\langle t'\rangle/dt < 0$. For cases $m < 1$, $p(0) = \infty$, and from (7c), $d\langle t'\rangle/dt > 0$. Thus there is a reversal in response between the cases $m < 1$ and $m > 1$, in agreement with the result of Ward and Goes.

In Figure A3a, we exhibit the interesting subcase of the Weibull distribution with $m = 2$, which is appropriate for rectified Gaussian noise and is known as the Rayleigh distribution. The Rayleigh distribution has a tail with similar properties to that of the Gaussian and decays faster than an exponential. We show $P(t')$ for times $t = t_0$ and $t = 2t_0$. It is clear that $P(t')$ has a progressively shrinking width to the origin as t increases; that is, the expected time decreases as the waiting time t increases. The answer A. is negative for both short times and long times, the latter property evidently connected with the rapid fall-off in $p(t)$ for large t.

The opposite situation is found in the case $m < 1$; in Figure A3b, we plot the case $m = \frac{1}{2}$ and show $P(t')$ for times $t = t_0$, $t = 2t_0$, and $t = 10t_0$, as well as $p(t)$. It is clear that $P(t')$ lies well above $p(t')$ at long times $t' > t_0$ and all the more so as t increases. Thus the longer we wait, the longer the time to the next event, in this case.

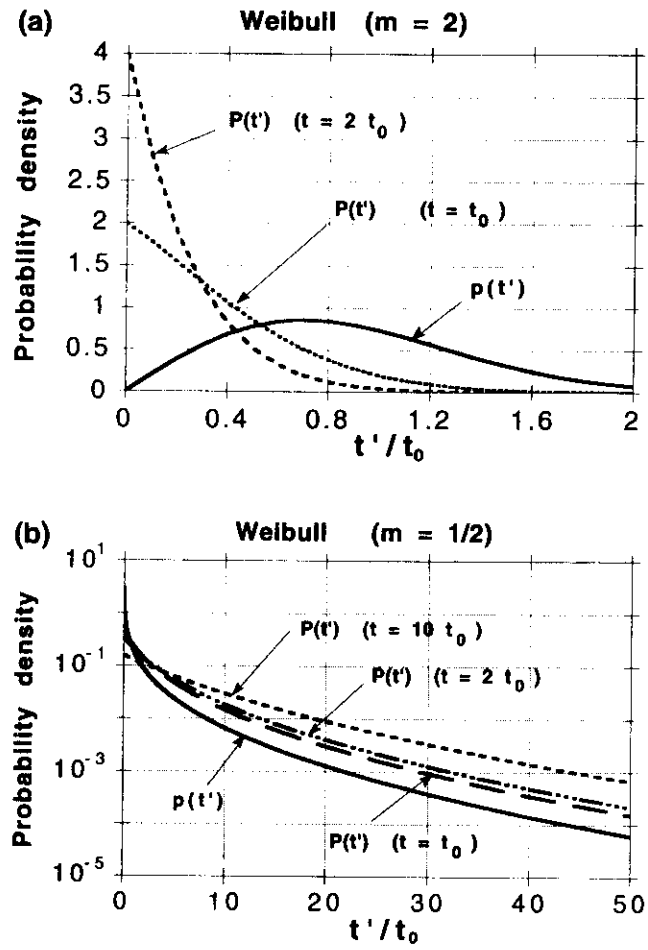

Figure A3. Weibull distribution. (a) $m = 2$ (Rayleigh distribution), corresponding to a tail decaying faster than an exponential. $P(t')$ is shown for $t = t_0$ and $t = 2t_0$ together with $p(t')$. (b) $m = \frac{1}{2}$ corresponding to a tail decaying slower than an exponential. $P(t')$ is shown for $t = t_0$, $t = 2t_0$, and $t = 10t_0$, together with $p(t')$.

Power-Law Distribution

The unconditional power-law distribution is

$$p(t) = 0, \quad 0 < t < t_0, \quad \text{(A5)}$$

$$p(t) = \frac{\mu}{t_0}\left(\frac{t}{t_0}\right)^{-(1+\mu)}, \quad t_0 \leqq t \leqq \infty, \quad 0 < \mu < \infty.$$

The characteristic timescale t_0 is proportional to the mean $(\mu/(\mu - 1))\,t_0$ for $\mu > 1$ and the median $t_0\,2^{1/\mu}$; for $\mu < 1$, the mean is infinite. This is an example of a distribution with a waiting time and has been used in the case $\mu = \frac{1}{2}$ in short-term earthquake prediction calculations by Kagan and Knopoff (1981, 1987).

For $\mu > 1$, we evaluate $d\langle t'\rangle/dt$ for this case by applying the criterion function (7a), which gives $(t_0/t)^{2\mu}\,1/(\mu - 1)$. Thus $d\langle t'\rangle/dt > 0$ for all $\mu > 1$ and all $t > t_0$.

For $\mu \leqq 1$, $\langle t \rangle$ diverges, and the criterion (7a) cannot be used. In this case, we have to examine the conditional distribution (2) directly and compare it with the unconditional distribution. This general method is also applicable to the case $\mu > 1$. Substitution of (A5) in equation (2) yields

$$P(t') = \frac{\mu}{t}\left(1 + \frac{t'}{t}\right)^{-(1+\mu)}. \qquad \text{(A6)}$$

Formula (A6) is almost the same as the unconditional distribution, except for the additional 1 in the parentheses; the two expressions are identical in the limit $t' \gg t$ except for obvious scaling factors. Thus, in this limit, the distribution $P(t')$ is also a power law with a characteristic scale given by the waiting time t, instead of t_0 for the unconditioned $p(t')$. Thus the longer it has been since the last earthquake, the longer the expected time until the next, for all cases $\mu > 1$.

Figure A4a shows $P(t')$ for $t = 10t_0$ and $t = 100t_0$ together with $p(t)$ for an exponent $\mu = 3$ (for this choice, $p(t)$ possesses a finite mean and variance). We observe the asymptotic power-law behavior of $P(t')$ at times $t' > t$ with amplitude significantly larger than $p(t')$, showing the enhanced probability for large conditional waiting times. Figure A4b shows $P(t')$ for $t = 10t_0$ and $t = 100t_0$ together with $p(t)$ for the threshold case of exponent $\mu = 1$; in this case, the mean and variance are not defined. This is an illustration of a power law with a very weighty tail. The behavior of $P(t')$ is qualitatively similar to the previous case.

Truncated Power-Law Distribution

Except for the uniform and periodic distributions, we have considered thus far only distributions of fluctuations in interval times that extend to infinity. In these cases of distributions with long-time tails, there is a finite but small probability that a second earthquake will occur after a very long time interval after the first. If the distributions describe the seismicity of a region, rather than that of an individual fault, the very long time intervals imply very large accumulations of deformational energy and hence very large fracture sizes. To avoid the problems of earthquake sizes greater than the size of a given region, we consider a cutoff in the distributions $p(t)$ (Knopoff, 1996). To demonstrate the influence of a cutoff, we restrict the previous case to

$$\begin{aligned} p(t) &= \frac{1}{1 - \left(\frac{t_{\max}}{t_0}\right)^{-\mu}} \frac{\mu}{t_0}\left(\frac{t}{t_0}\right)^{-(1+\mu)}, \quad t_0 \leqq t \leqq t_{\max}, \\ &= 0 \qquad\qquad\qquad\qquad\quad , \quad 0 < t < t_0, \end{aligned} \qquad \text{(A7)}$$

which is normalized. Substitution in equation (2) yields

$$P(t') = \frac{\mu}{(t + t')^{1+\mu}} \frac{1}{t^{-\mu} - t_{\max}^{-\mu}}. \qquad \text{(A8)}$$

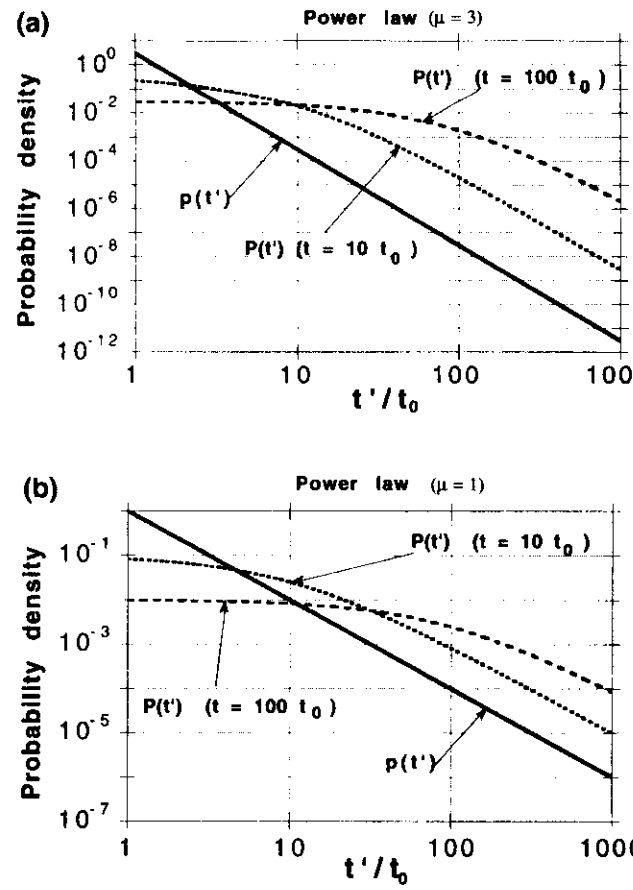

Figure A4. Power-law distribution. (a) $\mu = 3$; $p(t)$ possesses a finite mean and variance. $P(t')$ is shown for $t = 10t_0$ and $t = 100t_0$ together with $p(t')$. (b) $\mu = 1$; the mean and variance are not defined. $P(t')$ is shown for $t = 10t_0$ and $t = 100t_0$ together with $p(t')$.

For $t \ll t_{\max}$, the second factor of (A8) is t^{μ}, which is the same as letting $t_{\max} \to \infty$. Thus we recover the previous case of the simple power law without truncation.

The interesting regime is found when t is not very small compared to $t_{\max}$. Consider the case $t \to t_{\max}$. From equation (A8), we get

$$P(t') \approx \frac{1}{t_{\max} - t}, \qquad \text{(A9)}$$

which is independent of t' and becomes very large as $t \to t_{\max}$. This case is identical to that of the uniform distribution (A1) above. Thus it is not unexpected that the longer we wait, the shorter will be the expected time until the next event. Without truncation, the result is reversed. There is a crossover between the truncated and untruncated cases, as illustrated in Figure A5. In the figure, we take $\mu = 3$ as in Figure A4a, $t_{\max} = 100t_0$, and show $P(t')$ for $t = 10t_0$, $90t_0$, and $98t_0$. For $t = 10t_0$, $P(t')$ is found to be much larger than $p(t')$ in the tail, as in the previous untruncated case. For $t = 90t_0$, $P(t')$ is defined only for $0 \leqq t' \leqq 10t_0$. In agree-

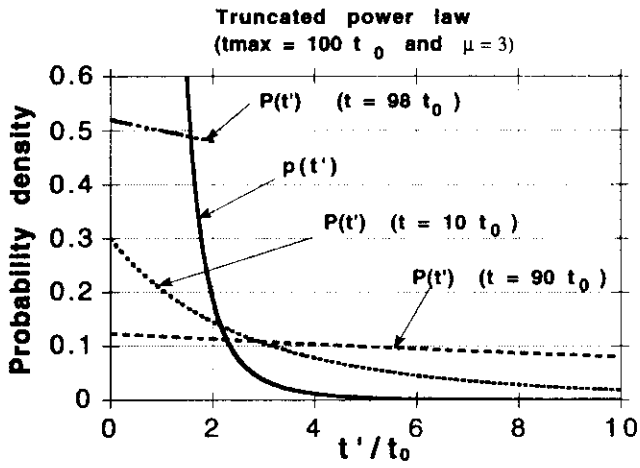

Figure A5. Truncated power-law distribution with $\mu = 3$ and $t_{max} = 100t_0$. $P(t')$ is shown for $t = 10t_0$, $90t_0$, and $98t_0$.

ment with (A8), we see that $P(t')$ becomes almost constant and close to $1/10t_0$. For $t = 98t_0$, $P(t')$ is defined only for $0 \leqq t' \leqq 2t_0$ and is close to $\frac{1}{2}t_0$. This illustrates the crossover from a longer expected time when t is small to a shorter expected time as t approaches t_{max}.

Since the truncated power-law distribution is very close to a uniform distribution for times near t_{max}, we expect that the truncated lognormal distribution and truncated Weibull distributions with $\mu < 1$ will also have a shorter time until the next event, the longer we have been waiting for an earthquake to happen; thus we expect a crossover in the response to Q. between these truncated and untruncated cases as well.

Department of Earth and Space Sciences and Institute of Geophysics and Planetary Physics
University of California
Los Angeles, California 90095
(D.S.)

Laboratoire de Physique de la Matière Condensée
CNRS URA190
Université des Sciences, B.P. 70
Parc Valrose, 06108 Nice Cedex 2, France
(D.S.)

Department of Physics and Institute of Geophysics and Planetary Physics
University of California
Los Angeles, California 90095
(L.K.)

Manuscript received 17 July 1996.